RESULTATS

-

Resultats (Capítol 1)

La Reelina i l'mDab1 regulen el desenvolupament de les connexions hipocampals

Els resultats presentats en aquest capítol han estat enviats per a la seva publicació a la revista **Molecular and Cellular Neuroscience**.

Lluís Pujadas [1*], Victor Borrell [1*], David Durà [1], Marta Solé [1], Sergi Simó [1], Jose A. Del Río [1] and Eduardo Soriano [1]

[*] Aquests autors han contribuït amb igualtat al desenvolupament del treball presentat.

[1] **Laboratori de Neurobiologia del Desenvolupament i la Regeneració Neuronal**, Parc Científic de Barcelona-IRB i Departament de Biologia Cel·lular, Universitat de Barcelona, E-08028 Barcelona.

RESUM

En l'anàlisi de la participació de la Reelina i l'mDab1 en el desenvolupament de les connexions hipocampals, en primer lloc hem observat que l'mDab1 és present als cons de creixement i als tractes dels axons en desenvolupament. Els mutants *mdab1-/-* tenen el mateix fenotip que els *reeler* en les alteracions observades en les connexions entorínico-hipocàmpica i commissural. S'observa innervació de regions ectòpiques, formació de patrons terminals erronis i un retard en el refinament de projeccions.

Els cultius organotípics mixtes de mutants *mdab1-/-* i controls demostren que les alteracions de la projecció entorínico-hipoàmpica és deguda a la deficiència de l'*mdab1* tant en les neurones que extenen l'axó com en les neurones diana. Els axons que innerven l'hipocamp reaccionen al tractament amb la Reelina incrementant la ramificació axonal i col·lapsant el con de creixement principal.

Els resultats obtinguts indiquen que la Reelina i l'mDab1 participen en el desenvolupament final i el refinament de les connexions hipocampals regulant les propietats d'adhesió i la ramificació axonal.

Resultats (Capítol 1)

Reelin and mDab1 regulate the development of hippocampal connections

ABSTRACT

To analyze the participation of Reelin and mDab1 in the development of hippocampal connections, we first show that mDab1 is present in growth cones and axonal tracts of developing of hippocampal afferents. *mdab1*-deficiency produce severe alterations in the entorhino-hippocampal and commissural connections identical to those described in *reeler* mice, including innervation of ectopic areas, formation of abnormal patches of fiber termination and a delay in the refinement of projections.

Organotypic slice cultures combining tissue from *mdab1*-mutant and control mice demonstrate that the abnormalities observed in the mutant entorhino-hippocampal projection are caused by *mdab1*-deficiency in both the projecting neurons and target hippocampal cells. Axonal afferents that innervate the hippocampus react to Reelin treatment by increasing the lateral branching and collapsing the principal growth cone.

Altogether these results indicate that Reelin and mDab1 participate in the final development and refinement of hippocampal connections by affecting the adhesion properties and the axonal branching.

INTRODUCTION

The correct functioning of the CNS requires both the proper positioning of neurons within layers or nuclei, and the formation of appropriate neuronal connections. Studies over the past few years point to the selective guidance of axonal growth cones by specific signals as the main mechanism by which neuronal connections are first established between brain areas (Huber et al., 2003; Mueller, 1999), while activity-dependent plasticity has been proposed as a mechanism for the final refinement and maturation of connections (Katz and Shatz, 1996).

A large number of extracellular diffusible and membrane-bound molecules, as well as extracellular matrix proteins, play a central role in the guidance and development of neural connections (Huber et al., 2003; Mueller, 1999). In some cases, such as Netrin-1, the same signal participates in both neuronal migration and axonal guidance. However, little is known about the intracellular molecules that transduce these environmental signals and thus participate in the elaboration of axonal growth cone responses. It has been shown that growth cone guidance is regulated through the signaling to the actin cytoskeleton, for instance, the Rho family of small GTPases play important roles in actin regulation during growth cone guidance and the development of connections (Gallo and Letourneau, 1998; Hall, 1998; Kuhn et al., 2000; Lin and Greenberg, 2000; Mueller, 1999; Wahl et al., 2000).

The hippocampus (HP) is a laminated structure that receives extrinsic and intrinsic inputs in a highly ordered fashion, where the different afferent systems terminate in non-overlapping layers. Thus, the entorhinal cortex (EC) innervates the stratum lacunosum-moleculare (SLM) of the HP proper, and the outer molecular layer (OML) of the dentate gyrus (DG). Conversely, the commissural/associational afferents terminate in the stratum radiatum (SR), stratum oriens(SO), and inner molecular layer (IML) (Blackstad, 1956; Ruth et al., 1982; Steward, 1976; Steward and Scoville, 1976; Swanson and Cowan, 1977; Swanson et al., 1978). In previous studies we have shown the importance of Cajal-Retzius (CR) cells in the orderly development of the hippocampal connections (Borrell et al., 1999b; Del Rio et al., 1997; Super et al., 1998).

The CR cells, first identified as a special class of pioneer neurons in the marginal zone of the neocortex, are also present in the marginal zone of the HP, prior to and during the ingrowth of hippocampal afferents (Del Rio et al., 1996; del Rio et al., 1995; Marin-Padilla, 1998; Soriano et al., 1994; Super and Soriano, 1994). CR cells express Reelin, a large extracellular molecule which lack produces the *reeler* phenotype (Alcantara et al., 1998; D'Arcangelo et al., 1995; D'Arcangelo et al., 1997; Ogawa et al., 1997; Schiffmann et al., 1997).

Shortly after the discovery of Reelin, a new molecule was identified: the mouse homolog of the *Drosophila* Disabled, mDab1, an intracellular adaptor protein whose mutation leads to migration disorders indistinguishable to those observed in *reeler* (Howell et al., 1997a; Howell et al., 1997b; Sheldon et al., 1997). mDab1 protein functions downstream of Reelin in the signaling pathway activated by Reelin stimulation. Later on, other molecules like lipoprotein receptors VLDLR and ApoER2, Src family kinases (SFKs), PI3K, Akt1, GSK3β and MAP1B were also been implicated in the same Reelin signaling pathway (Ballif et al., 2003; Beffert et al., 2002; Bock and

Herz, 2003; D'Arcangelo et al., 1999; Gonzalez-Billault et al., 2004; Trommsdorff et al., 1999). Moreover we recently found an implication of the ERK signaling pathway underlying Reelin stimulation, which induces the transcription of Egr-1 early gene.

Several studies show that the development of hippocampal connections requires the coordinated participation of a number of molecules, including Netrin-1, Semaphorin 3A and 3F, Slit-2, Ephrins, and Cell Adhesion Molecules (Barallobre et al., 2000; Chedotal et al., 1998; Dahme et al., 1997; Demyanenko et al., 1999; Nguyen Ba-Charvet et al., 1999; Pozas et al., 2001; Seki and Rutishauser, 1998; Stein et al., 1999; Steup et al., 2000; Steup et al., 1999). Moreover, we have shown that Reelin contributes to determine the layer-specific targeting of hippocampal afferents, and also stimulates their branching and synaptogenesis (Borrell et al., 1999a; Del Rio et al., 1997).

Here we analyze the development of the entorhino-hippocampal connections and the pattern of commissural projections in *mdab1* knock-out mice. Here we show that the *mdab1* gene is expressed in the EC and HP at embryonic and perinatal stages, when entorhino-hippocampal and commissural connections develop, and also that entorhinal and commissural afferents are mDab1 immunopositive. We next demonstrate that the absence of mDab1 leads to several alterations in the development of the entorhino-hippocampal pathway, including a delay in the appearance of the topographic patterns of projection, and the formation of ectopic patches of axonal termination. Some of these abnormalities are transient, while others persist to the adulthood. In addition, the analysis of the commissural/associational projection reveals that these afferents terminate ectopically in the hippocampal CA3 area in these mutants.

Altogether our results demonstrate that these abnormalities are very similar to those described earlier for the *reeler* mouse (Borrell et al., 1999a; Borrell et al., 1999b). Using mutant/wild-type mixed entorhino-hippocampal organotypic co-cultures, we demonstrate that both the absence of the protein mDab1 in both the entorhinal projecting neurons and in the target HP**,** are responsible for the abnormalities observed in *mdab1*-mutants. Finally, we analyzed the direct influence of Reelin stimulation of the axonal outgrowth of HP afferents. Reelin induce the collapse of CA3 axons and increase the lateral branching of HP neurons. Similarly, Reelin reduces the outgrowth of EC and DRG axons in explant cultures, indicating that Reelin may affect the final development those axons by collapsing the principal growth cone and increasing the lateral branching.

RESULTS

Pattern of *mdab1* mRNA expression and immunoreactivity in the developing hippocampal system

To understand the role of mDab1 in hippocampal development we first analyzed its expression at the gene and protein levels. In agreement with previous studies (Rice et al., 1998; Sheldon et al., 1997), *mdab1* expression was detected by *in situ* hybridization at E14-16 in a continuous band corresponding to the cortical plate of the entire developing cerebral cortex. In the EC, *mdab1* expression was also detected in the cortical plate, which contains postmitotic neurons, while in the developing HP expression was confined to the hippocampal plate, where postmitotic pyramidal neurons accumulate (Figure 1A). Lower expression levels were detected in the emerging DG at these stages (Figure 1A). In newborn mice, *mdab1* expression was detected in postmitotic neurons of the EC, including lower and upper layers (layers II-III), which also express *reelin* (Figures 1B,C). In the P0 HP, expression was detected in developing pyramidal and granule cells (Figure 1B). At later stages (P5-Adult) the pattern of *mdab1* expression remained essentially the same although levels of expression decreased with age, except in layer II of the EC (data not shown).

At E14, mDab1 immunostaining in the HP was mainly confined to the fimbria, containing developing commissural axons, moreover, the primitive plexiform layer was also immunopositive, although the intensity of staining was very faint at this stage (data not shown). At E16-E18 axonal bundles were heavily labeled in fimbria, the intermediate zone (specially in the CA1 and subicular areas), and in the angular bundle (Figures 1D,E). The hippocampal commissure, which was first visible at E18, also showed mDab1-immunostaining (data not shown). The hippocampal plate and the inner marginal zone showed a diffuse labeling, whereas the outer marginal zone was mDab1-negative at E16. Starting at E18, the lower aspect of the outer marginal zone became mDab1-positive (Figures 1D,F). In the DG the emerging granule cell layer was immunoreactive, and mDab1-positive cells were observed in the dentate ventricular zone and along the migratory pathway towards the developing DG (Figure 1D).

At P0, the overall level of mDab1 immunostaining increased witch respect to earlier stages. Numerous commissural axon bundles were labeled in the fimbria and white matter. The SLM exhibited a strong immunoreactivity in its lower aspect, where fiber bundles could be identified, however, mDab1 could not be detected in the upper aspect of the SLM (Figures 1D,F). In the DG the granule cell layer and the inner molecular layer (IML) were mDab1-positive, whereas the OML showed no immunoreactivity (data not shown). In order to ascertain whether entorhinal afferents terminating in the SLM are mDab1-positive, we compared the pattern of mDab1 immunolabeling with that of entorhino-hippocampal innervation in the CA1 area. mDab1 staining colocalizes with entorhinal axons, but only in the portion of the SLM closer to the SR (Figures 1G,I). Interestingly, the absence of mDab1 signal in the upper aspect of the SLM correlates with the presence of Reelin-expressing CR cells (Figures 1G,H). Suggesting that mDab1 protein levels in entorhinal axons that innervate the SLM may be locally downregulated by Reelin, as described for developing migrating neurons (Rice et al., 1998).

At P5-P8, the pattern of immunoreactivity changed in several ways from that observed at earlier stages. In the HP proper, the SO and white matter were strongly labeled, where axonal bundles could be recognized. In addition, the SLM displayed a strong and homogeneous immunoreactivity, with axon fascicles identified in area CA3. The SR displayed a diffuse immunostaining of low intensity, whereas the stratum lucidum was mDab1 negative. In the DG, a diffuse staining was observed in the MML, whereas no signal was visible in the outer or inner molecular layers (Figure 1J).

At P15 axon fascicles were mDab1 positive in the hippocampal commissure, fimbria, and in the hippocampal white matter. The HP proper displayed a diffuse immunostaining in the SO, SR, and SLM, being this latter the layer with the heaviest levels of stain. In the stratum lucidum mDab1 staining was undistinguishable from background levels. In the DG mDab1 immunolabeling was observed in the granule cell layer and also in the MML at the suprapyramidal blade, and both in the MML and OML at the infrapyramidal blade (data not shown).

In the adult brain, numerous axonal fascicles were immunopositive in the hippocampal commissure, but this staining was much more scarce in the fimbria and hippocampal white matter. The SO and SLM showed a very strong staining, whereas in the SR the staining intensity was lighter and mainly confined to the lower aspect of this layer. The stratum lucidum was almost devoid of staining, as observed during development. In the adult DG the ML was mDab1-positive in its middle and outer portions, both in the supragranular and infragranular blades, as opposed to the developmental stages analyzed (Figure 1K).

mDab1 protein is present in the developing axons that innervate the HP.

To evaluate the involvement of mDab1 in the stablishment of hippocampal connections, we first analyze whether Reelin is influencing the mDab1 content in axons that innervate the HP. mDab1 protein became phosphorylated after Reelin signaling, which induces its ubiquitination and degradation by proteosomal processing.

The overall levels of mDab1 are highly increased in *reelin*-deficient animals because of accumulation of unphosphorylated species. Augmented mDab1 protein levels can be detected by immunohistochemistry in *reeler* animals (Figure 2B) compared to wild types (Figure 2A). Moreover, *reeler* animals also show increased mDab1 content in axonal tracks that innervate the HP. In the fimbria, intense mDab1 immunoreactivity was detected in commissural axons incoming from CA3 area (Figure 2B,C). In the SLM, entorhinal afferents show high levels of mDab1 staining is the entire thickness of this layer, and mDab1 positive axons were detected in the immediacy of hippocampal fissure (HF) (Figure 2B,D), suggesting that the absence of Reelin avoids the local degradation of mDab1 in axons that innervate the SLM upper aspect.

To further confirm that mDab1 is present in CA3 and EC axons, and so it may contribute there to Reelin signaling, we cultured *in vitro* CA3 and EC explants and detected mDab1 protein presence by immunocytofluorescence. mDab1 was mainly present in the growth cones of CA3 axons, as well as detectable along the axonal tracks

(Figure 2E-G). Similarly, EC axons show an intense labeling of the growth cone, and also of the entire axonal track (Figure 2H-J). Altogether, our results indicate that Reelin signaling machinery is present in CA3 and EC axons, and they may be affected by hippocampal Reelin.

***mdab1*-deficient mice display abnormalities in the entorhino-hippocampal pathway**

To study the role of mDab1 in the development of the entorhino-hippocampal connections, postnatal mutant mice were injected in the EC with axonal tracers, and the patterns of innervation were compared to wild-type, to heterozygous mice, and also to previous analyses of the *reeler* phenotype (Borrell et al., 1999a). Since *mdab1 -/-* and *scm/scm* mice yielded identical patterns of labeling, both groups were pooled and will be described together. As described, the pattern of entorhinal innervation in P1 and P5 wild-type mice was restricted to the SLM. The innervation became denser at P5, with axons highly defasciculated, forming elaborate arbors and displaying numerous collaterals and axonal varicosities. In the DG, whereas at P1 the entorhinal fibers were just beginning to innervate the dentate OML, at P5 they had already formed a dense and elaborate innervation in this layer. The heterozygous (+/-) and (*+/scm*) mice, show the same pattern of innervation reported for wild type mice (Figures 3A,D).

The pattern of entorhinal innervation in *mdab1*-mutant mice at P1-P5 was very similar to that observed in *reeler* pups (Borrell et al., 1999a). At dorsal hippocampal levels most entorhinal fibers of *reeler* and *mdab1*-mutants were densely packed near the HF, following rather straight courses and exhibiting few collaterals or axonal varicosities (Figures 3B,C). Moreover, as in *reeler* mice, the CA3 area was almost devoid of entorhinal innervation. In the DG, entorhinal fibers were densely packed in the OML at P5, and many fibers were seen terminating ectopically in the IML and hilus (Figures 3B,C). In addition, entorhinal axons terminated aberrantly within the SR, specially at ventral levels, but also within the SP and SO, forming ectopic termination patches (Figures 3E,F).

The pattern of innervation from P16 onward was essentially the same that in adults, so these ages will be described together. In agreement with previous studies, tracer injections in the lateral or medial entorhinal areas of wild-type mice revealed two distinct patterns of entorhinal innervation to the HP (Borrell et al., 1999a; Ruth et al., 1982; Swanson and Cowan, 1977). Injections in the lateral EC of either wild type or heterozygous mice, form a dense patch of profusely branched fibers in the SLM of the CA3 area, and in the interface CA1-subiculum (Figure 4A). Conversely, medial entorhinal injections innervated selectively the molecular layer of the subiculum, the SLM of area CA1, and the lower aspect of the SLM in area CA3, where they formed elaborated axonal arbors (Figures 4B,I). In *mdab1*-mutant mice, innervation from the lateral EC was confined to the upper aspect of the SLM in the CA1 and subiculum, forming a continuous band of fibers without regional patches of termination, and with a virtual absence of innervation of the CA3 area (Figure 4C). The innervation of the SLM was narrower in the *mdab1*-mutants (44 $\pm$ 4.6 μm) than in control littermates (119 $\pm$ 4 μm), and numerous fibers in the CA1 area were fasciculated, displaying few axonal branches or varicosities. This pattern of innervation was essentially similar to that observed previously in *reeler* mice (Figure 4E) (Borrell et al., 1999a).

Following injections in the medial entorhinal area of *mdab1*-mutant mice, the typical two-patch pattern of axonal termination could be observed in the SLM of the CA1 area and subiculum, however, the CA3 region was devoid of any innervation (Figure 4D). Furthermore, a dense patch of ectopic afferent termination was observed in area CA1, where axons populated ectopically the SR, SO, and between the double pyramidal layer (Figures 4I,J). This feature was never observed in control mice, and was reminiscent to that observed in *reeler* mice (Figure 4F) (Borrell et al., 1999a).

In the DG of control (+/+ and +/-) mice, lateral entorhinal fibers were mainly detected in the OML, while innervation from the medial EC was largely confined to the MML (Figures 4A,B,G). In *mdab1*-mutants, lateral and medial entorhinal afferents terminated mostly in the OML and MML respectively, although in both cases a great number of ectopic fibers invaded inappropriate layers of the DG (Figures 4C,D,H).

The analysis of the development of entorhino-hippocampal projections in *mdab1*-deficient mice reveals that numerous and relevant alterations occur in this pathway in the absence of mDab1. These alterations have proved to be identical to those observed in *reeler* mice, in which extracellular Reelin is absent (Borrell et al., 1999a; Stanfield et al., 1979), strongly suggesting the participation of mDab1 in the transduction pathway of the Reelin signal that operates in the development of the entorhinal projection.

***mdab1*-deficient mice display abnormalities in the hippocampal commissural pathway**

We next analyzed the pattern of commissural connections in *mdab1* knock-out mice. The pattern of commissural projections observed at P16 were essentially similar to those observed in adult animals. Injections of BDA in the HP of P16-adult wild-type and heterozygous (+/-; *+/scm*) mice revealed the presence of commissural fibers in the contralateral hipocampus terminating in the SO and SR of the CA1-CA3 regions, where afferents arborized densely (Figure 5A). These commissural fibers did not invade the SLM, SL, or stratum pyramidale, in accordance with previous descriptions (Borrell et al., 1999b). In the DG, commissural afferents terminated mostly in the IML, although few fibers were occasionally seen in other layers such as the hilus (Figure 5C).

In *mdab1* knock-out mice, two patterns of commissural termination were detected, as occurs in *reeler* mice (Borrell et al., 1999b). In the CA1 area, either *mdab1*-deficient or *reeler* mice, show commissural axons terminating densely in SO, SR, and between the double-pyramidal layer (Figures 5B,E). At septal hippocampal levels, misrouted commissural fibers could also be observed terminating within the SLM (not shown). In area CA3 commissural afferents terminated also in the SO and SR, but in addition they densely innervated the entire thickness of the SLM, at all septo-temporal levels (Figures 5B,E). It is interesting to note that commissural fibers in the CA3 did not invade the SL, which was only populated by mossy fibers (immunolabeled with anti-calbindin antibodies; data not shown). The commissural projection to the DG terminated most densely in the IML, in close apposition to the granule cell area (Figure 5D). Moreover, a great number of ectopic fibers also terminated within this granule cell-

hilar area, forming small fiber clusters or being loosely distributed and intermingled between the misspositioned granule cells (Figure 5D).

These results show that the hippocampal commissural projections are deeply altered in *mdab1*-deficient mice. The strong parallelism between the abnormalities observed in these mice and those described in the reeler mouse (Borrell et al., 1999b; Stanfield et al., 1979) suggests that mDab1 is also necessary for the function of Reelin in the development of the commissural connections in the HP.

mDab1 is involved in the outgrowth and positioning of entorhino-hippocampal fibers.

Since *mdab1* is expressed in both the HP and the EC, the abnormalities observed in the entorhino-hippocampal projection of the *mdab1*-deficient mice could be due to the lack of *mdab1* in either the ingrowing developing axons or in the target region.

To discern between these possibilities, we prepared mixed organotypic entorhino-hippocampal co-cultures using slices obtained from newborn *mdab1*-mutants and their control littermates. After 7 days *in vitro* (DIV), homogenetic co-cultures ($EC^{+/+}/HP^{+/+}$, $EC^{+/-}/HP^{+/-}$, $EC^{-/-}/HP^{-/-}$) displayed patterns of entorhino-hippocampal innervation similar to those described *in vivo,* supporting the usefulness of this model to evaluate the characteristics of mixed co-cultures ($EC^{+/-}/HP^{-/-}$, $EC^{-/-}/HP^{+/+}$). In homogenetic wild-type ($EC^{+/+}/HP^{+/+}$) and heterozygous ($EC^{+/-}/HP^{+/-}$) co-cultures, entorhino-hippocampal fibers formed a dense innervation restricted to the OML and SLM (Figure 6A). Frequently, this co-cultures show distinct topographic patches of entorhinal termination that could be observed in the CA1 and CA3 areas, depending on the injection in the medial or lateral co-cultured EC (Figure 6A). In mutant homogenetic co-cultures ($EC^{-/-}/HP^{-/-}$) the innervation of the HP proper exhibited severe abnormalities (Figure 6D). Entorhinal projection to the SLM was compacted and restricted to its upper aspect, with fibers displaying abundant collaterals and axonal varicosities. Numerous entorhinal fibers descended from the SLM toward the SR, where they branched profusely and formed an ectopic patch of termination in the CA1 area (Figure 6D, white arrows) and CA3 area (Figure 6D, white arrowheads). Similarly, the perforant entorhinal axons innervate the DG near the HF with fibers packed very tightly, showing a great number of misrouted fibers ectopically innervating the hilus (Figure 6H,K).

When heterozygous entorhinal slices were co-cultured with mutant HP ($EC^{+/-}/HP^{-/-}$), a mixed pattern of projection between control and mutant homogenetic cultures was obtained (Figure 6B). Thus, afferent axons where not compacted close to the HF and they innervate the entire thickness of SLM and OML (Figure 6B). Topographic patches of termination were never formed at our time of culture (7 DIV), and misrouted fibers were frequently seen ectopically in the SR of the CA1 area (Figure 6B, white arrows) and CA3 area (Figure 6B, white arrowheads). Moreover, heterozygous entorhinal axons innervate profusely the mutant hilus through the perforant pathway (Figure 6F).

When mutant entorhinal slices were co-cultured with heterozygous hippocampal slices ($EC^{-/-}/HP^{+/-}$), the pattern of innervation also showed mixed characteristics of both

control and mutant homogenetic co-cultures (Figure 6C). Thus, entorhinal axons were targeted to the SLM, but while some ectopic axons descended to the SR of the CA3 area (Figure 6C, white arrowheads), ectopic fibers in the SR of the CA1 area were almost absent (Figure 6C, white arrow). The OML show an innervation mainly restricted to its upper aspect, where axons become tightly packed, even though, some fibers from the perforant pathway also innervate ectopically the hilus (Figure 6G,J).

To measure the severity of these abnormalities, we count the number of co-cultures that present moderate and severe defects in the entorhino-hippocampal projection (Figure 6I). In the CA1 area, moderate/severe grade of ectopic terminations was found in the 60-70% of co-cultures that contain *mdab1*-mutant HP; indicating that ectopies in this region are caused by misspositioning of target neurons (Figures 6A-D,I). In the CA3 area, the deficiency of *mdab1* in both axons and target neurons are responsible from the ectopies, mixed and homogenetic mutant co-cultures show moderate/severe ectopies in elevated percentages, with highest rigorous phenotype accomplished in $EC^{+/-}/HP^{-/-}$ co-cultures (Figures 6A-D,I). Similarly, in the hilus, the more severe ectopic innervation was achieved in $EC^{+/-}/HP^{-/-}$ co-cultures followed by *mdab1*-mutant homogenetic co-cultures indicating that heterozigous entorhinal axons growth more profusely into the *mdab1*-mutant HP than mutant fibers (Figures 6E-H,I). Finally, the phenotype showing compacted fibers in the HF was only present when the EC was *mdab1*-deficient, indicating that the tightly package of fibers was caused by the deficiency of *mdab1* in axonal tracks.

These *in vitro* experiments indicate that the abnormalities of the entorhino-hippocampal projection in *mdab1* knock-out mice may be attributable to the lack of the protein mDab1 in both the entorhinal projecting neurons and in the target HP. Ectopies are mainly caused by a misspositioning of target neurons, and are enhanced when the mutant HP is innerved by entorhinal axons not deficient in *mdab1*. Moreover, package of axons near the HF, especially in the OML, is a consequence of *mdab1* deficiency in EC projecting neurons. Altogether, these results suggest a role of mDab1 adaptor protein in the development of entorhinal axonal tracts and their adhesion properties.

Reelin affects axonal outgrowth:

The presence of mDab1 protein in the hippocampal afferents, and the phenotypic alterations observed in the hippocampal tracts of *reeler* and *mdab1*-deficient mice indicate that the Reelin signaling pathway may directly influence its outgrowth. For that reason we analyze the direct effect of Reelin treatment on the outgrowth of axons from the EC and CA3 region. We cultured explants from EC and CA3 from P0 mice on Reelin-coated coverslips and measured the total length of axons growing radially from the explant. Recombinant Reelin used in the coatings was produced by transitory transfection on 293T cells. The Reelin-containing supernatants of those cells, or from untransfected cells (Control Mock) were used in the coating treatments.

In Control Mock-treated coverslips, individualized axons growth out of the explant occupying the surrounding area (Figure 7A). When coverlips were coated with Reelin, the normal axonal growth is strongly reduced in both CA3 (Figure 7B,C) and

EC (Figure 7D) ; and also in non-hippocampal axons of the dorsal rooth ganglia (DRG) explants (Figure 7E-H). Moreover, in the CA3 explants, the number of individual growing axons decrease in Reelin-treatment conditions, and the outgrowth takes place in a more fasciculated manner in comparison to controls (Figure 7A,B).

Reelin affects hippocampal axonal branching and adhesion properties:

Since axons of the CA1/CA3 explants appear to growth out of the explant correctly before being affected by Reelin, we assayed an acute treatment with Reelin on those axons. CA3 explants were cultured for 3 DiV and then treated with supernatants containing Reelin (Figure 8A) or with control Mock supernatants (Figure 8B) for 1 hour. The analysis of axonal collapse promoted by Reelin indicates that Reelin increases significantly the number of collapsed CA3 axons (Figure 8C).

We then analyzed the effect of Reelin treatment on axonal growth of hippocampal primary cultures. Hippocampal neurons cultured on Reelin-coated coverlips tend to increase its homophilic interactions, indicating that Reelin influence their adhesion properties (Figures 8D,E). We where then also interested in quantifying the Reelin influence on axonal branching of hippocampal neurons. For that reason we maintained a low-density hippocampal primary culture for 3DiV in a collagen-based matrix with Reelin-containing (Figure 8G) or Control Mock-containing (Figure 8F) media. Images of individual neurons were captured and used for axonal length quantification and to count the branching points. Our results indicate that Reelin increases the number of axonal branching points per cell and also the total axonal arbor length in Reelin-treated cells comparing to Control Mock treatments (Figure 8H).

DISCUSSION

Reelin, an extracellular molecule secreted by Cajal-Retzius cells in the marginal zone, is essential for proper neuronal migration during the development of the cerebral cortex and HP (D'Arcangelo et al., 1995; Ogawa et al., 1995; Nakajima et al., 1997). Phenotypic analyses of mutant mice and biochemical studies have revealed that the Reelin signaling cascade involves the phosphorylation of the adapter protein mDab1 (Howell et al., 1997a,b, 1999, 2000; Sheldon et al., 1997; Rice et al., 1998). In earlier studies we have shown that Reelin is also involved in the development of the hippocampal connections, and that *reeler* mice display a number of abnormalities in the entorhinal and commissural projections to the HP, including invasion of inappropriate target layers, formation of ectopic patches of fiber termination, and deficient elaboration of axonal arbors and synaptogenesis (Del Río et al., 1997; Borrell et al., 1999a,b). These studies prompted the present analysis of the function of mDab1 in the development of hippocampal connections.

mDab1 is expressed in developing hippocampal axons

The *mdab1* gene was first discovered in *Drosophila* as a genetic modifier of the Abl cytoplasmic tyrosine kinase (Gertler et al., 1989). It was also shown that both Abl and Dab colocalize in major axon tracts in the CNS of the *Drosophila* larva, where they are required for proper axogenesis and formation of longitudinal and commissural axon bundles in the nerve cord (Gertler et al., 1989, 1993). In the present study we have shown that *mdab1* mRNA is expressed in the EC and HP during mouse development, including those stages when hippocampal connections are first established. In newborn pups *mdab1* is expressed in upper layers of the EC, where hippocampal-projecting neurons are located, and in the hippocampal plate, where commissural-projecting neurons reside. We have also shown that developing entorhino-hippocampal axons contain the mDab1 protein, not only in the axon shaft but also in the growth cone, in agreement with previous observations in mouse peripheral nerves, and in neocortical and hippocampal neurons in culture (Howell et al., 1997a; Howell et al., 1999b). These data support the notion that mDab1 may also have a function in the early development of hippocampal connections in the mouse. Furthermore, we have shown that entorhinal axons running through the upper aspect of the SLM of the HP display severely reduced levels of mDab1 protein at perinatal stages, which is coincident with the presence of Reelin-expressing CR cells in that particular sublayer, indicating that Reelin may induce the phosphorylation and subsequent degradation of mDab1 in this region. Previous studies have described that the absence of Reelin in the developing brain of the *reeler* mouse leads to increased levels of mDab1 protein, indicating that mDab1 may be degraded after fulfilling a signaling function evoked by Reelin (Arnaud et al., 2003; Bock et al., 2004; Howell et al., 1999a; Rice et al., 1998). Our observations showing that entorhinal axons located in the SLM of the *reeler* HP express high levels of mDab1, not only demonstrate that these fibers contain mDab1 in the target layer also, but further support the observations that developing entorhino-hippocampal afferents are Reelin-responsive, and are indicative that mDab1 participates in the Reelin signaling pathway within the developing entorhinal axons. Moreover, the presence of mDab1 within the growth cone suggests a direct role for the Reelin-mDab1 signaling pathway

in axon growth and/or guidance. In addition, the presence in the adult brain of high levels of *mDab1* mRNA in pyramidal cells in layer II of the EC, and of mDab1 protein in entorhino-hippocampal axons, strongly suggests the involvement of this molecule in lifely occurring phenomena, such as synaptic plasticity and learning/memory processes, as it has also been suggested to occur in GABAergic interneurons of the necortex (Rodriguez et al., 2000).

Alterations in hippocampal connections in mDab1 -/- are similar to those in reeler

The present analyses of the *mdab1*-mutant mouse show that the entorhinal and commissural connections are formed in the absence of mDab1, indicating that this protein is not essential for the early ingrowth of these afferents to the HP. Our study also shows that the patterns of termination of hippocampal afferents during the development of *mdab1*-mutants are largely similar to the patterns described for *reeler* mice (Borrell et al., 1999a; Borrell et al., 1999b). In the entorhino-hippocampal projection these abnormalities include an increase in ectopic fibers at inappropriate layers, both in the HP proper and the DG, the formation of aberrant projections from the medial EC to the SR and SO of the CA1-CA2 region, the presence of abundant misrouted fibers, and the virtual absence of innervation of the CA3 area. The main alterations observed in the commissural pathway are the invasion of the SLM in area CA3, and the intermingling of fibers with the granule cells in the DG and hilus. These results indicate that mDab1 plays a key role in the correct patterning of hippocampal afferents termination, and favor the hypothesis that Reelin signaling cascade modulate the development of such connections though mDab1.

Mechanisms of action of the Reelin-mDab1 signal

To ascertain whether the abnormal pattern of entorhino-hippocampal projections in the *mdab1*-mutant are due to the lack of mDab1 in the developing axons or in the target HP, mixed combinations of organotypic co-cultures were established. In these co-cultures, the pattern of entorhinal termination was a mixture between those observed in control and mutant homogenetic co-cultures. Thus, the entorhino-hippocampal projection pattern observed in the mutant mouse develops abnormally because of the absence of mDab1 in both the EC and the HP. Accordingly, the presence of mDab1 in either the projecting EC or the target HP is not sufficient to rescue the mutant phenotype, and in both cases only a mixed pattern is obtained. The mispositioning of target neurons in *mdab1*-deficient HP is responsible for the ectopies observed in CA1, CA3 and hilar regions; when the axons innerving the mutant HP are not deficient in mDab1, this ectopic projection is even favored, indicating that mDab1 protein is somehow involved in the final growth process and terminal positioning of entorhinal axons. Moreover, the single absence of mDab1 in the EC projection neurons is sufficient to produce the compactation of fibers near the HF, supporting the involvement of mDab1 in the positioning of EC axons possibly modulating the adhesion properties of ingrowing axons.

Reelin also modulates the adhesion properties of hippocampal neurons and their axons, and induces axonal growth cone collapse of CA3 afferents. This may be a mechanism of regulating the formation of associative/commissural connection.

MATERIALS AND METHODS:

Animals

OF1 mice (Charles River Laboratories) were used for the *in situ* hybridization and immunocytochemical studies, and for the *in vitro* explant assays. For tracing studies, two different colonies of *mdab1*-mutant mice were used: *scrambler* homozygous and heterozygous mice were obtained by mating *scrambler* homozygous (*scm*/*scm*) males with heterozygous (+/*scm*) females. *mdab1*-mutant, heterozygous and wild-type mice were obtained by mating heterozygous (+/-) mice. Genotypes were determined as described (Howell et al., 1997b). Since *mdab1*-mutant mice die at the third week of postnatal life, the adult stage could only be analized using *scrambler* animals, which survive through adulthood. *reeler* mice were obtained by mating *reeler* homozygous (*rl/rl*) males with heterozygous (+/*rl*) females. The day at which a vaginal plug was detected was considered embryonic day 0 (E0), and the day of birth was considered postnatal day 0 (P0).

All those experiments where carried out in accordance with the European Community Council Directive and the National Institute of Health guidelines for the care and use of laboratory animals.

In situ hybridization

Embryos from E14, E16 and E18 stages, and postnatal mice from stages P0, P5, P10, P15, P21, and adults (two animals each), were perfused with 0.1 M phosphate-buffered (PB) containing 4% of paraformaldehyde. The brains were postfixed overnight with the same solution, cryoprotected with 30% sucrose, and sectioned either coronally or horizontally at 25-50 μm. *mdab1* and *reelin* antisense riboprobes were labeled with digoxigenin-d-UTP (Boehringer-Mannheim, Germany) by *in vitro* transcription of a cDNA fragment encoding mouse *mdab1* (Rice et al., 1998), or mouse *reelin* (D'Arcangelo et al., 1995) using a T3 polymerase (Ambion). *In situ* hybridization was performed essentially as described elsewhere (Alcántara et al., 1998; Alvarez-Dolado et al., 1999). Sections were permeabilized in 0.2-0.5% Triton X-100 (15 min), treated with 2% H_2O_2 (15 min), deproteinized with 0.2 N HCl (10 min), fixed in 4% paraformaldehyde (10 min), and blocked in 0.2% glycine (5 min). Thereafter, sections were prehybridized at 60°C for 3 hr in a solution containing 50% formamide, 10% dextran sulfate, 5× Denhardt's solution, 0.62 M NaCl, 10 mM EDTA, 20 mM PIPES, pH 6.8, 50 mM DTT, 250 μg/ml yeast tRNA, and 250 μg/ml denatured salmon sperm DNA. Labeled antisense RNA was added to the prehybridization solution (500 ng/ml) and hybridization was carried out at 60°C overnight. Sections were then washed in 2× SSC (30 min, room temperature), digested with 20 μg/ml RNAse A (37°C, 1 hr), washed in 0.5× SSC/50% formamide (4 hr, 55°C) and in 0.1× SSC/0.1% sarkosyl (1 hr, 60°C). Sections were blocked in 10% normal goat serum (2 hr) and incubated overnight with an alkaline phosphatase-conjugated antibody to digoxigenin (Boehringer Mannheim, 1:2000). After washing, sections were developed with nitroblue tetrazolium (NBT) and 5-bromo-4-chloro-3-indolyl phosphate (BCIP) both purchased from Roche, mounted on gelatin-coated slides and coverslipped with Mowiol.

Immunocytochemistry

Embryos from E14, E16, and E18 stages, postnatal mice stages from stages P0, P5, P8, P15, and adults were perfused, cryoprotected and sectioned as above. After

several rinses in PB, sections were blocked with 10% goat serum during 2 hrs, and then incubated overnight at 4ºC with a rabbit polyclonal antibody against mDab1 (B3; dilution 1:800) (Howell et al., 1997a). Primary antibodies were visualized using biotinylated anti-rabbit antibodies (1:200), and a Streptavidin-biotinylated horseradish peroxidase complex (Amersham, Life Science) (1:400). The peroxidase reaction was developed using diaminobenzidine (DAB) and H_2O_2 as substrates. Sections were mounted, dehydrated and coverslipped.

Tracing of the entorhino-hippocampal and commissural pathways in vivo

Postnatal wild-type, heterozygous, *mdab1*-mutant mice obtained from either *scrambler* (*scm/scm*) or *mdab1*-mutant (-/-) strains (P0: 3 +/+, 7 +/-, 4 *+/scm*, 3 -/-, 1 *scm/scm*; P4: 9 +/+, 14 *+/scm*, 6 *scm/scm*; P16: 4 +/+, 6 +/-, 1 -/-) and adult mice from the Scrambler strain (4 *+/scm*, 2 -/-) were iontophoretically injected with biotinylated Dextran-Amine (BDA, MW=10.000; Molecular Probes) (+7.6 μA, 2 sec. On, 1 sec. Off) in the EC to trace the entorhino-hippocampal projection. Alternatively, P16 (4 +/+, 2 +/-, 4 -/-) and adult mice (2 *+/scm*, 1 *scm/scm*) were injected in the CA3 and hilus to trace the commissural connections. In addition, a similar collection of postnatal and adult *reeler* (*rl/rl*) mice were also injected in the EC and in the HP, to compare their phenotype with that of the *mdab1*-mutant mice. After 24-48 hrs of survival, animals were perfused, cryoprotected and sectioned either coronally or horizontally (50 μm thick) as described above. After blocking endogenous peroxidase activity, sections were incubated with ABC complex and developed with a DAB nickel-enhanced reaction (black reaction product); sections were counterstained with Nissl stain, dehidrated and coverslipped.

Explant cultures

EC explants were obtained from E16 or P0 OF1 brains as described elsewhere (Chedotal et al., 1998). Tissue pieces were then plated on poly-D-lysin/laminin (SIGMA) coated coverslips, and cultured for 2 days in a 5% CO_2, 37ºC, 95% humidity incubator in Neurobasal medium supplemented with 1% horse serum, L-glutamine, $NaHCO_3$, D-glucose, and B-27 supplement (all from GIBCO Life Technologies). Explants were fixed in 4% paraformaldehyde for 40 min, and washed several times with PBS 1X. Next cultures were blocked with 10% goat serum during 2 hrs, and then incubated overnight at 4ºC with a rabbit polyclonal antibody against mDab1 (B3; dilution 1:800) (Howell et al., 1997a) and with Texas-red tagged phalloidin (1:500). Primary antibody was visualized using Alexa Fluor 488 F(ab')2 fragment of goat anti-rabbit IgG (H+L) (1:500; Molecular probes). Explants were visualized using Olympus Fluoview FV300 confocal microscope.

Organotypic co-culture experiments

Entorhino-hippocampal co-cultures were prepared from P0-P1 pups essentially as described (Borrell et al., 1999a; Del Rio et al., 1997; Frotscher and Heimrich, 1993). Animals were anaesthetized by hypothermia, and the HP and prospective parietal neocortex were dissected out. Tissue pieces were cut into transverse slices (325 μm thick) using a McIIwain Tissue Chopper, and the slices were maintained in Minimum Essential Medium (MEM) supplemented with L-Glutamine (2mM) at 4ºC. Selected slices were co-cultured using the membrane interface technique (Stoppini et al., 1991). The phenotype of the pups was determined by the cytoarchitectonics of the HP (Borrell et al., 1999a), and later confirmed by genotyping. Four types of entorhino-hippocampal

co-cultures were prepared: (1) Control co-cultures ($EC^{+/+ \text{ or } +/-}/HP^{+/+ \text{ or } +/-}$) (n=22), where both slices were from wild-type or heterozygous pups; (2) *mdab1*-mutant co-cultures ($EC^{-/-}/HP^{-/-}$) (n=19); (3) mixed co-cultures using HP from (-/-) mice and EC from control mice ($EC^{+/-}/HP^{-/-}$) (n=31); and (4) mixed co-cultures combining control HP and (-/-) EC slices ($EC^{-/-}/HP^{+/-}$) (n= 25). To assess the formation of entorhino-hippocampal connections, a crystal of biocytin was injected in the entorhinal slice at 6 days *in vitro*. Co-cultures were fixed 24 hr after injection of the tracer, with 4% paraformaldehyde in 0.1 M PB. After several rinses, 40 μm thick sections were obtained, incubated with ABC overnight at 4ºC, and developed with a nickel-enhanced DAB reaction. Sections were counterstained with Nissl stain.

ABBREVIATIONS

DG	dentate gyrus
DRG	dorsal rooth ganglia
EC	entorhinal cortex
f	fimbria
GL	granule cell layer
HF	hippocampal fissure
HP	hippocampus
IML	inner molecular layer
ML	molecular layer
MML	medial molecular layer
NC	neocortex
H	hilus
OML	outer molecular layer
SC	subicular complex
SLM	stratum lacunosum-moleculare
SO	stratum oriens
SP	stratum piramidale
SR	stratum radiatum
WM	white matter

ACKNOWLEDGEMENTS

The authors would like to thank D. Goldowitz (Memphis) for the *scrambler* colony, and J. A. Cooper (Seattle) for the *mdab1* knock-out mouse colony and for generously providing the B3 antibody. We would also like to thank R. Rycroft and T. Yates for editorial help, and S. Maqueda for technical assistance. This work was supported by the Human Frontier Science Program, and CICYT SAF98-106 to E. Soriano, and MEC grant PM98-047 to J.A. Del Río. V. Borrell was a recipient of a CIRIT-FPI fellowship, L. Pujadas and M. Solé hold FPU postgraduate fellowships from the MEC, S. Simó hold an FPI postgraduate fellowship from the MEC, and D. Durà was funded by the Institute for Research in Paraplegia.

REFERENCES

Alcantara, S., M. Ruiz, G. D'Arcangelo, F. Ezan, L. de Lecea, T. Curran, C. Sotelo, and E. Soriano. 1998. Regional and cellular patterns of reelin mRNA expression in the forebrain of the developing and adult mouse. *J Neurosci*. 18:7779-99.

Arnaud, L., B.A. Ballif, and J.A. Cooper. 2003. Regulation of protein tyrosine kinase signaling by substrate degradation during brain development. *Mol Cell Biol*. 23:9293-302.

Ballif, B.A., L. Arnaud, and J.A. Cooper. 2003. Tyrosine phosphorylation of Disabled-1 is essential for Reelin-stimulated activation of Akt and Src family kinases. *Brain Res Mol Brain Res*. 117:152-9.

Barallobre, M.J., J.A. Del Rio, S. Alcantara, V. Borrell, F. Aguado, M. Ruiz, M.A. Carmona, M. Martin, M. Fabre, R. Yuste, M. Tessier-Lavigne, and E. Soriano. 2000. Aberrant development of hippocampal circuits and altered neural activity in netrin 1-deficient mice. *Development*. 127:4797-810.

Beffert, U., G. Morfini, H.H. Bock, H. Reyna, S.T. Brady, and J. Herz. 2002. Reelin-mediated signaling locally regulates protein kinase B/Akt and glycogen synthase kinase 3beta. *J Biol Chem*. 277:49958-64.

Blackstad, T.W. 1956. Commissural connections of the hippocampal region in the rat, with special reference to their mode of termination. *J Comp Neurol*. 105:417-537.

Bock, H.H., and J. Herz. 2003. Reelin activates SRC family tyrosine kinases in neurons. *Curr Biol*. 13:18-26.

Bock, H.H., Y. Jossin, P. May, O. Bergner, and J. Herz. 2004. Apolipoprotein E receptors are required for reelin-induced proteasomal degradation of the neuronal adaptor protein Disabled-1. *J Biol Chem*. 279:33471-9.

Borrell, V., J.A. Del Rio, S. Alcantara, M. Derer, A. Martinez, G. D'Arcangelo, K. Nakajima, K. Mikoshiba, P. Derer, T. Curran, and E. Soriano. 1999a. Reelin regulates the development and synaptogenesis of the layer-specific entorhino-hippocampal connections. *J Neurosci*. 19:1345-58.

Borrell, V., M. Ruiz, J.A. Del Rio, and E. Soriano. 1999b. Development of commissural connections in the hippocampus of reeler mice: evidence of an inhibitory influence of Cajal-Retzius cells. *Exp Neurol*. 156:268-82.

Chedotal, A., J.A. Del Rio, M. Ruiz, Z. He, V. Borrell, F. de Castro, F. Ezan, C.S. Goodman, M. Tessier-Lavigne, C. Sotelo, and E. Soriano. 1998. Semaphorins III and IV repel hippocampal axons via two distinct receptors. *Development*. 125:4313-23.

Dahme, M., U. Bartsch, R. Martini, B. Anliker, M. Schachner, and N. Mantei. 1997. Disruption of the mouse L1 gene leads to malformations of the nervous system. *Nat Genet*. 17:346-9.

D'Arcangelo, G., R. Homayouni, L. Keshvara, D.S. Rice, M. Sheldon, and T. Curran. 1999. Reelin is a ligand for lipoprotein receptors. *Neuron*. 24:471-9.

D'Arcangelo, G., G.G. Miao, S.C. Chen, H.D. Soares, J.I. Morgan, and T. Curran. 1995. A protein related to extracellular matrix proteins deleted in the mouse mutant reeler. *Nature*. 374:719-23.

D'Arcangelo, G., K. Nakajima, T. Miyata, M. Ogawa, K. Mikoshiba, and T. Curran. 1997. Reelin is a secreted glycoprotein recognized by the CR-50 monoclonal antibody. *J Neurosci*. 17:23-31.

Del Rio, J.A., B. Heimrich, V. Borrell, E. Forster, A. Drakew, S. Alcantara, K. Nakajima, T. Miyata, M. Ogawa, K. Mikoshiba, P. Derer, M. Frotscher, and E. Soriano. 1997. A role for Cajal-Retzius cells and reelin in the development of hippocampal connections. *Nature*. 385:70-4.

Del Rio, J.A., B. Heimrich, H. Super, V. Borrell, M. Frotscher, and E. Soriano. 1996. Differential survival of Cajal-Retzius cells in organotypic cultures of hippocampus and neocortex. *J Neurosci*. 16:6896-907.

del Rio, J.A., A. Martinez, M. Fonseca, C. Auladell, and E. Soriano. 1995. Glutamate-like immunoreactivity and fate of Cajal-Retzius cells in the murine cortex as identified with calretinin antibody. *Cereb Cortex*. 5:13-21.

Demyanenko, G.P., A.Y. Tsai, and P.F. Maness. 1999. Abnormalities in neuronal process extension, hippocampal development, and the ventricular system of L1 knockout mice. *J Neurosci*. 19:4907-20.

Frotscher, M., and B. Heimrich. 1993. Formation of layer-specific fiber projections to the hippocampus in vitro. *Proc Natl Acad Sci U S A*. 90:10400-3.

Gallo, G., and P.C. Letourneau. 1998. Axon guidance: GTPases help axons reach their targets. *Curr Biol*. 8:R80-2.

Gonzalez-Billault, C., J.A. Del Rio, J.M. Urena, E.M. Jimenez-Mateos, M.J. Barallobre, M. Pascual, L. Pujadas, S. Simo, A. La Torre, R. Gavin, F. Wandosell, E. Soriano, and J. Avila. 2004. A role of MAP1B in Reelin-dependent Neuronal Migration. *Cereb Cortex*.

Hall, A. 1998. Rho GTPases and the actin cytoskeleton. *Science*. 279:509-14.

Howell, B.W., F.B. Gertler, and J.A. Cooper. 1997a. Mouse disabled (mDab1): a Src binding protein implicated in neuronal development. *Embo J*. 16:121-32.

Howell, B.W., R. Hawkes, P. Soriano, and J.A. Cooper. 1997b. Neuronal position in the developing brain is regulated by mouse disabled-1. *Nature*. 389:733-7.

Howell, B.W., T.M. Herrick, and J.A. Cooper. 1999a. Reelin-induced tryosine phosphorylation of disabled 1 during neuronal positioning. *Genes Dev*. 13:643-8.

Howell, B.W., L.M. Lanier, R. Frank, F.B. Gertler, and J.A. Cooper. 1999b. The disabled 1 phosphotyrosine-binding domain binds to the internalization signals of transmembrane glycoproteins and to phospholipids. *Mol Cell Biol*. 19:5179-88.

Huber, A.B., A.L. Kolodkin, D.D. Ginty, and J.F. Cloutier. 2003. Signaling at the growth cone: ligand-receptor complexes and the control of axon growth and guidance. *Annu Rev Neurosci*. 26:509-63.

Katz, L.C., and C.J. Shatz. 1996. Synaptic activity and the construction of cortical circuits. *Science*. 274:1133-8.

Kuhn, T.B., P.J. Meberg, M.D. Brown, B.W. Bernstein, L.S. Minamide, J.R. Jensen, K. Okada, E.A. Soda, and J.R. Bamburg. 2000. Regulating actin dynamics in neuronal growth cones by ADF/cofilin and rho family GTPases. *J Neurobiol*. 44:126-44.

Lin, M.Z., and M.E. Greenberg. 2000. Orchestral maneuvers in the axon: trio and the control of axon guidance. *Cell*. 101:239-42.

Marin-Padilla, M. 1998. Cajal-Retzius cells and the development of the neocortex. *Trends Neurosci*. 21:64-71.

Mueller, B.K. 1999. Growth cone guidance: first steps towards a deeper understanding. *Annu Rev Neurosci*. 22:351-88.

Nguyen Ba-Charvet, K.T., K. Brose, V. Marillat, T. Kidd, C.S. Goodman, M. Tessier-Lavigne, C. Sotelo, and A. Chedotal. 1999. Slit2-Mediated chemorepulsion and collapse of developing forebrain axons. *Neuron*. 22:463-73.

Ogawa, M., T. Miyata, K. Nakajima, and K. Mikoshiba. 1997. [The action of reelin in the layering of cortical neurons in cerebrum]. *Tanpakushitsu Kakusan Koso*. 42:577-83.

Pozas, E., M. Pascual, K.T. Nguyen Ba-Charvet, P. Guijarro, C. Sotelo, A. Chedotal, J.A. Del Rio, and E. Soriano. 2001. Age-dependent effects of secreted Semaphorins 3A, 3F, and 3E on developing hippocampal axons: in vitro effects and phenotype of Semaphorin 3A (-/-) mice. *Mol Cell Neurosci*. 18:26-43.

Rice, D.S., M. Sheldon, G. D'Arcangelo, K. Nakajima, D. Goldowitz, and T. Curran. 1998. Disabled-1 acts downstream of Reelin in a signaling pathway that controls laminar organization in the mammalian brain. *Development*. 125:3719-29.

Rodriguez, M.A., C. Pesold, W.S. Liu, V. Kriho, A. Guidotti, G.D. Pappas, and E. Costa. 2000. Colocalization of integrin receptors and reelin in dendritic spine postsynaptic densities of adult nonhuman primate cortex. *Proc Natl Acad Sci U S A*. 97:3550-5.

Ruth, R.E., T.J. Collier, and A. Routtenberg. 1982. Topography between the entorhinal cortex and the dentate septotemporal axis in rats: I. Medial and intermediate entorhinal projecting cells. *J Comp Neurol*. 209:69-78.

Schiffmann, S.N., B. Bernier, and A.M. Goffinet. 1997. Reelin mRNA expression during mouse brain development. *Eur J Neurosci*. 9:1055-71.

Seki, T., and U. Rutishauser. 1998. Removal of polysialic acid-neural cell adhesion molecule induces aberrant mossy fiber innervation and ectopic synaptogenesis in the hippocampus. *J Neurosci*. 18:3757-66.

Sheldon, M., D.S. Rice, G. D'Arcangelo, H. Yoneshima, K. Nakajima, K. Mikoshiba, B.W. Howell, J.A. Cooper, D. Goldowitz, and T. Curran. 1997. Scrambler and yotari disrupt the disabled gene and produce a reeler-like phenotype in mice. *Nature*. 389:730-3.

Soriano, E., J.A. Del Rio, A. Martinez, and H. Super. 1994. Organization of the embryonic and early postnatal murine hippocampus. I. Immunocytochemical characterization of neuronal populations in the subplate and marginal zone. *J Comp Neurol*. 342:571-95.

Stanfield, B.B., V.S. Caviness, Jr., and W.M. Cowan. 1979. The organization of certain afferents to the hippocampus and dentate gyrus in normal and reeler mice. *J Comp Neurol*. 185:461-83.

Stein, E., N.E. Savaskan, O. Ninnemann, R. Nitsch, R. Zhou, and T. Skutella. 1999. A role for the Eph ligand ephrin-A3 in entorhino-hippocampal axon targeting. *J Neurosci*. 19:8885-93.

Steup, A., M. Lohrum, N. Hamscho, N.E. Savaskan, O. Ninnemann, R. Nitsch, H. Fujisawa, A.W. Puschel, and T. Skutella. 2000. Sema3C and netrin-1 differentially affect axon growth in the hippocampal formation. *Mol Cell Neurosci*. 15:141-55.

Steup, A., O. Ninnemann, N.E. Savaskan, R. Nitsch, A.W. Puschel, and T. Skutella. 1999. Semaphorin D acts as a repulsive factor for entorhinal and hippocampal neurons. *Eur J Neurosci*. 11:729-34.

Steward, O. 1976. Topographic organization of the projections from the entorhinal area to the hippocampal formation of the rat. *J Comp Neurol*. 167:285-314.

Steward, O., and S.A. Scoville. 1976. Cells of origin of entorhinal cortical afferents to the hippocampus and fascia dentata of the rat. *J Comp Neurol*. 169:347-70.

Super, H., A. Martinez, J.A. Del Rio, and E. Soriano. 1998. Involvement of distinct pioneer neurons in the formation of layer-specific connections in the hippocampus. *J Neurosci*. 18:4616-26.

Super, H., and E. Soriano. 1994. The organization of the embryonic and early postnatal murine hippocampus. II. Development of entorhinal, commissural, and septal connections studied with the lipophilic tracer DiI. *J Comp Neurol*. 344:101-20.

Swanson, L.W., and W.M. Cowan. 1977. An autoradiographic study of the organization of the efferent connections of the hippocampal formation in the rat. *J Comp Neurol*. 172:49-84.

Swanson, L.W., J.M. Wyss, and W.M. Cowan. 1978. An autoradiographic study of the organization of intrahippocampal association pathways in the rat. *J Comp Neurol*. 181:681-715.

Trommsdorff, M., M. Gotthardt, T. Hiesberger, J. Shelton, W. Stockinger, J. Nimpf, R.E. Hammer, J.A. Richardson, and J. Herz. 1999. Reeler/Disabled-like disruption of neuronal migration in knockout mice lacking the VLDL receptor and ApoE receptor 2. *Cell*. 97:689-701.

Wahl, S., H. Barth, T. Ciossek, K. Aktories, and B.K. Mueller. 2000. Ephrin-A5 induces collapse of growth cones by activating Rho and Rho kinase. *J Cell Biol*. 149:263-70.

FIGURE 1

Pattern of mdab1 and reelin expression during mouse hippocampal development

A-C, Low power views of the hippocampal region illustrating the distribution of *mDab1* (*A*,*B*) and *reelin* (*C*) mRNA-expressing cells (blue reaction product) at E16 (*A*) and P0 (*B*,*C*) in horizontal sections. At E16 (*A*), *mDab1*-positive cells are mainly located in the hippocampal and cortical plates, including the entorrinal cortex (EC). At P0 (*B*), *mDab1*-expressing cells are located in the hippocampal plate (HPP) and in the emerging dentate plate, in the subicular complex (SC), as well as in the upper layers of the entorhinal cortex (EC) (arrowheads). *reelin* (*C*) is strongly expressed by cells in cortical layer I and in the hippocampal fissure (HF), as well as by layer II cells in the EC (arrowheads).
D-F, Low (*D*) and high (*E*,*F*) magnification photomicrographs of the hippocampal region at E18 immunoreacted for the detection of mDab1. The HPP as well as the inner marginal zone (IMZ) and the inner portion of the outer marginal zone (OMZ) are immunostained (*F*). mDab1-positive axon fascicles are seen in the neocortex (NC) and EC (*D,* open arrowheads), as well as in the SC and the hippocampal intermediate zone (IZ) (*D-F*, arrowheads). The angular bundle is also stained (arrow in *D*,*E*).
G-I, Medium power parallel views of P0 (G,H) and P1 (I) hippocampal CA1 area showing the pattern of mDab1 immunoreactivity (*G*), *reelin* mRNA expression (*H*), and entorhino-hippocampal projection (*I*). mDab1 is only detected in the lower aspect of the stratum lacunosum-moleculare (SLM) but not in its upper aspect (*G*), where Reelin-expressing cells are located (*H*).
J,*K*, Low power views of coronal sections of the hippocampus (HP) at P5 (*J*) and adult (*K*) immunostained for mDab1. mDab1 immunoreactivity is mostly detected in the SLM (arrowheads) and stratum oriens (SO) at both stages, and also in the molecular layer (ML) of the adult (*K*). At P5, the hippocampal commissure is also mDab1-positive (arrow in *J*).
DG, dentate gyrus; VZ, ventricular zone; SR, stratum radiatum; SP, stratum pyramidale; WM, white matter; GL, granule cell layer; f, fimbria.
Scale bars: *A-C*, *D*, 250 μm; *E*,*F*, 100 μm; *G-I*, 65 μm; *J*,*K*, 400 μm.

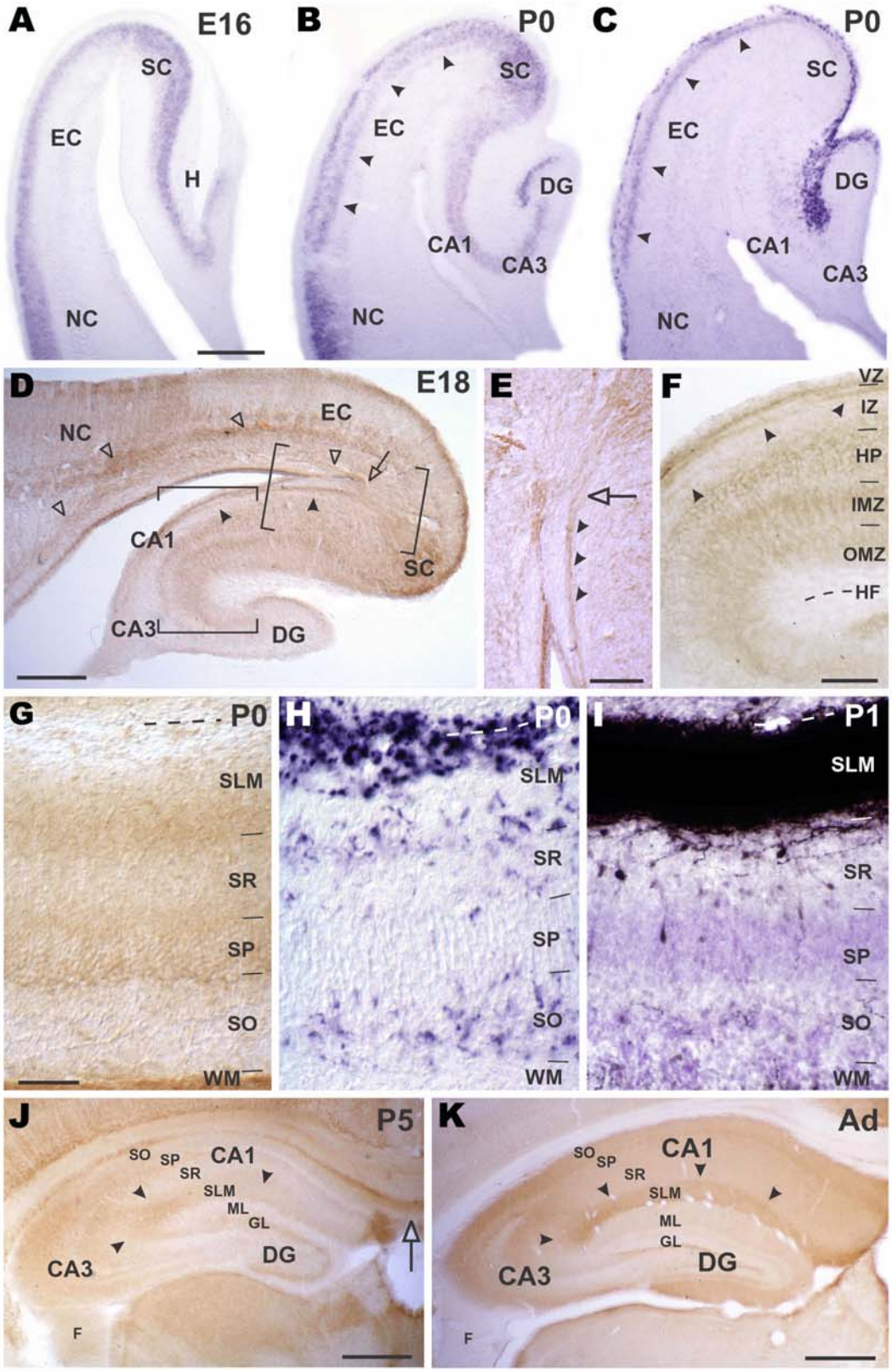
A
E16
SC
EC
H
NC
B
P0
SC
EC
DG
CA1
CA3
NC
C
P0
SC
EC
DG
CA1
CA3
NC
D
E18
NC
EC
CA1
SC
CA3
DG
E
F
VZ
IZ
HP
IMZ
OMZ
HF
G
P0
SLM
SR
SP
SO
WM
H
P0
SLM
SR
SP
SO
WM
I
P1
SLM
SR
SP
SO
WM
J
P5
SO
SP
SR
CA1
SLM
ML
GL
CA3
DG
F
K
Ad
SO
SP
SR
CA1
SLM
ML
GL
CA3
DG
F

Figure 1

FIGURE 2

mDab1 is present in hippocampal afferents and upregulated in reeler mice.

A,*B*, Low power micrographs of wild-type (+/+) and *reeler* (rl/rl) P0 hippocampus (HP) immunostained for mDab1, showing that the overall intensity of immunoreactivity is stronger in *reeler* (*B*) than in wild type mice (*A*); in *reeler* the entire thickness of the stratum lacunosum-moleculare (SLM) is immunopositive (*B,D*), whereas the upper aspect of the SLM in +/+ is not labeled (*A*).
C,*D*, High power micrographs of fimbria (f) (*C*) and CA1 region (*D*) immunostained for mDab1 from *reeler* P0 animals. *C,* Commissural fibers from the CA3 area are detected in the fimbria (black arrows) with enhanded mark compared to wild types. *D,* The entire thickness of the SLM of the CA1 region of *reeler* is stained and axonal tracts can be seen in the immediacy of hipocampal fissure (HF).
E-J, High magnification images of axons from cultured CA3 (*E-G*) and entorhinal cortex (EC) (*H-J*) explants immunostained for mDab1 (*C,H*) and actin (*F,I*); mDab1 is mainly localized in the growth cone although it is also present along the axon shaft; merge images show that mDab1 is not present in the elongating filopodia of the growth cone (G,J).
DG, dentate gyrus; ML, molecular layer; SR, stratum radiatum; SP, stratum pyramidale; SO, stratum oriens; WM, white matter.
Scale bars: *A*,*B*, 200 μm; *C,D,* 100 μm *E-J*, 10 μm.

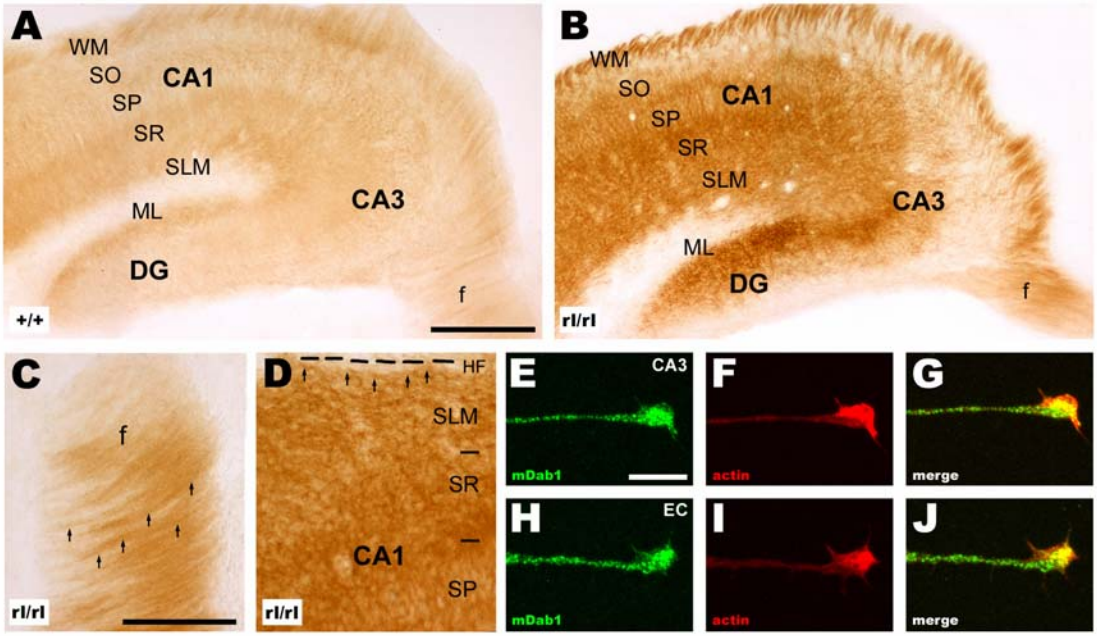
A
WM
SO
CA1
SP
SR
SLM
ML
CA3
DG
f
+/+
B
WM
SO
CA1
SP
SR
SLM
CA3
ML
DG
f
rl/rl
C
f
rl/rl
D
HF
SLM
SR
CA1
SP
rl/rl
E
CA3
mDab1
F
actin
G
merge
H
EC
mDab1
I
actin
J
merge

Figure 2

FIGURE 3

Development of the entorhino-hippocampal pathway in mDab-mutant, reeler and control mice.

A-E, Low power photomicrographs illustrating the distribution of entorhinal afferents labeled after dextran-amine injections in the entorhinal cortex (EC) at P1-P2 and P5 in mDab1 heterozygous (+/-) and knock-out (-/-) mice, and reeler (rl/rl) mice. In heterozygous mice at P1 (*A*) EC afferents innervate the entire thickness of the stratum lacunosum-moleculare (SLM). EC fibers in -/- (*B*) and rl/rl (*C*) mice, in contrast, appear packed densely near the hippocampal fissure (HF), but many axons also descend toward lower aspects of the SLM and to the stratum radiatum (SR). At P5 (*D*), lateral EC axons in the hippocampus (HP) proper innervate exclusively the SLM, when the characteristic patch distribution of axons in the CA3 and CA1 subicular border begins to be visible. In addition, fibers innervate the molecular layer (ML) of the dentate gyrus (DG). *E*, In P5 -/- mice, most entorhino-hippocampal fibers are still in the vicinity of the HF, at the molecular layer as well as the neighboring SLM, although abundant fibers are also present in the inner portion of the SLM and the SR.
F, High magnification of the inset box in *E*, showing misrouted EC fibers (arrowheads) terminating in the SR and stratum pyramidale (SP).
Scale bars: *A-C*, 200 μm; *D*,*E*, 300 μm; *F*, 125 μm.

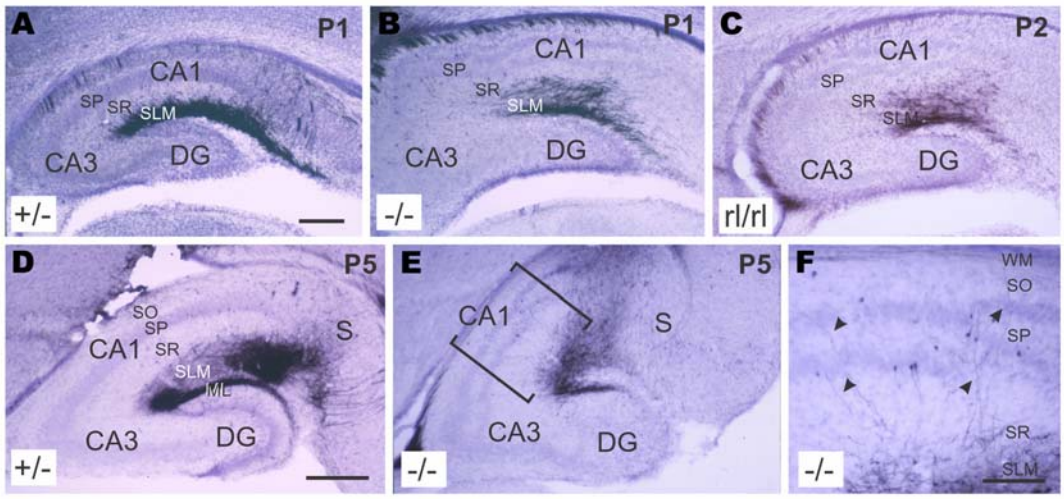
A
P1
CA1
SP
SR
SLM
CA3
DG
+/-
B
P1
CA1
SP
SR
SLM
CA3
DG
-/-
C
P2
CA1
SP
SR
SLM
CA3
DG
rl/rl
D
P5
SO
SP
CA1
SR
SLM
ML
S
CA3
DG
+/-
E
P5
CA1
S
CA3
DG
-/-
F
WM
SO
SP
SR
SLM
-/-

Figure 3

FIGURE 4

Patterns of entorhino-hippocampal projection in adult mDab1 knock-out (-/-), control (+/-), and reeler (rl/rl) mice.

A,*C*,*E*, Photomicrographs illustrating the pattern of entorhino-hippocampal innervation after dextran-amine injection in the lateral entorhinal cortex (EC). *A*, Injections in the lateral EC in +/- mice yield a dense patch of fibers in the stratum lacunosum-moleculare (SLM) of the CA3 region and the subicular-CA1 interface (data not shown). Some fibers are also observed in CA1. In the dentate gyrus (DG) axons are restricted to the outer third of the molecular layer (ML). In -/- (*C*) and rl/rl (*E*) mice, lateral EC injections result in a narrow band of fibers in the SLM of the CA1 region and in the outer part of the ML of the DG, near the hippocampal fissure (HF). Note that the characteristic patch of termination in the SLM of the CA3 region is not observed.
B,*D*,*F*, Pattern of entorhino-hippocampal innervation after medial EC injections of dextran-amine. In +/- (*B*) mice, EC axons innervate two patches in the subiculum (data not shown) and in the SLM of the proximal CA1 region, in continuation with a narrow band of fibers in the lower SLM of the CA3 region. In the DG, fibers are restricted to the middle third of the ML. *D*,*F*, Injections in -/- and rl/rl mice show two patches of termination in the SLM of the CA1 region, and subiculum (not shown in *D*), reminiscent of those in control animals. In addition, numerous aberrant fibers are present in the stratum radiatum (SR), stratum pyramidale (SP) and stratum oriens (SO) of the CA1 subfield. The pattern of medial innervation in the DG involves the medial molecular layer (MML).
G,*H*, Photomicrographs of the DG showing the pattern of innervation of lateral EC injections in -/- (*H*) mice compared with +/- (*G*) mice. In heterozygous (*G*) mice the lateral EC afferents occupy the outer molecular layer (OML) without invading lower layers such as media molecular layer (MML), inner molecular layer (IML), granule cell layer (GL) or hilus (H). In *mDab1*-mutant (-/-) mice (*H*), fiber also innevate mainly the OML, but also numerous fibers are detected in lower layers.
I,*J*, Photomicrographs of area CA1 showing the pattern of innervation of medial EC injections in +/- (*I*) and -/- (*J*) mice. *I*, In +/- mice medial EC fibers are evenly and exclusively distributed within the SLM, and they are also seen bundled within the white matter (WM). *J*, In -/- mice numerous axons descend through the SR toward the SP and SO, where they terminate forming big patches of fibers.
Scale bars: *A-D*, 500 μm; *E*, *F*, 400 μm; *G-J*, 100 μm.

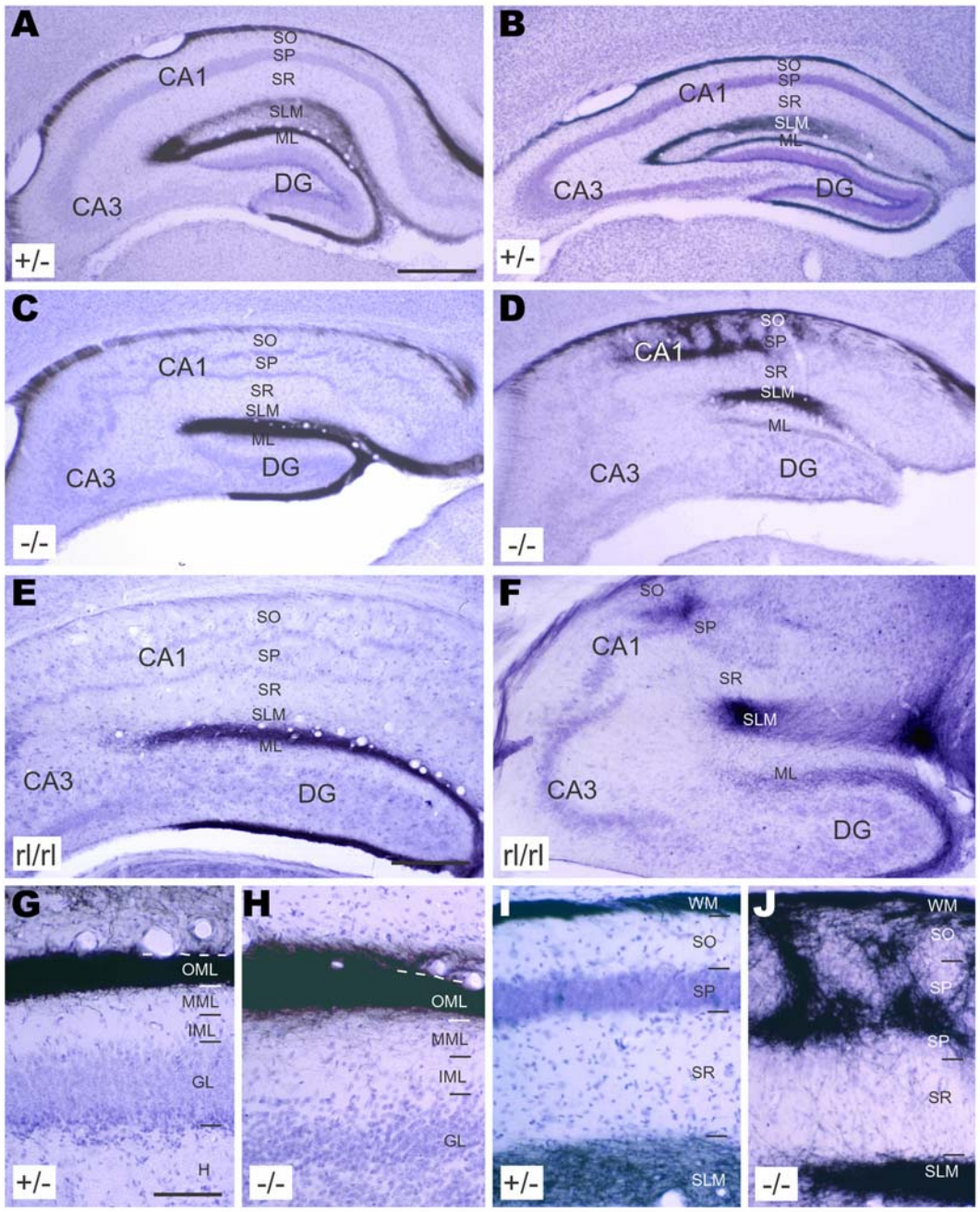
A
SO
SP
SR
SLM
ML
CA1
CA3
DG
+/-
B
SO
SP
SR
SLM
ML
CA1
CA3
DG
+/-
C
SO
SP
SR
SLM
ML
CA1
CA3
DG
-/-
D
SO
SP
SR
SLM
ML
CA1
CA3
DG
-/-
E
SO
SP
SR
SLM
ML
CA1
CA3
DG
rl/rl
F
SO
SP
SR
SLM
ML
CA1
CA3
DG
rl/rl
G
OML
MML
IML
GL
H
+/-
H
OML
MML
IML
GL
-/-
I
WM
SO
SP
SR
SLM
+/-
J
WM
SO
SP
SP
SR
SLM
-/-

Figure 4

FIGURE 5

Patterns of commissural projection in mDab1-mutant (-/-), heterozygous (+/-) and reeler (rl/rl) mice.

A,*B*,*E*, Photomicrographs illustrating the pattern of commissural innervation after dextran-amine injections in the CA3 region and dentate gyrus (DG) of the contralateral hippocampus (HP). *A*, In +/- mice tracer injections revealed a uniformly dense innervation restricted to the stratum oriens (SO) and stratum radiatum (SR) in the HP proper, and a narrow band of fibers occupying the inner part of the molecular layer (ML) in the DG. In -/- (*B*) and *reeler* (*C*) mice, commissural fibers terminated in the SO and SR in the CA1 and CA3 areas, and in the stratum lacunosum-moleculare (SLM) of the CA3 area. Commissural fibers innervate the disrupted granule cell layer (GL), where an increase in density of innervation was noted in the inner part of the molecular layer (ML) (not shown in *E*). Some retrogradely labeled cells can be seen in the pyramidal cell layer of the CA3 region and in the hilus in *A*,*B*, and *E*.
C,*D*, High magnification photomicrographs of the DG showing the pattern of commissural innervation in +/- (*C*) and -/- (*D*) mice. In heterozygous mice (*C*) the commissural afferents occupy the inner molecular layer (IML), whereas in knock-out mice (*D*) the projection to the DG terminates densely in the lower aspect of the inner molecular layer, but also numerous ectopic fibers are distributed in the GL.
OML, outer molecular layer; MML, medial molecular layer.
Scale bars: *A*,*B*,*E*, 125 μm; *C*,*D*, 60 μm.

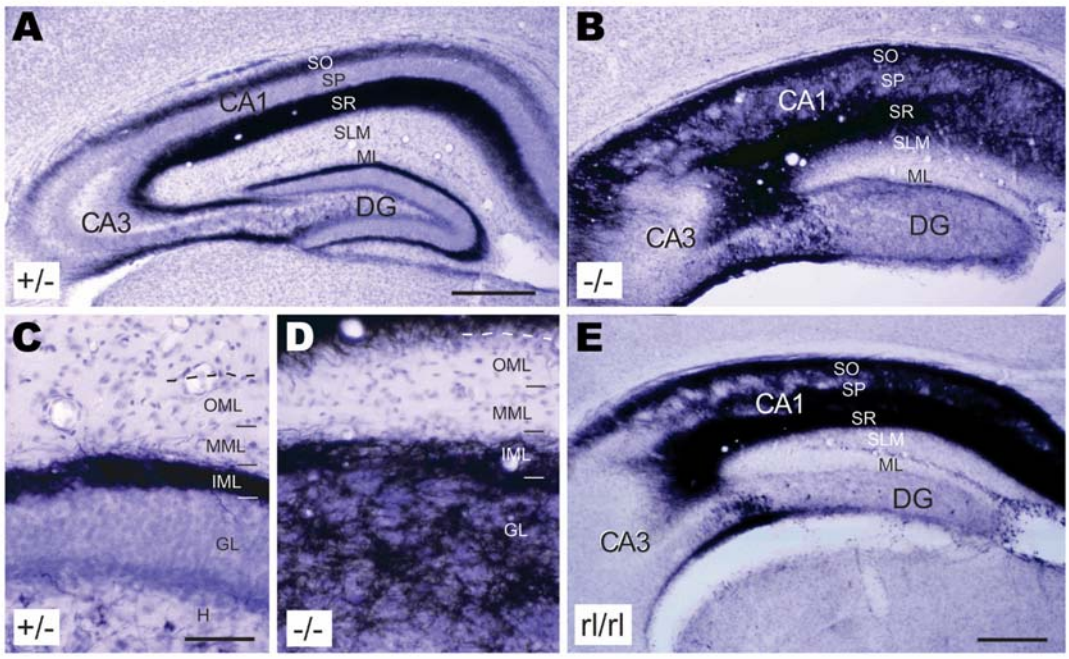
A
SO
SP
CA1
SR
SLM
ML
CA3
DG
+/-
B
SO
SP
CA1
SR
SLM
ML
CA3
DG
-/-
C
OML
MML
IML
GL
+/-
H
D
OML
MML
IML
GL
-/-
E
SO
SP
CA1
SR
SLM
ML
DG
CA3
rl/rl

Figure 5

FIGURE 6

In vitro formation of the entorhino-hippocampal projection in mDab1-deficient organotypic slice co-cultures.

A-D, Low power micrographs of co-cultures from entorhinal cortex (EC) and hippocampus (HP). Entorhino-hippocampal axons were labeled with biocytin and visualized by immunohistochemistry with DAB precipitates. *A,* In wild type co-cultures ($EC^{+/-}/HP^{+/-}$), EC afferents terminated in the entire thickness of the stratum lacunosum moleculare (SLM) and the outer aspect of the molecular layer (ML), forming topographic patches of termination, reminiscent to the *in vivo* phenotype. *B,* In *mDab1*-mutant homogenic co-cultures ($EC^{-/-}/HP^{-/-}$) numerous misrouted fibers ectopically innervate the CA1 area (white arrows) whereas other axons switch to the CA3 region (white arrowheads), as well as occur *in vivo*. *B,* Mixed $EC^{-/-}/HP^{+/-}$ co-cultures present the similar ectopies in the CA1 and CA3 regions as mutant homogenic co-cultures, but in the CA3 region these ectopies are even more abundant. *D*, Mixed $EC^{-/-}/HP^{+/-}$ co-cultures present very rarely ectopies in the CA1 area, but severe ectopies in CA3 are as frequent as in homogenic mutant co-cultures.

E-H, High power micrographs of the hilar region of the DG from organotypic co-cultures. In wild type homogenic co-cultures the perforant pathway afferents are restricted to the ML (*E*). Whereas, misrouted fibers from the perforant pathway descended to the hilus from the ML (black arrows) when at least one part of the co-cultures is *mDab1*-defective (*F-H*). The most severe ectopies are formed when wild type axons innervate mutant HP ($EC^{+/-}/HP^{-/-}$) (*G*).

I-L, Severe compactation of fibers near the hippocampal fissure (HF) is only observed when the EC axons are *mDab1*-defective. Both $EC^{-/-}/HP^{-/-}$ (*L*) and $EC^{-/-}/HP^{+/-}$ (*K*) co-cultures, but not $EC^{+/-}/HP^{+/-}$ (*I*) or $EC^{+/-}/HP^{-/-}$ (*J*), present compacted fibers in the HF. These results indicate that mDab1 play a key role in the adhesion properties of EC outgrowing axons.

M, Quantification of the observed abnormalities was performed by analyzing the percentage of cultures showing from moderate to severe ectopic innervation in the different regions. The basal percentage of wild-type homogenic co-cultures presenting abnormalities (10 to 30%) is attributable to defective biocytin injections. Ectopies in CA1 are merely attributable to the mispositioning of neurons in the target HP. By the other hand, ectopic innervation of CA3 and hilus is responsible of both defect in *mDab1* in the EC and HP, with highest percentage of severely misrouted projection in wild type EC fibers innervating mutant HP (75%).

Scale bar: *A-D*, 500 μm; *E-H*, 100 μm; *J,K*, 50 μm.

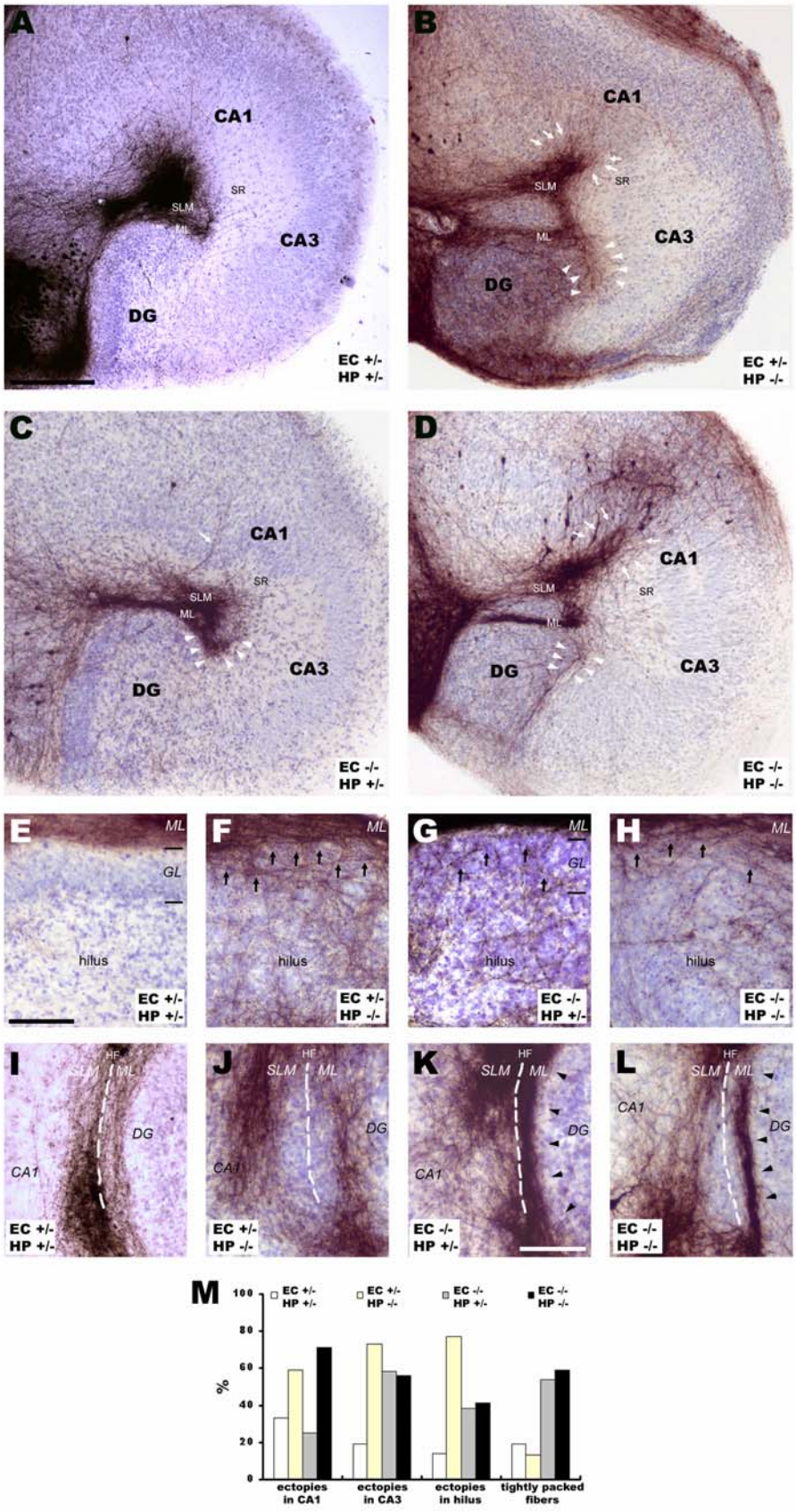
A
CA1
SR
SLM
ML
CA3
DG
EC +/-
HP +/-
B
CA1
SLM
SR
ML
CA3
DG
EC +/-
HP -/-
C
CA1
SR
SLM
ML
CA3
DG
EC -/-
HP +/-
D
CA1
SLM
SR
ML
DG
CA3
EC -/-
HP -/-
E
ML
GL
hilus
EC +/-
HP +/-
F
ML
hilus
EC +/-
HP -/-
G
ML
GL
hilus
EC -/-
HP +/-
H
ML
hilus
EC -/-
HP -/-
I
HF
SLM
ML
DG
CA1
EC +/-
HP +/-
J
HF
SLM
ML
DG
CA1
EC +/-
HP -/-
K
HF
SLM
ML
DG
CA1
EC -/-
HP +/-
L
HF
SLM
ML
CA1
DG
EC -/-
HP -/-
M
EC +/-
HP +/-
EC +/-
HP -/-
EC -/-
HP +/-
EC -/-
HP -/-
%
100
80
60
40
20
0
ectopies
in CA1
ectopies
in CA3
ectopies
in hilus
tightly packed
fibers

Figure 6

FIGURE 7

Reelin reduces axonal outgrowth.

A,*B*, β-III-tubulin immunostaining of CA3 explants cultured for 3 DiV in Reelin-coated (*B*) or in Control Mock-coated (*A*) coverslips; in Reelin-treated coverslips the axonal outgrowth is reduced and individualized axons are difficultly observed.
C,D, Quantification of length of axons growing out of the EC (*C*) or CA1/CA3 (*D*) explants grown in Control Mock- or Reelin-treated coverslips for 3 DiV. Histograms summarize the data obtained in independent/separate experiments expressed in percentages. Data represent mean±SEM (*,$p<0.05$)
E,*F*, β-III-tubulin immunostaining of DRG explants cultured for 3 DiV with NT3 containing media in Reelin-coated (*B*) or in Control Mock-coated (*A*) coverslips; in Reelin-treated coverslips the axonal outgrowth is reduced.
G,H, Quantification of length of axons growing out of the DRG explants supplemented with NT3- or NGF-containing media (*G,H* respectively) in Control Mock- or Reelin-treated coverslips for 3 DiV. Histograms summarize the data obtained in independent/separate experiments expressed in percentages. Data represent mean±SEM (*,$p<0.05$)
Scale bar: *A-B*, 200μm; *E-F*, 200μm

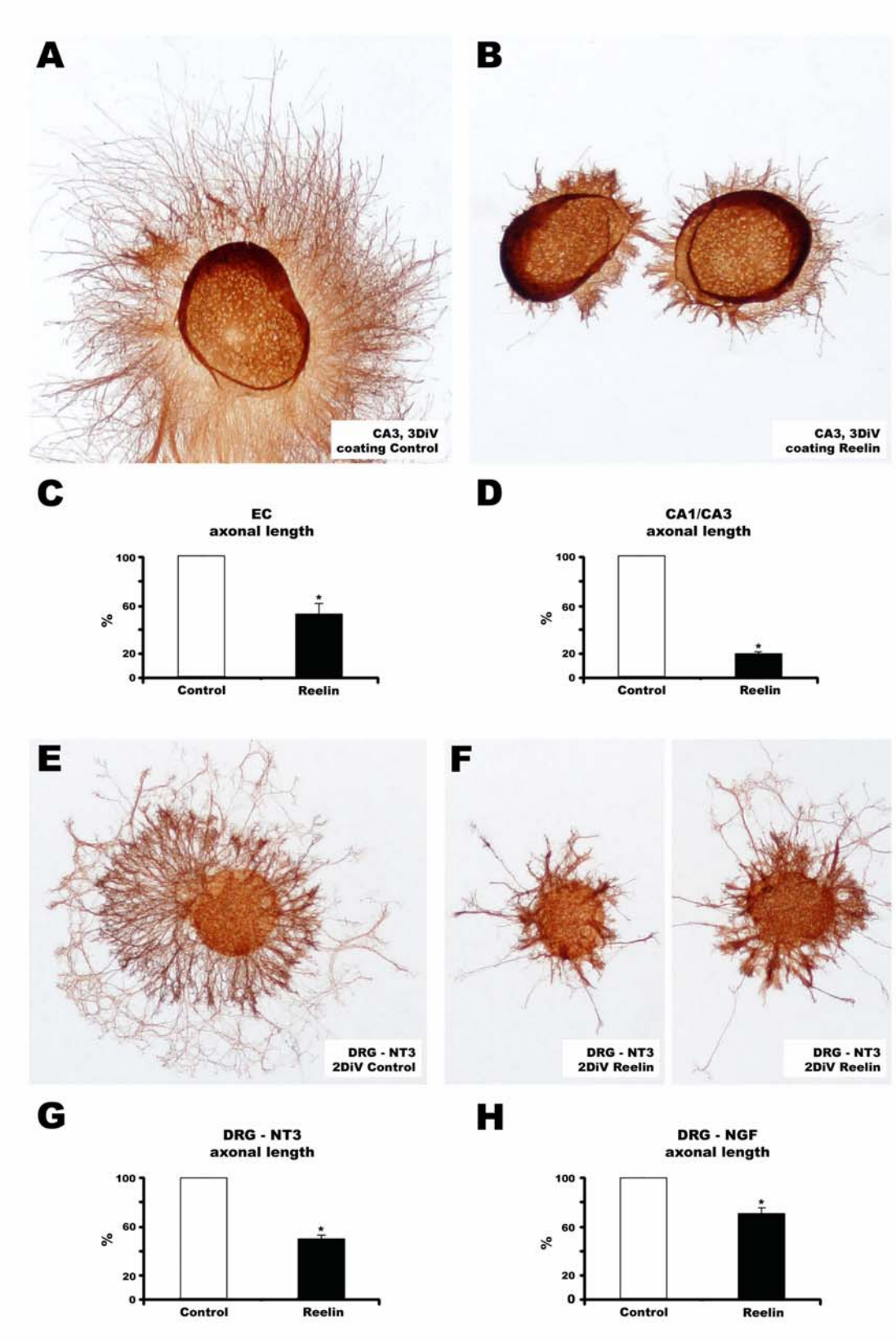
A
CA3, 3DiV
coating Control
B
CA3, 3DiV
coating Reelin
C
EC
axonal length
100
60
20
0
%
*
Control
Reelin
D
CA1/CA3
axonal length
100
60
20
0
%
*
Control
Reelin
E
DRG - NT3
2DiV Control
F
DRG - NT3
2DiV Reelin
DRG - NT3
2DiV Reelin
G
DRG - NT3
axonal length
100
60
20
0
%
*
Control
Reelin
H
DRG - NGF
axonal length
100
60
20
0
%
*
Control
Reelin

Figure 7

FIGURE 8

Reelin induce axonal growth cone collapse and lateral branching.

A,*B*, Phalloidin-texas-red staining of CA3 explants cultured for 3 DiV. Reelin-treatment for 1 hour (*B*) increases the number of collapsed axons in comparison to Control Mock-treatment (*A*).
C, Quantification of the percentage of collapsed axons in CA3 explants at 3 DiV. Reelin induce collapse to CA3 axons. Histograms summarize the data obtained in independent/separate experiments. Data represent mean±SEM (*,$p<0.05$).
D,*E*, β-III-tubulin immunostaining of hippocampal primary culture at 3 DiV in Reelin-coated (*E*) or in Control Mock-coated (*D*) coverslips; in Reelin-treated coverslips the cell neurites fasciculate by homophillic interaction (arrowheads).
F,*G*, β-III-tubulin immunostaining of hippocampal primary culture at 3 DiV in collagen matrix. Reelin-treatment for 3 DiV (*B*) increases the number of branching points in the axon in comparison to Control Mock-treatment (*A*). Reelin also increases the total axonal arbor length due to the increased collateral branches.
H, Quantification of the number of axonal branching points and the total axonal arbor length of individualized hippocampal neurons grown in Control Mock- or Reelin-treatement conditions in collagen matrixs. Histograms summarize the data obtained by analyzing 63 neurons for each group. Data represent mean±SEM (*,$p<0.05$; **, $p<0.001$).
Scale bar: *A-B*, 20 μm; *D-E*, 100 μm; *F-G*, 50 μm.

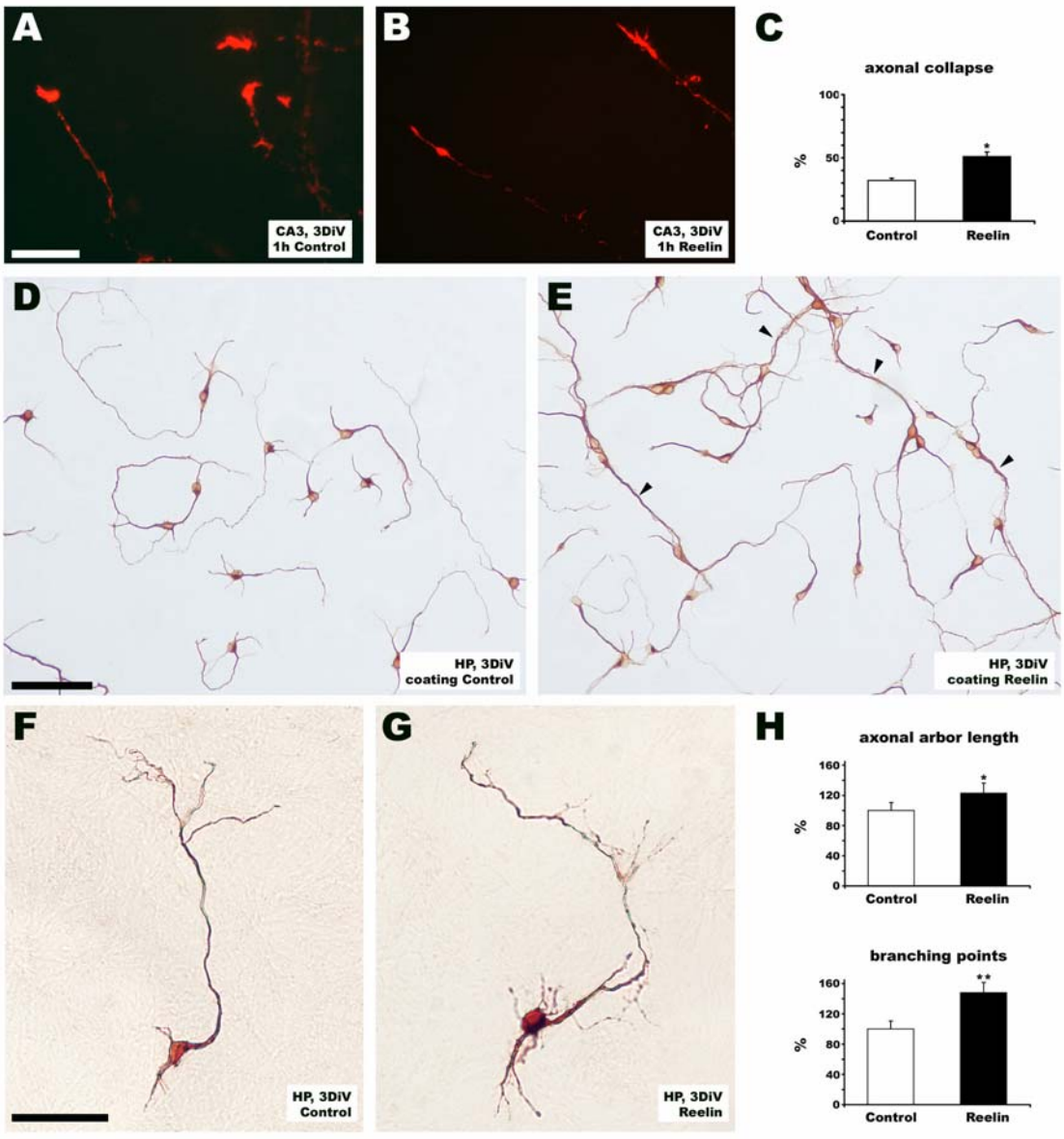
A
CA3, 3DiV
1h Control
B
CA3, 3DiV
1h Reelin
C
axonal collapse
100
50
0
%
*
Control
Reelin
D
HP, 3DiV
coating Control
E
HP, 3DiV
coating Reelin
F
HP, 3DiV
Control
G
HP, 3DiV
Reelin
H
axonal arbor length
160
120
80
40
0
%
*
Control
Reelin
branching points
160
120
80
40
0
%
**
Control
Reelin

Figure 8

Resultats (Capítol 2)

La Reelina indueix la desadhesió de les neurones de la zona subventricular i l'expressió de l'Egr-1 mitjançant l'activació de les proteïnes Erk1/2

Els resultats presentats en aquest capítol han estat enviats per a la seva publicació a la revista **Cerebral Cortex.**

Lluís Pujadas [1*], Sergi Simó [1*], Miguel F. Segura [2], Anna La Torre [1], José A. del Río [1], Jesús M. Ureña [1], Joan X. Comella [2], and Eduardo Soriano [1#]

[*] Aquests autors han contribuït amb igualtat al desenvolupament del treball presentat.

[1]**Laboratori de Neurobiologia**, Parc Científic de Barcelona-IRB i Departament de Biologia Cel·lular, Universitat de Barcelona, E-08028 Barcelona. [2]**Grup de Senyalitzacio i Apoptosi**, Departament de Ciències Mèdiques Bàsiques, Universitat de Lleida, E-08028 Lleida.

RESUM

La Reelina s'uneix als receptors VLDLR i ApoER2 receptors, induint la fosforilació de l'mDab1 i l'activació de la via de PI3K. En aquest treball es demostra que la Reelina activa la via de MAPK/ERK, que induiex la fosforilació de les proteïnes Erk1/2. La inhibició de les SFKs bloqueja l'activació d'Erk1/2 dependent de la Reelina. En cultius neuronals de mutants *mdab1* tampoc s'observa activació d'Erk1/2 depenent de la Reelina. Tot i detectar-se una lleugera activació de la proteïna Ras en resposta a la Reelina, el fet que la inhibició de la PI3K comporti el bloqueig de l'activació de la via d'ERK indica una senyalització creuada entre les vies d' ERK i de PI3K.

D'altra banda, el bloqueig de la via d'ERK no evita la migració en cadena de les neurones de la SVZ, però en canvi sí que n'inhibeix la desadhesió causada per tractaments amb Reelina. Finalment també es mostra que la Reelina indueix la transcripció del factor de transcripció Egr-1.

Els resultats presentats demostren que la Reelina indueix la senyalització de la via d'ERK de forma depenent de SFK/mDab1 i de PI3K, i que l'activació d'ERK és necessària per a l'activació transcripcional i la desadhesió de les neurones de la SVZ.

Resultats (Capítol 2)

Reelin induces the detachment of subventricular zone cells and the expression of the Egr-1 through Erk1/2 activation

ABSTRACT

Reelin binds to VLDLR and ApoER2 receptors, thereby inducing mDab1 phosphorylation and activation of the PI3K pathway. Here we demonstrate that Reelin activates the MAPK/ERK pathway, which leads to the phosphorylation of Erk1/2 proteins. The inhibition of SFKs blocked Reelin-dependent Erk1/2 activation. This was also shown in neuronal cultures from *mdab1*-deficient mice. Although Ras was weakly activated upon Reelin treatment, pharmacological inhibition of the PI3K pathway blocked Reelin-dependent ERK activation, which indicates cross-talk between the ERK and PI3K pathways.

We show that blockade of the ERK pathway does not prevent the chain migration of neurons from the SVZ but does inhibit the Reelin-dependent detachment of migrating neurons. We also show that Reelin induces the transcription of the Egr-1 transcription factor.

Our findings demonstrate that Reelin triggers ERK signaling in an SFK/mDab1- and PI3K-dependent manner, and that ERK activation is required for Reelin-dependent transcriptional activation and the detachment of neurons migrating from the SVZ.

INTRODUCTION

The migration and positioning of neurons are essential steps during the development of the Central Nervous System. Several molecules direct and modulate these migratory processes, including Netrins, Slits, Ephrins and Reelin, through the activation of complex signaling cascades (Hatten, 1999; Huber et al., 2003; Marin and Rubenstein, 2003).

Reelin is a 385 kD extracellular protein that controls neuronal migration in a variety of laminated brain regions (D'Arcangelo et al., 1997; Rice and Curran, 2001). *reeler* mice, defective in Reelin, show devastating layering alterations in many regions of the brain (Rice and Curran, 2001). Near its N-terminal region, Reelin contains a segment with no homology to other proteins that includes the CR-50 epitope, which is essential for Reelin functions (Kubo et al., 2002; Nakajima et al., 1997).

Although the exact functions of Reelin *in vivo* remain to be elucidated, it has been proposed that this protein is a stop signal or a detachment factor (Curran and D'Arcangelo, 1998; Dulabon et al., 2000; Frotscher, 1998; Hack et al., 2002). For instance, in the olfactory bulb (OB), Reelin produced by mitral cells induces the shift from tangential/chain to radial/individual neuronal migration and the detachment of precursors in the rostral migratory stream (RMS) originated in the subventricular zone (SVZ) (Alcantara et al., 1998; Hack et al., 2002).

Reelin binds the apolipoprotein E receptor 2 (ApoER2) and the very low density lipoprotein receptor (VLDLR), thereby triggering the phosphorylation of the adaptor protein mDab1 (Benhayon et al., 2003; D'Arcangelo et al., 1999; Hiesberger et al., 1999; Howell et al., 1999). The double mutant for *apoer2* and *vldlr* or the *mdab1* knock-out mouse have a migratory phenotype that is indistinguishable from that of *reeler* mice (Rice et al., 1998; Sheldon et al., 1997; Trommsdorff et al., 1999). Moreover, it has also been proposed that Reelin binds $\alpha 3\beta 1$ integrins and proteins of the Cadherin-related neuronal receptor (CNR) family (Dulabon et al., 2000; Senzaki et al., 1999).

mDab1 phosphorylation is performed by the Src family kinases (SFK), which are activated by Reelin in a mDab1-dependent manner, indicating that mDab1 is both a substrate and an activator of SFK in neurons (Arnaud et al., 2003; Bock and Herz, 2003). Moreover, tyrosine phosphorylation of mDab1 is essential for Reelin function (Howell et al., 2000).

Phosphorylated mDab1 binds to several intracellular signaling molecules, such as Nckβ, the Crk family of adapter proteins, the GTPase-activating protein Dab2IP or the p85 subunit of phosphatidylinositide 3 kinase (PI3K) (Bock et al., 2003; Homayouni et al., 2003; Huang et al., 2004; Pramatarova et al., 2003). The binding of mDab1 to p85 may activate the p110 PI3K subunit and the subsequent phosphorylation of Akt1 (Ballif et al., 2003; Beffert et al., 2002; Bock et al., 2003).

To further elucidate the functions of Reelin in neuronal migration and CNS development, we analyzed the downstream signaling events activated by this protein in neurons. We recently showed that Reelin induces the phosphorylation of the microtubule-associated protein 1B (MAP1B), and that *map1b*-deficient mice show *reeler*-like migration deficits (González-Billault et al., 2004). In the present study, we show that Reelin activates the MAPK Erk1 and Erk2 proteins, in a way that depends on both SFK and mDab1 phosphorylation. We also demonstrate a Reelin-dependent transcriptional activation of the early gene *egr-1* (also known as *zif268*, *krox-24*, *NGFI-A* or *zenk*), a transcriptional target of ERK (Harada et al., 1996; Hodge et al., 1998; Watson et al., 1997) and that the Reelin-induced detachment of cells migrating from the SVZ requires MAPK Erk1/2 activation.

RESULTS

Reelin induces Erk1 and Erk2 phosphorylation through MEK:

To test whether Reelin induces the activation of the ERK pathway, primary neuronal cultures from telencephalon were cultured for 4 days and treated with either recombinant Reelin supernatant or supernatant from control Mock-transfected cells. As reported (Howell et al., 1999), Reelin treatment for 15 minutes led to mDab1 phosphorylation, as detected by Western Blot (WB) with anti-phosphotyrosine antibody after mDab1 immunoprecipitation (Figure 1A). Reelin-treated cultures exhibited increased Akt1 phosphorylation, in agreement with Beffert et al. (2002). Cultures treated with control Mock supernatant did not exhibit phosphorylation of either the mDab1 or Akt1 protein (Figure 1A).

We next focused on the activation of p38, JNK, Erk1 and Erk2 proteins. Although we did not detect activation of p38 and JNK upon Reelin treatment (Figure 1A), strong Erk1/2 phosphorylation was found when neuronal cultures were treated with Reelin for 15 minutes, compared to the control Mock treatment (Figure 1B). Similar findings were observed when cultures were treated with partially purified Reelin (2ng/ml) (Figure 1C). Reelin-dependent Erk1/2 activation reached maximum levels between 5 and 15 minutes of treatment, and returned to basal activation states by 2 hours (Figure 1D). This short-term profile of Erk1/2 activation occurs after stimulation with numerous trophic factors, including GDNF, BDNF and NGF growth factors, and with axonal guidance cues such as Netrin-1 (Forcet et al., 2002; Gavalda et al., 2004; Harada et al., 2001; Trupp et al., 1999).

To confirm that Erk1/2 was dependent on Reelin, we used the CR-50 Reelin antibody (Nakajima et al., 1997). Reelin and control Mock supernatants were preincubated for 1 hour with the CR-50 antibody or with control mouse IgGs (0.1mg/ml). The Reelin supernatant preincubated with control IgGs led to Erk1/2 activation, while the CR-50-treated supernatants failed to induce the phosphorylation of these kinases (Figure 1E). We conclude that preincubation with the CR-50 antibody, but not with control IgGs, blocks Reelin-induced Erk1/2 activation. Taken together, these results indicate that Reelin signaling activates MAPK Erk1/2, but not JNK or p38.

To determine whether Reelin-dependent Erk1/2 phosphorylation is mediated through the classical MAPK activator MAPK kinase (MEK, MAPKK), we used the MEK specific inhibitor PD 98059. Pharmacological blockade of MEK inhibited Reelin-induced Erk1/2 phosphorylation (Figure 2A). Moreover, we also determined the activity of Erk1/2 on an artificial substrate, myelin basic protein (MBP), by the addition of γ-P^{32} (Aronica et al., 1997). A 2.1-fold increase in activity was detected in Reelin-treated samples in comparison with untreated, control Mock-treated or PD 98059-incubated samples (Figure 2B). These results show that Erk1/2 phosphorylation corresponds to an increased enzymatic activity and that the Reelin-induced activation of Erk1/2 is performed through MEK.

Reelin-dependent ERK phosphorylation requires SFK, mDab1 and PI3K activation:

Erk1/2 induction by many extracellular factors requires Ras activation. We thus studied whether this protein is activated by the Reelin signaling pathway. Reelin led to a weak activation of Ras at 5 min (1.5 fold) that was not significant in comparison to controls ($p>0.05$) (Figure 3A). No Ras activation was found at longer treatment times (15 minutes, unpublished data), indicating that this activation may not be the only signaling pathway through which Reelin induces ERK phosphorylation. We compared the activation of Ras and the phosphorylation levels induced by Reelin on Akt1 and Erk1/2 proteins with the activation levels induced by a classical factor, BDNF (Huang and Reichardt, 2003). BDNF-treated cultures exhibited robust Ras activation after 5 minutes (9-fold) (Figure 3A).

Consistent with this, the phosphorylation of Akt1 and Erk1/2 proteins was notably stronger in BDNF-treated samples than in Reelin-stimulated cultures (Figure 3B). Interestingly, the effect of Reelin on Akt1 and Erk1/2 phosphorylation levels was similar. These results indicate that Reelin induces similar, but not maximal, Akt1 and Erk1/2 activation levels, and that the contribution of Ras to Reelin-dependent Erk1/2 phosphorylation is limited.

Ras-independent Erk1/2 phosphorylation is involved in a number of events (Schmidt et al., 2004; Takeda et al., 1999; Wandzioch et al., 2004; Yart et al., 2002; York et al., 1998). To analyze the possible crosstalk between downstream Reelin-signaling events and Erk1/2 activation, we treated neuronal cultures with Reelin in the presence of pharmacological inhibitors for SFK, MEK or PI3K (see Figure 7). As expected, the blockade of SFK with PP2 inhibited Reelin-dependent mDab1 phosphorylation, which was not inhibited by the MEK inhibitor PD 98059 or by the PI3K inhibitor LY 294002 (Figure 3C). Similarly, activation of the downstream Reelin effector Akt1 was inhibited by SFK and by PI3K inhibitors (Figure 3E,F), but not by PD 98059 (Figure 3D). These results are consistent with previous studies showing that mDab1 phosphorylation requires the SFKs Fyn and Src (Arnaud et al., 2003; Bock et al., 2003) and indicate that the PI3K and ERK pathways may be two coordinated Reelin-dependent cascades downstream of mDab1.

We analyzed the effect of pharmacological kinase blockade on Erk1/2 activation. Treatment of cultures with PP2 blocked Reelin-dependent Erk1/2 phosphorylation (Figure 3E, left panel), indicating that SFK-dependent mDab1 phosphorylation is required for ERK activation. To confirm these findings, we cultured neurons from *mdab1*-deficient mice and the phosphorylation of Akt1 and Erk1/2 proteins was analyzed after Reelin stimulation. In agreement with other studies, Reelin did not phosphorylate Akt1 in *mdab1* -/- neuronal cultures (Figure 3E, right panel) (Beffert et al., 2002). Similarly, Reelin did not induce the phosphorylation of Erk1/2 in cultures lacking the mDab1 protein (Figure 3E, right panel).

Interestingly, the blockade of PI3K by LY 294002 also inhibited Reelin-induced Erk1/2 phosphorylation, as occurred with PD 98059, implying that PI3K activation is required for Reelin-induced Erk1/2 activation (Figure 3F). In contrast, LY 294002 did not affect the Erk1/2 phosphorylation induced by BDNF (Figure 3F), indicating that the crosstalk of the PI3K and ERK pathways is specific for the Reelin signaling cascade. Altogether, these results show that Reelin leads to the sequential activation of SFK and mDab1, and of the PI3K, which in turn activates in parallel both the Akt1 and the ERK pathway.

Reelin-induced Erk1/2 activation facilitates the detachment of SVZ cells:

Next, we analyzed the involvement of ERK in a Reelin-regulated migratory process, i.e. the detachment of neurons migrating from the RMS. Explants from postnatal SVZ were dissected out and cultured in Matrigel matrix. In these conditions, neuronal precursors migrate in chains, as occurs *in vivo* (Wichterle et al., 1997).

As described, the neurons migrated out of the explants and formed neuronal chains, which became disorganized after 3 days *in vitro* (DIV) (Figure 4A). We first studied whether proteins of the Reelin signaling pathway were expressed by SVZ neurons *in vitro*. Using immunofluorescence analysis of neuronal cultures, we found that chains of neurons migrating from the SVZ expressed mDab1, Erk, Ras (Supplemental Figure 1) as well as Akt1 (Unpublished data). We used PD 98059 to analyze the effect of ERK blockade on the detachment of SVZ cells *in vitro*. This treatment did not inhibit the migration of SVZ cells nor the formation of neuronal chains. In contrast, PD 98059 inhibited the detachment of the SVZ cells at 3 DIV (Figure 4A). Interestingly, PI3K inhibition with LY 294002 also blocked the detachment of the cultured SVZ neurons after 3 DIV (Figure 4A).

In agreement with a previous study, the incubation of SVZ explants with Reelin caused a dramatic detachment of SVZ neurons already after 2 DIV. (Figure 4B,C) (Hack et al., 2002). We also found that explants obtained from *reeler* mice showed a response to Reelin incubation that was indistinguishable from that of wild-type SVZ explants, indicating that wild-type and *reeler* SVZ cultured neurons show a similar response when exposed to Reelin (Unpublished data). Incubation of Reelin-treated SVZ explants with the MEK inhibitor PD 98059 prevented the Reelin-induced neuronal detachment of SVZ chains. Instead, neuronal chains treated with Reelin 50μM PD 98059 showed a compact appearance with virtually no detached neurons (Figure 4B).

Similar effects were observed with 25μM PD 98059, as shown by the lack of detached cells in Reelin-treated cultures, although the thickness of neuronal chains was thinner than in cultures incubated with 50μM PD 98059 (Supplemental Figure 2B). These findings indicate that ERK activation is required for Reelin-induced detachment of neurons migrating from the SVZ.

Blockade of SFK using PP2 also inhibited the Reelin-induced detachment of SVZ neurons, indicating that mDab1 phosphorylation may be crucial in this migration process (Figure 4D). To address this issue, SVZ explant cultures were prepared from *mdab1* -/- mice and were cultured with control Mock or Reelin-containing supernatants for 2 DIV. Reelin did not induce neuronal detachment in the absence of mDab1 protein (Figure 4D).

Finally, we also examined whether an independent activator of ERK (BDNF), induces the detachment of SVZ neuronal chains. Incubation with BDNF (25μg/ml) did not cause detachment, either in the absence or presence of LY 294002 (Supplemental Figure 3), suggesting that the Reelin-induced detachment of SVZ neurons occurs upon specific activation of the Reelin transduction cascade. Taken together, our results indicate that Reelin induces the detachment of migrating neurons from SVZ explants through activation of the Reelin signaling cascade, which includes SFKs, mDab1, PI3K and Erk1/2.

Reelin-dependent Erk1/2 activation up-regulates the expression of the transcription factor Egr-1

Activated Erk1/2 translocates to the nucleus and phosphorylates substrates like the transcription factor Elk1, which in turn enhances the expression of genes containing Serum Response Element (SRE) (Buchwalter et al., 2004; Shaw and Saxton, 2003). We next explored the possible regulation of ERK target genes by Reelin.

To test whether the ERK/Elk1 downstream effector, Egr-1 (Hodge et al., 1998), is regulated by Reelin, we analyzed Egr-1 expression in neuronal cultures. First, Reelin-treated cultured neurons (15 min) were incubated with anti-Erk1/2 phospho-specific antibodies. Reelin induced increased levels of phospho-Erk1/2 immunolabeling and translocation of phospho-Erk1/2 to the nucleus, both in telencephalic primary cultures (Figure 5A) and in dissociated SVZ neuronal cultures (Supplemental Figure 2A). Similarly, incubation with Reelin for 1 hour increased the expression of Egr-1 protein, as detected by immunofluorescence in neuronal cultures, which showed a nuclear localization (Figure 5B).

WB performed after Reelin treatment of neuronal cultures showed that Egr-1 was up-regulated in comparison with control Mock-treated or untreated cultures (Figure 6A). As expected for an early gene, increased protein levels were already observed at 30 min, reaching a maximal plateau at 60-90 minutes, decreasing thereafter (Figure 6B). To confirm that increased Egr-1 protein levels were due to transcriptional activation of *egr-1*, we performed a semi-quantitative RT-PCR analysis. Neuronal cultures showed a marked increase in *egr-1* mRNA after Reelin treatment for 30 minutes compared to cultures treated with control Mock supernatant (Figure 6C).

Moreover, pharmacological experiments showed that Reelin-induced Egr-1 protein levels were not up-regulated when PD 98059 or PP2 were present, thereby confirming that Egr-1 expression depends on Reelin-dependent SFK and ERK activation (Figure 6D). Finally, Egr-1 up-regulation was also blocked by LY 294002 (Figure 6D), thus reinforcing the notion of crosstalk between the PI3K and ERK pathways in the Reelin signaling cascade.

DISCUSSION

Here we demonstrate that, in addition to the PI3K/Akt1 pathway, Reelin activates the ERK pathway. Moreover, Reelin regulates the transcriptional activation of *egr-1* and cell adhesion of SVZ neurons during neuronal chain migration in an ERK-dependent manner. We also report a model in which SFK, and the PI3K and ERK pathways, cooperate to transduce Reelin signaling, thus involving Reelin receptors and the adaptor protein mDab1. These findings show a novel Reelin signaling mechanism (Figure 7).

Reelin stimulates the ERK pathway through activation of the PI3K signaling cascade

A previous study reports that Reelin does not stimulate the MAPK pathway (Ballif et al., 2003). The differences with our findings may result from the distinct cell preparations tested or the different Reelin preparations used. In our hands, however, Erk1/2 activation of telencephalic cultured neurons was observed after treatment with two Reelin preparations (Reelin-containing supernatant and partially purified Reelin) and was specifically inhibited by preincubation with the CR-50 blocking antibody and by SFK inhibitors, which block mDab1 phosphorylation.

Similarly, Erk1/2 activation was dependent on mDab1, which is an essential transducer of the Reelin signal. Moreover, although Reelin-induced Erk1/2 phosphorylation was not maximal (compared with BDNF treatment), it was comparable with the levels of Akt1 phosphorylation induced by Reelin. Finally, we show that Reelin induces nuclear translocation of phospho-Erk1/2, and that both Reelin-dependent transcriptional activation of *egr-1* and cell detachment of SVZ cells require Erk1/2 activation. Altogether, our findings support the view that ERK activation is a crucial event in the signaling cascade triggered by Reelin.

Our findings indicate that Reelin leads to weak Ras activation. Ras activation could be due to the classical Shc/Grb2/Sos induction (Hunter, 2000). However, we were unable to find consistent association of Shc with mDab1 after Reelin treatment (Unpublished data). Thus, although the participation of Shc in the Ras stimulation induced by Reelin cannot be discarded, we favor other mechanisms. For instance, similar to mDab1, the PTB domain of Shc may bind to the NPXY motifs of intracellular receptor tails, which would suggest a direct VLDLR/ApoER2 interaction with Shc, as occurs with the LDL receptor-related protein 1 (LRP1), another NPXY-containing lipoprotein receptor (Barnes et al., 2001). This process may be facilitated by receptor

multimerization since receptor clustering is required for Reelin signaling and mDab1 phosphorylation, and for the activation of the SFK and PI3K pathways (Strasser et al., 2004).

In neurons, the ERK pathway can be activated via Rap1, in a Ras-independent manner, leading to sustained ERK activity (Stork, 2005; York et al., 1998). Although it is known that Reelin weakly activates Rap1 (Ballif et al., 2004), we did not observe a sustained ERK activation upon Reelin stimulation. Our pharmacological experiments with the SFK inhibitor PP2 and the PI3K inhibitor LY 294002 indicate that the sequential SFK/mDab1/PI3K activation is the most relevant pathway that leads to MAPK-activation and phosphorylation of Erk1/2. Consistent with this view, similar crosstalk between the PI3K and the ERK pathways has been reported (e.g. in LPA and Erythropoietin signaling) (Schmidt et al., 2004; Takeda et al., 1999; Yart et al., 2002). Multiple models of crosstalk between the PI3K and ERK pathways have been observed, including a Ras-independent pathway leading to ERK activation mediated by PI3K and PKC (Takeda et al., 1999). The precise mechanism used by PI3K to activate the ERK pathway after treatment with Reelin remains to be clarified.

Reelin/ERK activation regulates the transcription of egr-1

Here we report that Reelin regulates transcriptional activation. This opens the possibility of new mechanisms for Reelin action in neural development. A number of genes show altered expression in *reeler* mice (Kuvbachieva et al., 2004). Several extracellular proteins, for instance Fibronectin or Tenascin-C, modulate gene expression (Ogawa et al., 2002; Ruiz et al., 2004). Interestingly, Netrin-1, another neuronal cue involved in migration and axonal growth, has been shown to activate the transcription factor NFAT (Graef et al., 2003).

Here we demonstrate that Reelin treatment of cultured neurons results in the up-regulation of another immediate early gene, the *egr-1* gene, through activation of the ERK pathway. Egr-1 target genes include a variety of factors such as other transcriptional regulatory proteins, the p35 neuron-specific activator of Cdk5, extracellular matrix proteins such as Collagen III and Fibronectin, the phosphatase PTEN, and the tumor suppressor protein p53 (Fu et al., 2003; Harada et al., 2001; Nair et al., 1997; Virolle et al., 2001). Moreover, constitutive expression of *egr-1* mRNA in brain is detected in several areas, including the neocortex, hippocampus, entorhinal cortex and cerebellum, all of which are severely targeted in *reeler* and *reeler*-like mutants (Bozon et al., 2002; Rice and Curran, 2001).

egr-1 transcription in neurons is dynamically regulated by a variety of pharmacological and physiological stimuli (Beckmann and Wilce, 1997). Interestingly, this gene is essential, in an ERK-dependent manner, for long-term potentiation (LTP) and long-term memory, as well as for memory reconsolidation (Jones et al., 2001; Lee et al., 2004). On its own, Erk1 also participates in the regulation of long-term adaptive changes, as reported in studies of the *erk1*-deficient mouse (Mazzucchelli et al., 2002; Pages et al., 1999).

Moreover, Egr-1 is strongly down-regulated in memory-deficient doubly transgenic mice over-expressing APP and PS1, a mouse model for Alzheimer's disease (Dickey et al., 2003). Similarly, Reelin and the Reelin receptors VLDLR/ApoER2 are also involved in memory formation and LTP (Beffert et al., 2005; Larson et al., 2003; Weeber et al., 2002). On the basis of our data, we propose that ERK/Egr-1 activation is one of the signaling events by which Reelin controls memory formation in the mature brain.

Reelin-dependent ERK activation is required for the detachment of neurons migrating from the SVZ.

Reelin induces the detachment of neurons migrating from the SVZ *in vitro* (Hack et al., 2002). This finding agrees with the observations *in vivo* showing that the lack of Reelin (Hack et al., 2002) or the adaptor mDab1 (Unpublished data) leads to the accumulation of SVZ-derived olfactory neurons before entry to the OB. These data have led to the notion that Reelin in the OB controls the change of neuronal chain migration to radial glia-guided migration and the subsequent detachment of migrating neurons. Here we have shown that the Reelin-induced detachment of migrating neurons in SVZ-derived explants is induced through ERK activation and can be prevented by ERK inhibitors, indicating that MAPK activation participates in the biological functions of Reelin.

The observation that the addition of ERK inhibitors alone also increases the thickness of migrating neuronal chains and alters their adhesion implies that ERK is involved in the regulation of neuron-to-neuron adhesion during neuronal migration, at least in neurons fated to the OB. Our pharmacological and genetic experiments also show that the Reelin-induced detachment of SVZ neurons also involves mDab1 and PI3K phosphorylation. Thus, together with a previous study showing that SFK and activation of atypical PKC are necessary for Reelin-dependent neuronal migration in an *in vitro* model of corticogenesis (Jossin et al., 2003), our results indicate that a complex scenario of signaling cascades is required for Reelin-dependent neuronal migration, which includes ERK activation.

MATERIALS AND METHODS

Antibodies and reagents:

Anti-phospho-p44/42MAP Kinase (Thr202/Tyr204) and anti-phospho-Akt (Ser473) antibodies were purchased from Cell Signaling Technology; antibodies against Egr-1 (588) and Akt1 (C-20) were from Santa Cruz Biotechnology; mouse monoclonal antibody against Erk (pan Erk) was from Transduction Laboratories, mouse monoclonal antibody against β Tubulin isotype III was from Sigma (clone SDL.3D10) or from Covance (TUJ1); anti-mDab1 antibody was purchased from ExAlpha Biologicals; anti-phospho-tyrosine (clone 4G10) was from Upstate Biotechnology; anti-pan-Ras (Ab-3) antibody was from Oncogene; affinity purified antibody anti-mDab1 (B3) used in WBs was a generous gift from J.A. Cooper (Seattle, USA); mouse monoclonal anti-Reelin antibody (clone G10) was provided by A.M. Goffinet and mouse monoclonal anti-Reelin blocking antibody (clone CR50) was provided by K. Nakajima. Phalloidin-Texas Red-conjugated was provided by Sigma. Alexa Fluor 488 goat anti-mouse IgG (H+L) and Alexa Fluor 488 $F(ab')_2$ fragment of goat anti-rabbit IgG (H+L) were from Molecular Probes. Goat-anti-mouse-HRP and rabbit-anti-goat-HRP secondary antibodies used in WB were purchased from DAKO; goat-anti-rabbit-HRP was from Sigma.

Protein G-Sepharose 4B Fast Flow was purchased from Sigma and Glutathion-Sepharose 4B beads from Amersham. rhBDNF was from Promega. All inhibitors used in the experiments were purchased from Calbiochem: PP2, PD 98059 and LY 294002.

Reelin production and neuronal primary culture treatment:

Transfection of 293T cells with full-length mouse Reelin expression construct pCrl or control Mock vector (pcDNA3.1) was done using Lipofectamine (Invitrogen) (D'Arcangelo et al., 1997). The culture medium was replaced with Opti-MEM I medium (GibcoBRL) the following day. Cells were maintained for 4 days and the conditioned medium was collected, filtered through 0.2 μm membranes (Orange Scientific), concentrated 60-fold using Amicon Ultra-15 100,000 MWCO (Millipore) filters, and maintained at 4ºC. Reelin production was confirmed by WB using anti-Reelin (G10) antibody. Control Mock supernatants were treated in the same way. Quantification of Reelin-containing supernatants was performed by Comassie Blue gel staining using Laminin (Sigma) as protein standard; band intensities were studied using GeneTools software. About 40ng/ml of full-length Reelin and cleaved products were obtained. Reelin working concentration was around 2ng/ml.

Telencephalic neurons were obtained from E16 mouse embryos (OF1 mice, Charles River Laboratories). The experiments were carried out in accordance with the European Community Council Directive and the National Institute of Health guidelines for the care and use of laboratory animals. Brains were dissected in PBS containing 0.6% glucose, and were trypsinized and mechanically dissociated. Cells were cultured in 6-well plates (Nunc) coated with Poly-D-Lysine at a density of 3-5 million per well and maintained in Neurobasal medium (GibcoBRL) with B27 supplement (GibcoBRL). Prior to treatment, neuronal cultures were starved using Neurobasal-based medium. Reelin or control Mock conditioned media were then used for treatment at a 1/20 dilution from the stock. Partially purified recombinant Reelin was a generous gift from Drs. T. Curran and D. Benhayon (Memphis, USA); Reelin, used at a concentration of 2ng/ml (including the full-length and cleavage fragments), was produced in 293T cells and the supernatant brought to 45% saturation with a solution of saturated ammonium

sulfate (4.1M), centrifuged, air-dried and resuspended in 10mM HEPES (pH 7.5) containing 10% glycerol before storage at -80 ºC (Keshvara et al., 2001).

For pharmacological inhibition of protein kinases, 1 hour before treatment, cultures were supplemented with 10μM of PP2, 50μM of LY 294002, or 50μM of PD 98059 to inhibit SFK, PI3K or MEK, respectively.

Cultures from *mdab1* -/- mice were obtained from E16 mouse embryos and treated in a similar way as the wild-type animals described previously.

For blocking experiments, Reelin and control Mock supernatants were preincubated for 1 hour with the CR-50 antibody or with control mouse IgGs (0.1mg/ml) at 4ºC, and then tested in cultured neurons. rhBDNF treatments were performed at a concentration of 25μg/ml.

Erk kinase assay:

Stimulated cortical neurons were washed with PBS and lysed directly on the plate in radioimmunoprecipitation assay (RIPA) buffer (50mM Tris-Cl (pH 8.0) 150mM NaCl, 1.0% Nonidet P-40, 0.5% sodium deoxycholate and 0.1% sodium dodecyl sulfate). Lysates were incubated with an agarose-conjugated antibody directed against ERK2 (Santa Cruz Biotechnology) overnight at 4°C. Immunoprecipitates were washed once in RIPA buffer and twice in assay buffer (25mM Tris-Cl [pH 7.4], 5mM b-glycerophosphate, 2mM dithiothreitol, 0.1mM Na3VO4, 10mM MgCl2 and 1mM phenylmethylsulfonyl fluoride). Reactions were initiated by resuspending immunoprecipitates in 30 μl of assay buffer containing 20μM unlabeled ATP, 5 μCi of [γ-^{32}P] ATP, and 5 μg of myelin basic protein (MBP; UBI). Reaction mixtures were incubated at 30°C for 15 min and were terminated by the addition of 7 μl of 5× Laemmli sample buffer. Reaction products were electrophoresed on a 12% polyacrylamide protein gel and transferred to an Immobilon membrane. Membranes were dried, exposed overnight to a phosphorimager screen (Fuji), and 32P-MBP levels were quantitated using a Fuji BAS1000 phosphorimager and PCBAS 2.0 software (Fuji Photo Film Co. Ltd.).

Immunoprecipitation, pull-down assays and WB:

For WBs, lysates were collected in hot (95ºC) Loading Buffer (75mM Tris (pH 6.5), 0.5mM β-mercaptoethanol, 0.5% SDS, 5% glycerol and 0.0125% bromophenol blue), boiled for 10 minutes at 95ºC and stored at -20ºC. For immunoprecipitation or activity assays, cells were collected in Lysis Buffer (Hepes 50mM (pH 7.5), 150mM sodium chloride, 1.5mM magnesium chloride, 1mM EGTA, 10% glycerol and 1% Triton X-100) containing Complete Mini protease inhibitor cocktail (Roche, cat. 1836153) and phosphatase inhibitors (10mM tetra-sodium pyrophosphate, 200μM sodium orthovanadate and 10mM sodium fluoride); insoluble debris were removed by centrifugation (30 min, 16000*g*) and supernatants were stored at -80ºC.

For immunoprecipitation, samples were incubated with the primary antibody overnight (o/n) at 4ºC (4μg/sample). Protein G-Sepharose beads were added for 90 min at 4ºC, recovered by centrifugation, washed 3 times with Lysis Buffer and boiled for 10 min at 95ºC in Loading Buffer before WB processing.

Pull-down assays of activated Ras were performed using purified RBD-GST (GST-conjugated Ras Binding Domain of Raf1) as described (de Rooij and Bos, 1997). 15 μg of protein was incubated o/n in Lysis Buffer with Glutathion sepharose 4B beads (Amersham) prebound to RBD-GST for 2.5 hours. The beads were then recovered by

centrifugation, washed and boiled in Loading Buffer. Immunoprecipitates, pull-down samples and cell lysates were resolved by SDS-polyacrylamide gels and transferred onto nitrocellulose membranes.

Nitrocellulose membranes were blocked for 1 hour at room temperature (RT) in TBST (Tris 10mM pH 7.4, sodium chloride 140mM (TBS) with 0.1% Tween 20) containing 5% non-fat milk. Primary antibodies were incubated for 90 min in TBST-0.02% azide (anti-phospho-p44/42MAP Kinase (Thr202/Tyr204) 1:5000, anti-phospho-Akt (Ser473) 1:5000, anti-Egr-1 (588) 1:1000, anti-Akt1 (C-20) 1:5000, anti-Erk (pan Erk) 1:5000, anti-beta-tubulin isotype III (clone SDL.3D10) 1:20000, anti-phospho-tyrosine (clone 4G10) 1:5000, anti-mDab1 (B3) 1:3000, anti-Reelin antibody (clone G10) 1:10000). After incubation with secondary HRP-labeled antibodies for 1 hour at RT (diluted 1:5000 in TBST-5% non-fat milk), membranes were developed with the ECL+ system (Amersham).

Semi-quantitative RT-PCR

cDNA was reverse-transcribed from RNA extracted from neuronal cultures treated with Reelin or control Mock supernatants using Oligo (dT)15 (Promega cat. C1101). Care was taken to arrest amplification during the linear phase.

Multiplex PCR was performed by co-amplification of egr-1 and the house- keeping gene gapdh. Primers used to amplify 505 bp and 435 bp specific fragments corresponding to egr-1 and gadph, respectively, are described below: Egr-1-F: 5'-ATCCCAGCCAAACGACTCG-3', Egr-1-R: 5'-GTGGAGTGAGCGAAGGCTGCT-3', GAPDH-(+): 5'-GGCCCCTCTGGAAAGCTGTGG-3', GAPDH-(-): 5'-CCTTGGAGGCCATGTAGGCCAT-3'.

Pictures were taken using a Gene Genius Bio Imaging System and band intensities were studied using GeneTools software, both from Syngene.

SVZ explant and primary cultures:

Explants from the SVZ of the anterior horn of the lateral ventricle were dissected from P5 OF1 mice (Charles River Laboratories) and cultured for 2-3 days in Matrigel matrix (Bioscience), as described (Wichterle et al., 1997). Explants were maintained in serum-free Neurobasal (GibcoBRL) medium with 2mM L-glutamine, 30 mM D-(+)-glucose, 5mM sodium bicarbonate, Penicillin/Streptomycin (100U/ml, 100µg/ml) and B27 supplement diluted 1:50 (GibcoBRL). SVZ explants, when indicated, were cultured with control Mock (control) or Reelin-containing media at 1/20 dilution from the stock. Some cultures were incubated with 25 or 50µM of PD 98059. LY 294002 was used at 50µM and SFK inhibitor was used 10µM̃. Other SVZ explants were cultured with 25µg/µl BDNF. Fixation was performed at 2-3 days using 4% paraformaldehyde in PB for 45 minutes at 4ºC, and cultures were immunolabeled for β-III-tubulin.

For SVZ dissociated cultures, cells were cultured in coverslips coated with Poly-D-Lysine and Matrigel at a density of 70.000 cells per coverslip.

Quantification of detached cells was done as in Hack *et al.* (2002). Thus random fields of control Mock-treated, Reelin-treated or untreated SVZ explants were taken and detached cells were harvested at the microscope (40x objective) and percentages of detached cells were calculated. Five independent experiments were counted (21-28 explants per group).

Immunofluorescence:

Cultured neurons or explants *in vitro* were fixed with 4% paraformaldehyde and blocked with 0.2% gelatin and 10% Normal Goat Serum (NGS) for 1 hour at RT. Anti-β-III-tubulin (TUJ1), anti-phospho-p44/42MAP Kinase, anti-Egr-1, anti-mDab1, anti-pan-Erk, anti-pan-Ras antibodies or phalloidin-Texas Red-conjugated were then used at 1:3000, 1:500, 1:200, 1:300, 1:500, 1:100 or 1:500 dilution, respectively. Secondary Alexa Fluor 488-tagged antibodies were incubated at a 1:500 dilution for 2 hours. Cultures were mounted with Mowiol (Calbiochem) and visualized under an Olympus Fluoview FV300 confocal microscope.

Statistics:

Statistical significances were tested using the Statgraphics Plus 4.0 (including an ANOVA test).

Online Supplemental Material:

Supplemental Figure 1 shows expression of mDab1, pan-Erk and Ras in SVZ cells.

Supplemental Figure 2 shows increased phospho-Erk immunostaining in SVZ cells nuclei after Reelin treament and dose response of cells migrating from SVZ explants to MEK inhibition.

Supplemental Figure 3 shows that BDNF does not induce detachment of SVZ neurons.

ABBREVIATIONS

ApoER2	apolipoprotein E receptor 2
BDNF	brain-derived neurotrophic factor
DIV	days *in vitro*
Egr-1	early growth response 1
Erk	extracellular signal-regulated kinase
MAPK	mitogen-activated protein kinase
OB	olfactory bulb
PI3K	phosphatidylinositide 3 kinase
RMS	rostral migratory stream
SFK	Src family kinases
SVZ	subventricular zone
VLDLR	very low-density lipoprotein receptor
WB	Western Blot

ACKNOWLEDGEMENTS

We thank Drs. J. A. Cooper, K. Nakajima, T. Curran, D. Benhayon and A. M. Goffinet for generously providing the materials used in this study, M.J. Barallobre for help in preliminary experiments, C. Solé for scientific assistance and T. Yates for technical assistance. L. Pujadas, S. Simó and M. F. Segura hold postgraduate fellowships from the Spanish Ministry of Education and Science. J. M. Ureña is a recipient of a "Ramón y Cajal" contract from the Spanish Ministry of Education and Science. This work was supported by grants from La Caixa Foundation, the Pfizer Foundation and the Spanish Ministry of Education and Science (SAF2001-3290, SAF2004-07929, FIS-PI042280 and BFI2003-03594) to E. Soriano, J.A. Del Río and J.M. Ureña, and from the Spanish Ministry of Health (FIS), La Caixa Foundation (*Convocatòria de Malalties Neurodegeneratives*), and the Government of Catalonia (*Suport als Grups de Recerca, and Distinció Joves Investigadors*) to J. X. Comella.

REFERENCES

Alcantara, S., M. Ruiz, G. D'Arcangelo, F. Ezan, L. de Lecea, T. Curran, C. Sotelo, and E. Soriano. 1998. Regional and cellular patterns of reelin mRNA expression in the forebrain of the developing and adult mouse. *J Neurosci*. 18:7779-99.

Arnaud, L., B.A. Ballif, E. Forster, and J.A. Cooper. 2003. Fyn tyrosine kinase is a critical regulator of disabled-1 during brain development. *Curr Biol*. 13:9-17.

Aronica, S.M., A.C. Gingras, N. Sonenberg, S. Cooper, N. Hague, and H.E. Broxmeyer. 1997. Macrophage inflammatory protein-1alpha and interferon-inducible protein 10 inhibit synergistically induced growth factor stimulation of MAP kinase activity and suppress phosphorylation of eukaryotic initiation factor 4E and 4E binding protein 1. *Blood*. 89:3582-95.

Ballif, B.A., L. Arnaud, W.T. Arthur, D. Guris, A. Imamoto, and J.A. Cooper. 2004. Activation of a Dab1/CrkL/C3G/Rap1 pathway in Reelin-stimulated neurons. *Curr Biol*. 14:606-10.

Ballif, B.A., L. Arnaud, and J.A. Cooper. 2003. Tyrosine phosphorylation of Disabled-1 is essential for Reelin-stimulated activation of Akt and Src family kinases. *Brain Res Mol Brain Res*. 117:152-9.

Barnes, H., B. Larsen, M. Tyers, and P. van Der Geer. 2001. Tyrosine-phosphorylated low density lipoprotein receptor-related protein 1 (Lrp1) associates with the adaptor protein SHC in SRC-transformed cells. *J Biol Chem*. 276:19119-25.

Beckmann, A.M., and P.A. Wilce. 1997. Egr transcription factors in the nervous system. *Neurochem Int*. 31:477-510; discussion 517-6.

Beffert, U., G. Morfini, H.H. Bock, H. Reyna, S.T. Brady, and J. Herz. 2002. Reelin-mediated signaling locally regulates protein kinase B/Akt and glycogen synthase kinase 3beta. *J Biol Chem*. 277:49958-64.

Beffert, U., E.J. Weeber, A. Durudas, S. Qiu, I. Masiulis, J.D. Sweatt, W.P. Li, G. Adelmann, M. Frotscher, R.E. Hammer, and J. Herz. 2005. Modulation of synaptic plasticity and memory by Reelin involves differential splicing of the lipoprotein receptor Apoer2. *Neuron*. 47:567-79.

Benhayon, D., S. Magdaleno, and T. Curran. 2003. Binding of purified Reelin to ApoER2 and VLDLR mediates tyrosine phosphorylation of Disabled-1. *Brain Res Mol Brain Res*. 112:33-45.

Bock, H.H., and J. Herz. 2003. Reelin activates SRC family tyrosine kinases in neurons. *Curr Biol*. 13:18-26.

Bock, H.H., Y. Jossin, P. Liu, E. Forster, P. May, A.M. Goffinet, and J. Herz. 2003. Phosphatidylinositol 3-kinase interacts with the adaptor protein Dab1 in response to Reelin signaling and is required for normal cortical lamination. *J Biol Chem*. 278:38772-9.

Bozon, B., S. Davis, and S. Laroche. 2002. Regulated transcription of the immediate-early gene Zif268: mechanisms and gene dosage-dependent function in synaptic plasticity and memory formation. *Hippocampus*. 12:570-7.

Buchwalter, G., C. Gross, and B. Wasylyk. 2004. Ets ternary complex transcription factors. *Gene*. 324:1-14.

Curran, T., and G. D'Arcangelo. 1998. Role of reelin in the control of brain development. *Brain Res Brain Res Rev*. 26:285-94.

D'Arcangelo, G., R. Homayouni, L. Keshvara, D.S. Rice, M. Sheldon, and T. Curran. 1999. Reelin is a ligand for lipoprotein receptors. *Neuron*. 24:471-9.

D'Arcangelo, G., K. Nakajima, T. Miyata, M. Ogawa, K. Mikoshiba, and T. Curran. 1997. Reelin is a secreted glycoprotein recognized by the CR-50 monoclonal antibody. *J Neurosci*. 17:23-31.

de Rooij, J., and J.L. Bos. 1997. Minimal Ras-binding domain of Raf1 can be used as an activation-specific probe for Ras. *Oncogene*. 14:623-5.

Dickey, C.A., J.F. Loring, J. Montgomery, M.N. Gordon, P.S. Eastman, and D. Morgan. 2003. Selectively reduced expression of synaptic plasticity-related genes in amyloid precursor protein + presenilin-1 transgenic mice. *J Neurosci*. 23:5219-26.

Dulabon, L., E.C. Olson, M.G. Taglienti, S. Eisenhuth, B. McGrath, C.A. Walsh, J.A. Kreidberg, and E.S. Anton. 2000. Reelin binds alpha3beta1 integrin and inhibits neuronal migration. *Neuron*. 27:33-44.

Forcet, C., E. Stein, L. Pays, V. Corset, F. Llambi, M. Tessier-Lavigne, and P. Mehlen. 2002. Netrin-1-mediated axon outgrowth requires deleted in colorectal cancer-dependent MAPK activation. *Nature*. 417:443-7.

Frotscher, M. 1998. Cajal-Retzius cells, Reelin, and the formation of layers. *Curr Opin Neurobiol*. 8:570-5.

Fu, M., X. Zhu, J. Zhang, J. Liang, Y. Lin, L. Zhao, M.U. Ehrengruber, and Y.E. Chen. 2003. Egr-1 target genes in human endothelial cells identified by microarray analysis. *Gene*. 315:33-41.

Gavalda, N., E. Perez-Navarro, E. Gratacos, J.X. Comella, and J. Alberch. 2004. Differential involvement of phosphatidylinositol 3-kinase and p42/p44 mitogen activated protein kinase pathways in brain-derived neurotrophic factor-induced trophic effects on cultured striatal neurons. *Mol Cell Neurosci*. 25:460-8.

González-Billault, C., J.A. Del Río, J.M. Ureña, E.M. Jiménez-Mateos, M.J. Barallobre, M. Pascual, L. Pujadas, S. Simó, A. La Torre, R. Gavin, F. Wandosell, E. Soriano, and J. Ávila. 2004. A role of MAP1B in Reelin-dependent Neuronal Migration. *Cerebral Cortex*.

Graef, I.A., F. Wang, F. Charron, L. Chen, J. Neilson, M. Tessier-Lavigne, and G.R. Crabtree. 2003. Neurotrophins and netrins require calcineurin/NFAT signaling to stimulate outgrowth of embryonic axons. *Cell*. 113:657-70.

Hack, I., M. Bancila, K. Loulier, P. Carroll, and H. Cremer. 2002. Reelin is a detachment signal in tangential chain-migration during postnatal neurogenesis. *Nat Neurosci*. 5:939-45.

Harada, S., R.M. Smith, J.A. Smith, M.F. White, and L. Jarett. 1996. Insulin-induced egr-1 and c-fos expression in 32D cells requires insulin receptor, Shc, and mitogen-activated protein kinase, but not insulin receptor substrate-1 and phosphatidylinositol 3-kinase activation. *J Biol Chem*. 271:30222-6.

Harada, T., T. Morooka, S. Ogawa, and E. Nishida. 2001. ERK induces p35, a neuron-specific activator of Cdk5, through induction of Egr1. *Nat Cell Biol*. 3:453-9.

Hatten, M.E. 1999. Central nervous system neuronal migration. *Annu Rev Neurosci*. 22:511-39.

Hiesberger, T., M. Trommsdorff, B.W. Howell, A. Goffinet, M.C. Mumby, J.A. Cooper, and J. Herz. 1999. Direct binding of Reelin to VLDL receptor and ApoE receptor 2 induces tyrosine phosphorylation of disabled-1 and modulates tau phosphorylation. *Neuron*. 24:481-9.

Hodge, C., J. Liao, M. Stofega, K. Guan, C. Carter-Su, and J. Schwartz. 1998. Growth hormone stimulates phosphorylation and activation of elk-1 and expression of c-

fos, egr-1, and junB through activation of extracellular signal-regulated kinases 1 and 2. *J Biol Chem*. 273:31327-36.

Homayouni, R., S. Magdaleno, L. Keshvara, D.S. Rice, and T. Curran. 2003. Interaction of Disabled-1 and the GTPase activating protein Dab2IP in mouse brain. *Brain Res Mol Brain Res*. 115:121-9.

Howell, B.W., T.M. Herrick, and J.A. Cooper. 1999. Reelin-induced tryosine phosphorylation of disabled 1 during neuronal positioning. *Genes Dev*. 13:643-8.

Howell, B.W., T.M. Herrick, J.D. Hildebrand, Y. Zhang, and J.A. Cooper. 2000. Dab1 tyrosine phosphorylation sites relay positional signals during mouse brain development. *Curr Biol*. 10:877-85.

Huang, E.J., and L.F. Reichardt. 2003. Trk receptors: roles in neuronal signal transduction. *Annu Rev Biochem*. 72:609-42.

Huang, Y., S. Magdaleno, R. Hopkins, C. Slaughter, T. Curran, and L. Keshvara. 2004. Tyrosine phosphorylated Disabled 1 recruits Crk family adapter proteins. *Biochem Biophys Res Commun*. 318:204-12.

Huber, A.B., A.L. Kolodkin, D.D. Ginty, and J.F. Cloutier. 2003. Signaling at the growth cone: ligand-receptor complexes and the control of axon growth and guidance. *Annu Rev Neurosci*. 26:509-63.

Hunter, T. 2000. Signaling--2000 and beyond. *Cell*. 100:113-27.

Jones, M.W., M.L. Errington, P.J. French, A. Fine, T.V. Bliss, S. Garel, P. Charnay, B. Bozon, S. Laroche, and S. Davis. 2001. A requirement for the immediate early gene Zif268 in the expression of late LTP and long-term memories. *Nat Neurosci*. 4:289-96.

Jossin, Y., M. Ogawa, C. Metin, F. Tissir, and A.M. Goffinet. 2003. Inhibition of SRC family kinases and non-classical protein kinases C induce a reeler-like malformation of cortical plate development. *J Neurosci*. 23:9953-9.

Keshvara, L., D. Benhayon, S. Magdaleno, and T. Curran. 2001. Identification of reelin-induced sites of tyrosyl phosphorylation on disabled 1. *J Biol Chem*. 276:16008-14.

Kubo, K., K. Mikoshiba, and K. Nakajima. 2002. Secreted Reelin molecules form homodimers. *Neurosci Res*. 43:381-8.

Kuvbachieva, A., A.M. Bestel, F. Tissir, I. Maloum, F. Guimiot, N. Ramoz, F. Bourgeois, J.M. Moalic, A.M. Goffinet, and M. Simonneau. 2004. Identification of a novel brain-specific and Reelin-regulated gene that encodes a protein colocalized with synapsin. *Eur J Neurosci*. 20:603-10.

Larson, J., J.S. Hoffman, A. Guidotti, and E. Costa. 2003. Olfactory discrimination learning deficit in heterozygous reeler mice. *Brain Res*. 971:40-6.

Lee, J.L., B.J. Everitt, and K.L. Thomas. 2004. Independent cellular processes for hippocampal memory consolidation and reconsolidation. *Science*. 304:839-43.

Marin, O., and J.L. Rubenstein. 2003. Cell migration in the forebrain. *Annu Rev Neurosci*. 26:441-83.

Mazzucchelli, C., C. Vantaggiato, A. Ciamei, S. Fasano, P. Pakhotin, W. Krezel, H. Welzl, D.P. Wolfer, G. Pages, O. Valverde, A. Marowsky, A. Porrazzo, P.C. Orban, R. Maldonado, M.U. Ehrengruber, V. Cestari, H.P. Lipp, P.F. Chapman, J. Pouyssegur, and R. Brambilla. 2002. Knockout of ERK1 MAP kinase enhances synaptic plasticity in the striatum and facilitates striatal-mediated learning and memory. *Neuron*. 34:807-20.

Nair, P., S. Muthukkumar, S.F. Sells, S.S. Han, V.P. Sukhatme, and V.M. Rangnekar. 1997. Early growth response-1-dependent apoptosis is mediated by p53. *J Biol Chem*. 272:20131-8.

Nakajima, K., K. Mikoshiba, T. Miyata, C. Kudo, and M. Ogawa. 1997. Disruption of hippocampal development in vivo by CR-50 mAb against reelin. *Proc Natl Acad Sci U S A*. 94:8196-201.

Ogawa, E., Y. Saito, K. Kuwahara, M. Harada, Y. Miyamoto, I. Hamanaka, N. Kajiyama, N. Takahashi, T. Izumi, R. Kawakami, I. Kishimoto, Y. Naruse, N. Mori, and K. Nakao. 2002. Fibronectin signaling stimulates BNP gene transcription by inhibiting neuron-restrictive silencer element-dependent repression. *Cardiovasc Res*. 53:451-9.

Pages, G., S. Guerin, D. Grall, F. Bonino, A. Smith, F. Anjuere, P. Auberger, and J. Pouyssegur. 1999. Defective thymocyte maturation in p44 MAP kinase (Erk 1) knockout mice. *Science*. 286:1374-7.

Pramatarova, A., P.G. Ochalski, K. Chen, A. Gropman, S. Myers, K.T. Min, and B.W. Howell. 2003. Nck beta interacts with tyrosine-phosphorylated disabled 1 and redistributes in Reelin-stimulated neurons. *Mol Cell Biol*. 23:7210-21.

Rice, D.S., and T. Curran. 2001. Role of the reelin signaling pathway in central nervous system development. *Annu Rev Neurosci*. 24:1005-39.

Rice, D.S., M. Sheldon, G. D'Arcangelo, K. Nakajima, D. Goldowitz, and T. Curran. 1998. Disabled-1 acts downstream of Reelin in a signaling pathway that controls laminar organization in the mammalian brain. *Development*. 125:3719-29.

Ruiz, C., W. Huang, M.E. Hegi, K. Lange, M.F. Hamou, E. Fluri, E.J. Oakeley, R. Chiquet-Ehrismann, and G. Orend. 2004. Differential gene expression analysis reveals activation of growth promoting signaling pathways by tenascin-C. *Cancer Res*. 64:7377-85.

Schmidt, E.K., S. Fichelson, and S.M. Feller. 2004. PI3 kinase is important for Ras, MEK and Erk activation of Epo-stimulated human erythroid progenitors. *BMC Biol*. 2:7.

Senzaki, K., M. Ogawa, and T. Yagi. 1999. Proteins of the CNR family are multiple receptors for Reelin. *Cell*. 99:635-47.

Shaw, P.E., and J. Saxton. 2003. Ternary complex factors: prime nuclear targets for mitogen-activated protein kinases. *Int J Biochem Cell Biol*. 35:1210-26.

Sheldon, M., D.S. Rice, G. D'Arcangelo, H. Yoneshima, K. Nakajima, K. Mikoshiba, B.W. Howell, J.A. Cooper, D. Goldowitz, and T. Curran. 1997. Scrambler and yotari disrupt the disabled gene and produce a reeler-like phenotype in mice. *Nature*. 389:730-3.

Stork, P.J. 2005. Directing NGF's actions: it's a Rap. *Nat Cell Biol*. 7:338-9.

Strasser, V., D. Fasching, C. Hauser, H. Mayer, H.H. Bock, T. Hiesberger, J. Herz, E.J. Weeber, J.D. Sweatt, A. Pramatarova, B. Howell, W.J. Schneider, and J. Nimpf. 2004. Receptor clustering is involved in Reelin signaling. *Mol Cell Biol*. 24:1378-86.

Takeda, H., T. Matozaki, T. Takada, T. Noguchi, T. Yamao, M. Tsuda, F. Ochi, K. Fukunaga, K. Inagaki, and M. Kasuga. 1999. PI 3-kinase gamma and protein kinase C-zeta mediate RAS-independent activation of MAP kinase by a Gi protein-coupled receptor. *Embo J*. 18:386-95.

Trommsdorff, M., M. Gotthardt, T. Hiesberger, J. Shelton, W. Stockinger, J. Nimpf, R.E. Hammer, J.A. Richardson, and J. Herz. 1999. Reeler/Disabled-like

disruption of neuronal migration in knockout mice lacking the VLDL receptor and ApoE receptor 2. *Cell*. 97:689-701.

Trupp, M., R. Scott, S.R. Whittemore, and C.F. Ibanez. 1999. Ret-dependent and -independent mechanisms of glial cell line-derived neurotrophic factor signaling in neuronal cells. *J Biol Chem*. 274:20885-94.

Virolle, T., E.D. Adamson, V. Baron, D. Birle, D. Mercola, T. Mustelin, and I. de Belle. 2001. The Egr-1 transcription factor directly activates PTEN during irradiation-induced signalling. *Nat Cell Biol*. 3:1124-8.

Wandzioch, E., C.E. Edling, R.H. Palmer, L. Carlsson, and B. Hallberg. 2004. Activation of the MAP kinase pathway by c-Kit is PI-3 kinase dependent in hematopoietic progenitor/stem cell lines. *Blood*. 104:51-7.

Watson, D.K., L. Robinson, D.R. Hodge, I. Kola, T.S. Papas, and A. Seth. 1997. FLI1 and EWS-FLI1 function as ternary complex factors and ELK1 and SAP1a function as ternary and quaternary complex factors on the Egr1 promoter serum response elements. *Oncogene*. 14:213-21.

Weeber, E.J., U. Beffert, C. Jones, J.M. Christian, E. Forster, J.D. Sweatt, and J. Herz. 2002. Reelin and ApoE receptors cooperate to enhance hippocampal synaptic plasticity and learning. *J Biol Chem*. 277:39944-52.

Wichterle, H., J.M. Garcia-Verdugo, and A. Alvarez-Buylla. 1997. Direct evidence for homotypic, glia-independent neuronal migration. *Neuron*. 18:779-91.

Yart, A., H. Chap, and P. Raynal. 2002. Phosphoinositide 3-kinases in lysophosphatidic acid signaling: regulation and cross-talk with the Ras/mitogen-activated protein kinase pathway. *Biochim Biophys Acta*. 1582:107-11.

York, R.D., H. Yao, T. Dillon, C.L. Ellig, S.P. Eckert, E.W. McCleskey, and P.J. Stork. 1998. Rap1 mediates sustained MAP kinase activation induced by nerve growth factor. *Nature*. 392:622-6.

FIGURE 1

Reelin-dependent phosphorylation of MAPK Erk1/2 proteins

Neuronal cultures were treated for 15 minutes (except in panel D) with control Mock supernatant (C), Reelin-containing supernatant (R), or kept untreated (t0).
(A) WB analyses of phospho-mDab1, phospho-Akt1, phospho-p38 and phospho-Jnk1/2/3 (lanes 1, 3, 5 and 7) and their loading controls (lanes 2, 4, 6 and 8). Reelin induces phosphorylation of mDab1 and Akt1, but not of p38 or Jnk1/2/3.
(B) WB assay demonstrating Reelin-dependent phosphorylation of Erk1/2 (lane 1); lane 2 shows the loading control. Densitometric analyses of five independent experiments (normalized to untreated samples (t0)) showing Reelin-dependent Erk1/2 phosphorylation. Differences between Reelin-treated and controls or untreated cultures are indicated (mean ± SEM; *, $p < 0.05$).
(C) Phosphorylation of Akt1 (left) and Erk1/2 (right) induced by treatment with partially purified Reelin (2ng/ml).
(D) Neuronal cultures were treated with Reelin for between 5 minutes to 24 hours. Erk1/2 activation was observed from 5 to 30 minutes, with maximal phosphorylation levels at 10-15 minutes.
(E) Reelin-dependent Erk1/2 phosphorylation is blocked by preincubation with the CR-50 antibody, but not with control IgGs.

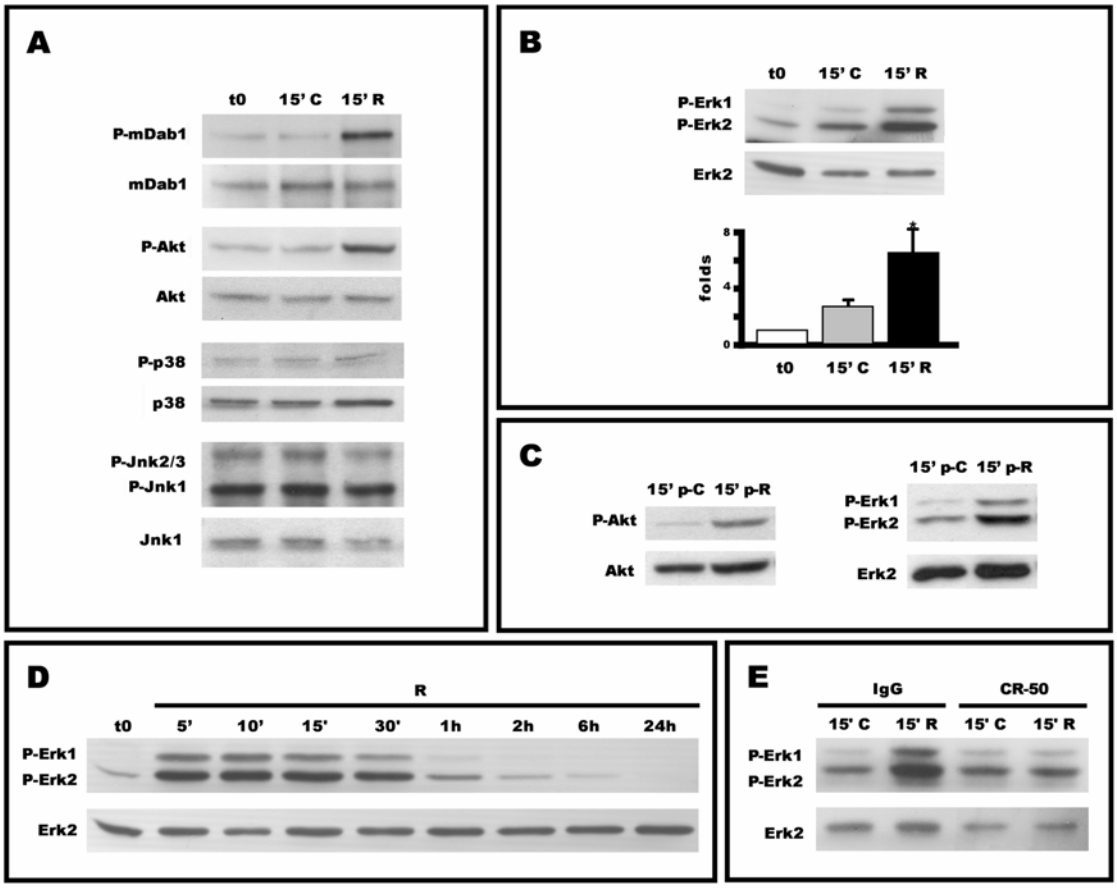
A
t0
15' C
15' R
P-mDab1
mDab1
P-Akt
Akt
P-p38
p38
P-Jnk2/3
P-Jnk1
Jnk1
B
t0
15' C
15' R
P-Erk1
P-Erk2
Erk2
folds
8
4
0
*
t0
15' C
15' R
C
15' p-C
15' p-R
P-Akt
Akt
15' p-C
15' p-R
P-Erk1
P-Erk2
Erk2
D
R
t0
5'
10'
15'
30'
1h
2h
6h
24h
P-Erk1
P-Erk2
Erk2
E
IgG
CR-50
15' C
15' R
15' C
15' R
P-Erk1
P-Erk2
Erk2

Figure 1

FIGURE 2

Reelin activates Erk1/2 in a MEK-dependent manner

Treatment of neuronal cultures with the MEK inhibitor PD 98059 blocks the Reelin-induced phosphorylation and activation of Erk1/2
(A) Starved neuronal cultures were preincubated for 1 hour with 25μM or 50μM of PD 98059 (PD). Cultures were then treated with Reelin and the phosphorylation state of Erk1/2 was analyzed by WB; lane 1 shows the phospho-Erk1/2 WB and lane 2 the loading control. PD 98059 blocked Reelin-induced phosphorylation of Erk1/2.
(B) An *in vitro* assay was performed to determine the enzymatic activity of Erk1/2 using the artificial substrate MBP. Samples treated with Reelin (R) showed an increase in the activity of Erk1/2, as detected by γ-P^{32} labeling of MBP. No differences with untreated samples are observed with control Mock treatments (C) or with PD 98059 preincubation before Reelin stimulation (R+PD). The histogram (mean ± SEM, from two separate experiments) shows the quantification of γ-P^{32}-MBP (lane 1), standardized with loading control of samples (lane 2).

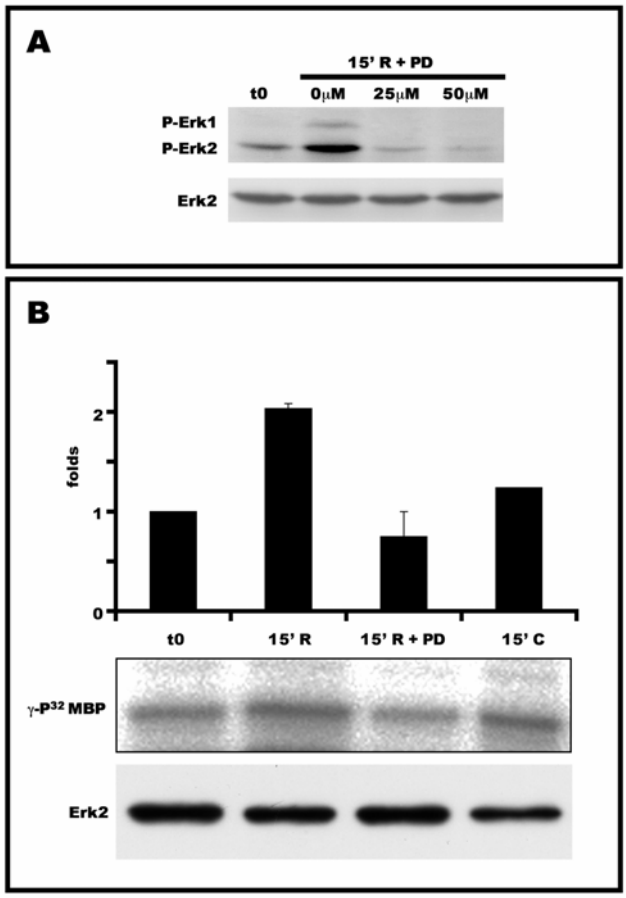
A
15' R + PD
t0
0μM
25μM
50μM
P-Erk1
P-Erk2
Erk2
B
folds
2
1
0
t0
15' R
15' R + PD
15' C
γ-P32 MBP
Erk2

Figure 2

FIGURE 3

Reelin-dependent ERK activation requires SFK, mDab1 and PI3K activation

Neuronal cultures were treated for 5 or 15 minutes with control Mock (C) or Reelin-containing (R) supernatant, or kept untreated (t0).
(A) Reelin (2ng/ml) induces a modest activation of Ras. BDNF (25μg/ml) was used as a positive control. Pull-downs of activated Ras were detected by WB using anti-Ras antibodies (left); Densitometric analyses (right) revealed non-significant Ras activation after Reelin treatment (1.5-fold) in comparison with BDNF treatment (9-fold). (*, $p \leq 0.05$)
(B) Comparison of Reelin- and BDNF-induced phosphorylation levels of Akt1 and Erk1/2 (lanes 1 and 3); Reelin induction of Erk1/2 and Akt1 is similar, and significantly weaker than BDNF induction. Loading controls for Akt1 and Erk2 are also shown (lanes 2 and 4).
(C) Analysis of Reelin-induced phosphorylation of mDab1 in the presence of inhibitors for SFK (PP2, 10μM), PI3K (LY 294002, 50μM) or MEK (PD 98059, 50μM). SFK inhibition blocks Reelin-induced phosphorylation of mDab1, but PI3K inhibition and MEK inhibition has no effect on mDab1 phosphorylation after Reelin treatment (lane 1; loading controls are in lane 2).
(D) Effect of MEK pathway inhibition on Reelin-induced phosphorylation of Akt1. MEK blockade with PD 98059 (50μM) has no effect on phosphorylation levels of Akt1 after Reelin treatment (lane 1; loading controls are in lane 2).
(E) Effect of SFK inhibition and *mdab1* deficiency on Reelin-induced phosphorylation of Akt1 and Erk1/2. SFK inhibition with PP2 (10μM) blocks Reelin-dependent phosphorylation on Akt1 and Erk1/2 proteins (lanes 1 and 3; loading controls are in lanes 2 and 4). Similarly, in cultures from *mdab1*-deficient (*mdab1* -/-) embryos, Akt1 and Erk1/2 were not phosphorylated after Reelin treatment (lane 1 and 3; loading controls are in lane 2 and 4).
(F) Effect of PI3K inhibition on phosphorylation levels of Akt1 and Erk1/2 proteins, induced by Reelin or BDNF. The PI3K inhibitor LY 294002 (50μM) blocks Reelin- and BDNF-induced phosphorylation of Akt1 (lane 1; loading controls are in lane 2). LY 294002 also inhibits Reelin-dependent, but not BDNF-dependent, phosphorylation of Erk1/2 (lane 3; loading controls are in lane 4).

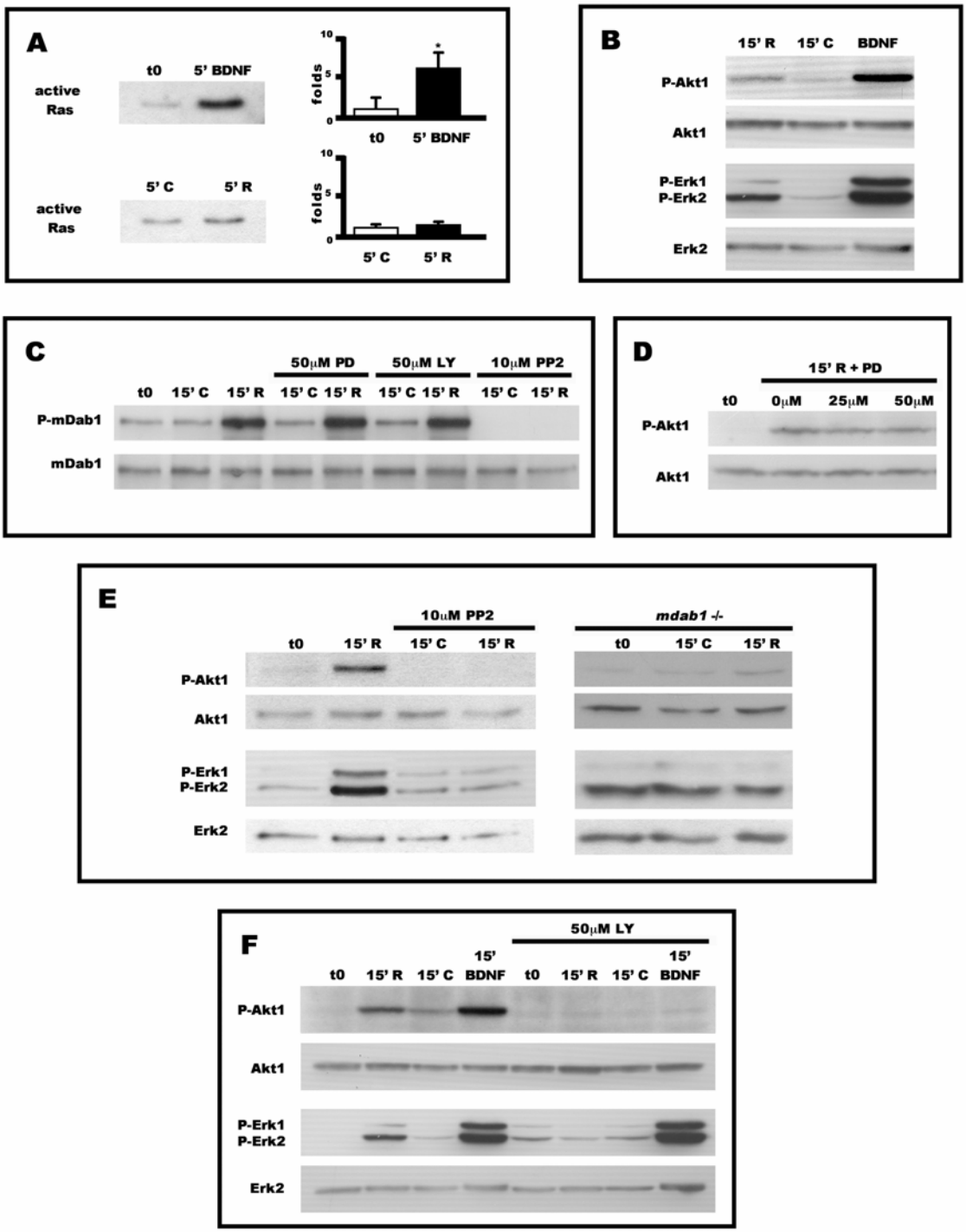
A
t0
5' BDNF
active Ras
folds
10
5
0
t0
5' BDNF
5' C
5' R
active Ras
folds
10
5
0
5' C
5' R
B
15' R
15' C
BDNF
P-Akt1
Akt1
P-Erk1
P-Erk2
Erk2
C
50μM PD
50μM LY
10μM PP2
t0
15' C
15' R
15' C
15' R
15' C
15' R
15' C
15' R
P-mDab1
mDab1
D
15' R + PD
t0
0μM
25μM
50μM
P-Akt1
Akt1
E
10μM PP2
mdab1 -/-
t0
15' R
15' C
15' R
t0
15' C
15' R
P-Akt1
Akt1
P-Erk1
P-Erk2
Erk2
F
50μM LY
15'
BDNF
15'
BDNF
t0
15' R
15' C
t0
15' R
15' C
P-Akt1
Akt1
P-Erk1
P-Erk2
Erk2

Figure 3

FIGURE 4

MAPKs are involved in Reelin-induced detachment of migrating neurons from the SVZ in vitro.

SVZ explants (P5) were cultured for 2 (A (left panels), B and D) or 3 (A (right panels)) DIV, fixed, and processed for immunostaining against β-III-tubulin.
(A) After 2 DIV, chains of neurons migrate out of the explants (top left panel). Neuronal chains start to disorganize at 3 DIV (top right panel). In the presence of the MEK inhibitor PD 98059 (50μM) or LY 294002 (50μM), neuronal chains are apparent both at 2 DIV and 3 DIV (middle and bottom panels).
(B) SVZ explants cultured for 2 DIV in the presence of control Mock (left panels) or Reelin-containing (right panels) supernatants. Reelin (top right panel) induces the detachment of migrating neurons from the SVZ at 2 DIV. The presence of the MEK inhibitor PD 98059 (50μM) in the culture medium blocks the detachment of SVZ neurons induced by Reelin (bottom panels).
(C) Quantification of the percentage of detached cells per field (0,03 mm^2) was performed at 2DIV. Reelin treatment produces a marked increase of detached cells compared with control Mock-treated or untreated samples (mean ± SEM; *, $p<0.05$).
(D) SVZ cultures from *mdab1*-deficient (*mdab1* -/-) (top panels) animals and PP2-treated cultures (bottom panels) were stimulated with control Mock (left panels) or Reelin-containing (right panels) supernatants. Reelin does not induce neuronal detachment in these conditions.
Scale bar, 20 μm (A,B,D).

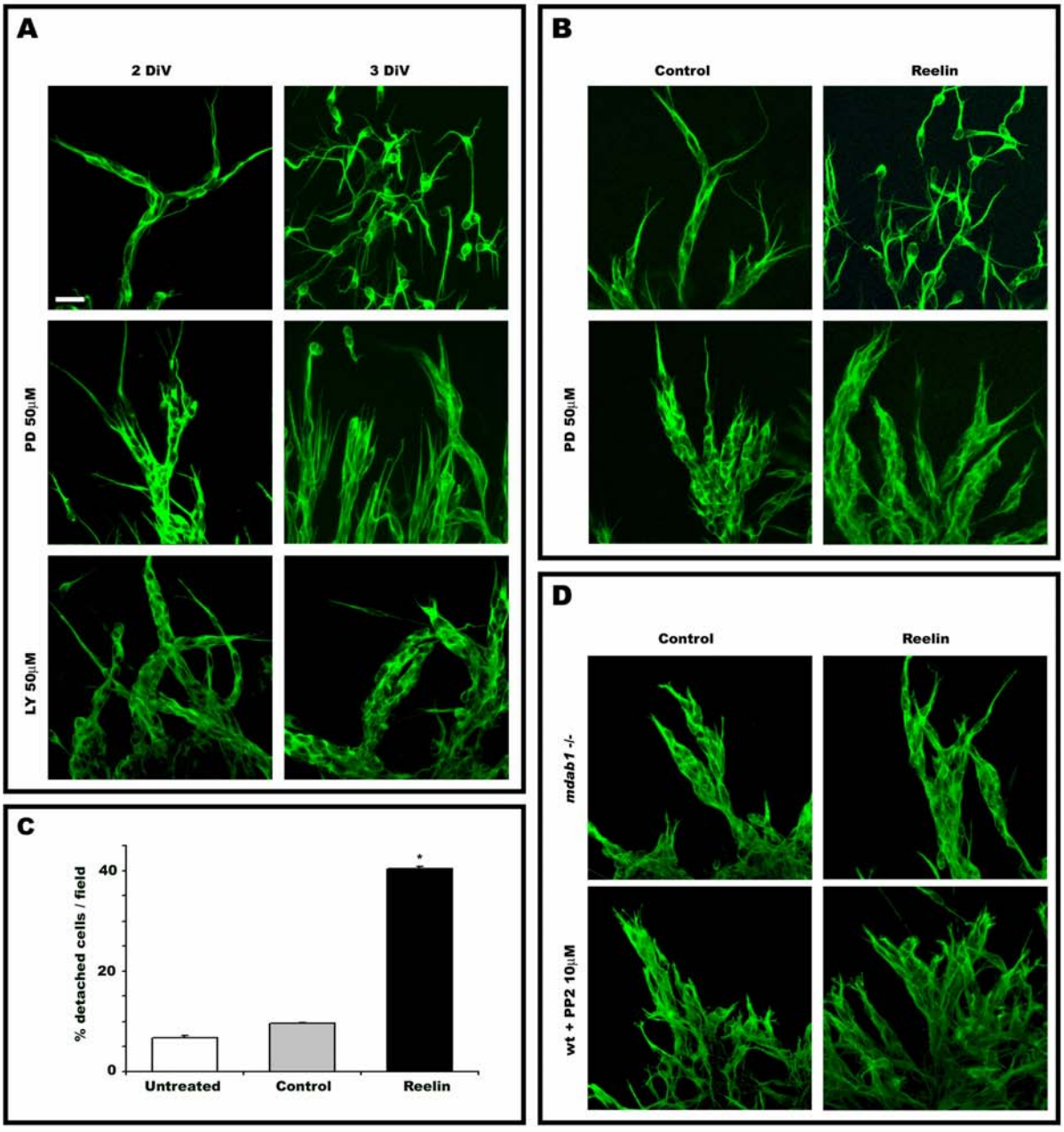
A
2 DiV
3 DiV
PD 50μM
LY 50μM
B
Control
Reelin
PD 50μM
C
% detached cells / field
40
20
0
*
Untreated
Control
Reelin
D
Control
Reelin
mdab1 -/-
wt + PP2 10μM

Figure 4

FIGURE 5

Reelin induces the translocation of P-Erk and the increase of Egr-1 protein levels in neuronal cultures

(A) Immunostaining of neuronal cultures with anti-phospho-Erk1/2 antibodies (left panels) after incubation with control Mock or Reelin-containing media for 15 minutes (Control or Reelin, respectively). Note increased phospho-Erk1/2-immunostaining and accumulation of labeling in the nuclei after Reelin treatment. Middle panels show counterstaining of actin filaments with Texas-Red-phalloidin and right panels show merged images.
(B) Reelin induces a similar increase in Egr-1 protein expression, which is localized in neuronal nuclei (bottom left panel), compared to controls (top left panel). An increase in Egr-1 protein is detected 1 hour after Reelin addition (bottom left panel). Middle panels show counterstaining of actin filaments with Texas-Red-phalloidin and right panels show merged images.
Scale bar, 30 μm (A), 50 μm (B).

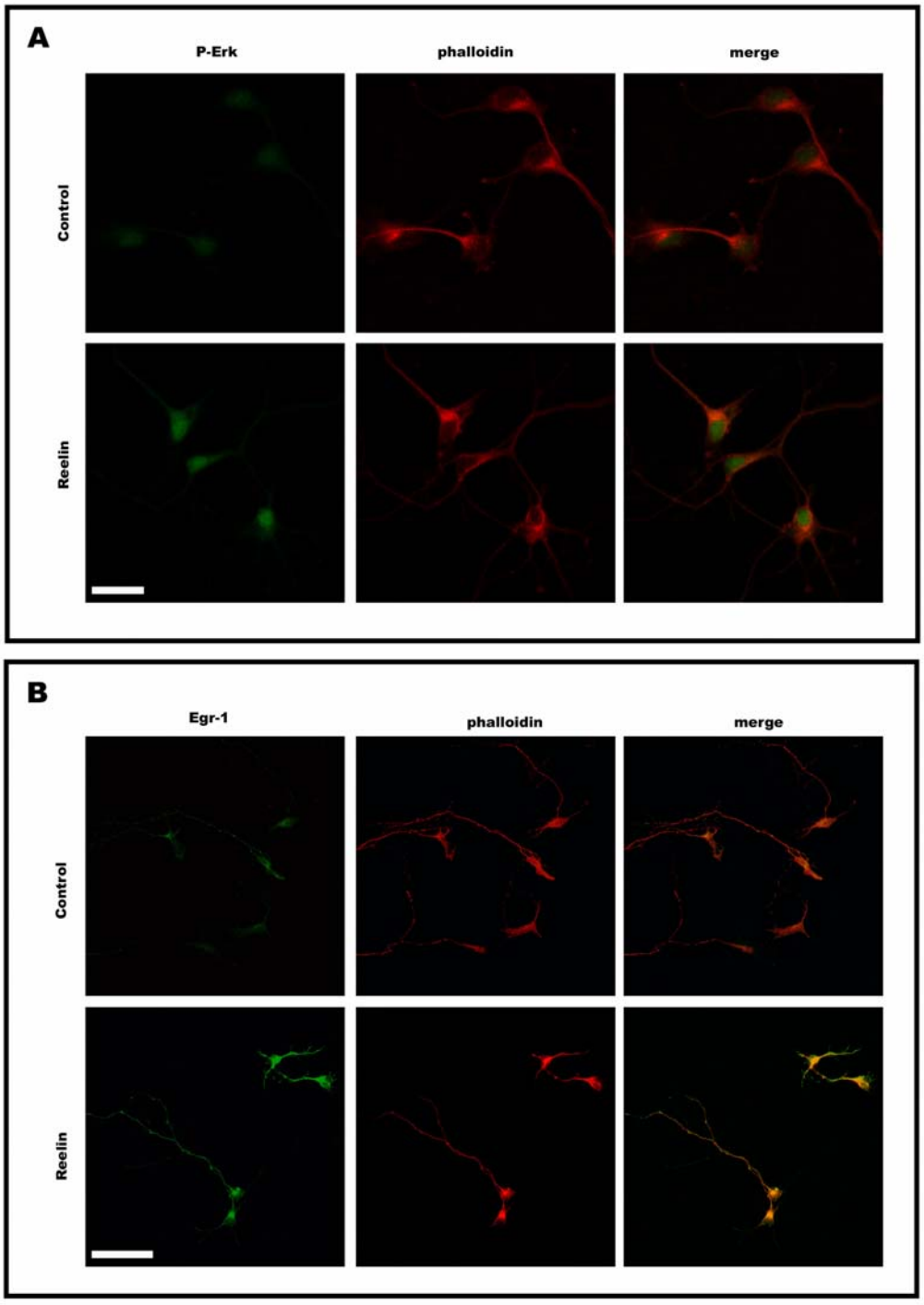
A
P-Erk
phalloidin
merge
Control
Reelin
B
Egr-1
phalloidin
merge
Control
Reelin

Figure 5

FIGURE 6

Reelin induces the expression of egr-1 through the ERK pathway

(A) Expression of Egr-1 protein was analyzed in neuronal cultures by WB after incubation with control Mock or Reelin-containing supernatants for 1 hour. The WB on the left shows a marked increase in Egr-1 protein content after Reelin treatment (lane 1); β-III-tubulin staining was used as a loading control (lane 2). A histogram summarizing the densitometric quantitative data obtained in 4 independent/separate experiments is shown on the right (mean ± SEM; *, $p<0.05$).
(B) Time course analysis of Egr-1 levels by WB in cultured neurons treated with Reelin (R) for 0-210 minutes, showing maximum content at 30-120 minutes (left panel). Comparison of the time course of Egr-1 up-regulation and Erk1/2 activation in the same neurons treated with Reelin (right panel). An antibody against β-III-tubulin was used as loading control blots (lane 2).
(C) Semi-quantitative RT-PCR analyses of *egr-1* mRNA. *gapdh* mRNA was used as a loading control. A marked significant increase in *egr-1* transcription occurs at 30-60 minutes when neuronal cultures are treated with Reelin-containing supernatant (left). Quantitative representation of 3 independent experiments (Right panel; *, $p\leq0.05$).
(D) Effects of 50μM PD 98059 (PD), 50μM LY 294002 (LY) or 10μM PP2 on Reelin-induced Egr-1 protein increase. Neuronal cultures were incubated with control Mock or Reelin-containing supernatants in the presence of the above inhibitors for 1 hour. WB analysis was probed for Egr-1 (lane 1), stripped and reprobed against β-III-tubulin as loading control (lane 2). All three pharmacological inhibitors prevent the Reelin-induced increase in Egr-1 at the protein level.

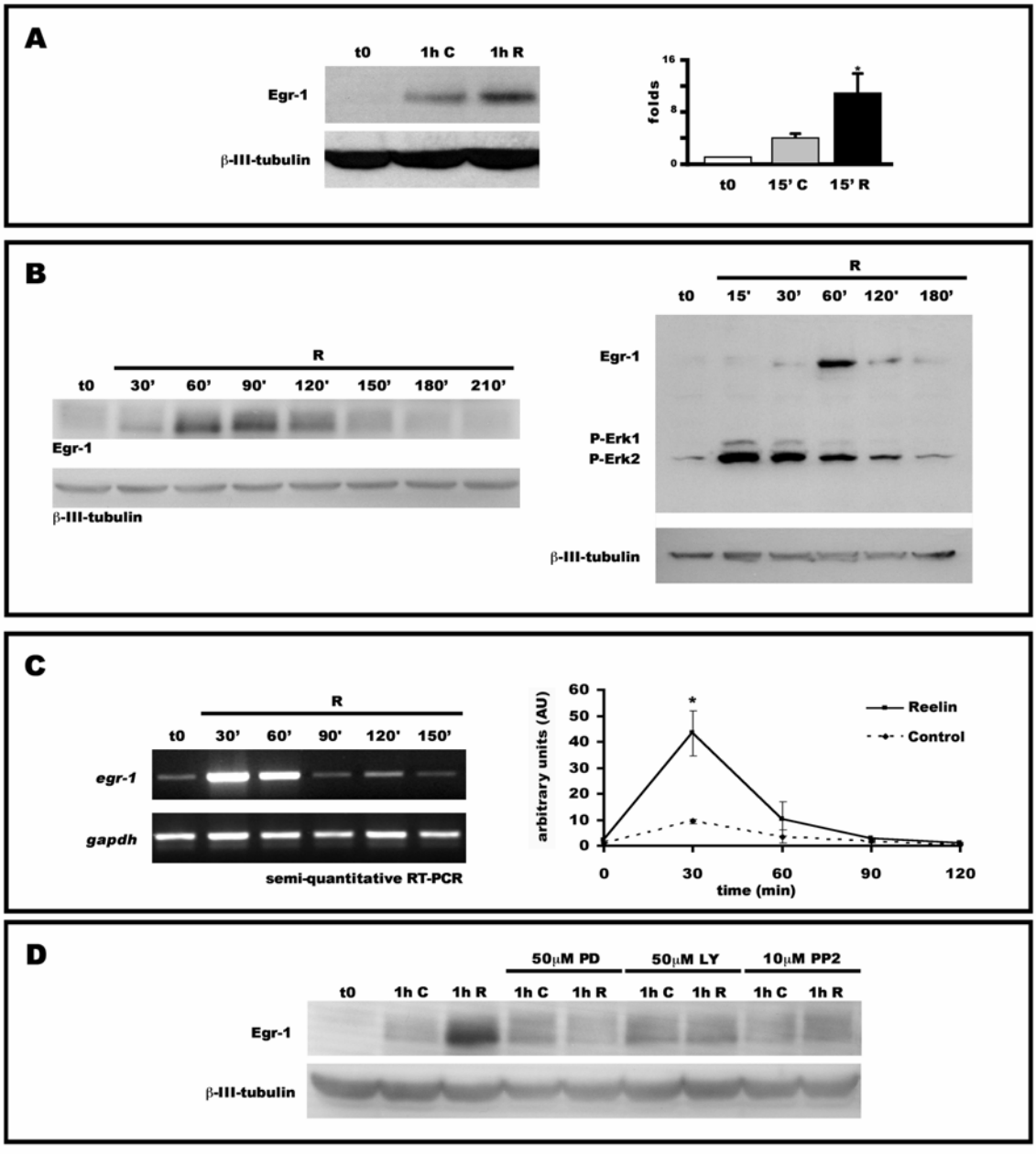
A
t0
1h C
1h R
Egr-1
β-III-tubulin
folds
16
8
0
*
t0
15' C
15' R
B
R
t0
30'
60'
90'
120'
150'
180'
210'
Egr-1
β-III-tubulin
R
t0
15'
30'
60'
120'
180'
Egr-1
P-Erk1
P-Erk2
β-III-tubulin
C
R
t0
30'
60'
90'
120'
150'
egr-1
gapdh
semi-quantitative RT-PCR
arbitrary units (AU)
60
50
40
30
20
10
0
*
Reelin
Control
0
30
60
90
120
time (min)
D
50μM PD
50μM LY
10μM PP2
t0
1h C
1h R
1h C
1h R
1h C
1h R
1h C
1h R
Egr-1
β-III-tubulin

Figure 6

FIGURE 7

Summary diagram integrating the ERK pathway in the Reelin signaling pathway.

Reelin binds VLDLR and ApoER2 receptors, thereby inducing the phosphorylation of mDab1 by SFK. Transduction involves the PI3K pathway and the subsequent phosphorylation of Akt1 and GSK3β, and downstream cytoskeletal proteins. PI3K is also required for the activation of the ERK pathway and phosphorylation of Erk1/2 proteins. The contribution of Ras to Reelin-dependent ERK activation cannot be discarded but the sequential activation of SFK and PI3K appears to be the major pathway that produces ERK activation. ERK activation leads, in turn, to the transcriptional activation of *egr-1,* which may in turn control several cellular events. The sites of action of the pharmacological inhibitors PP2, LY 294002 and PD 98059 are indicated in the context of Reelin signaling.

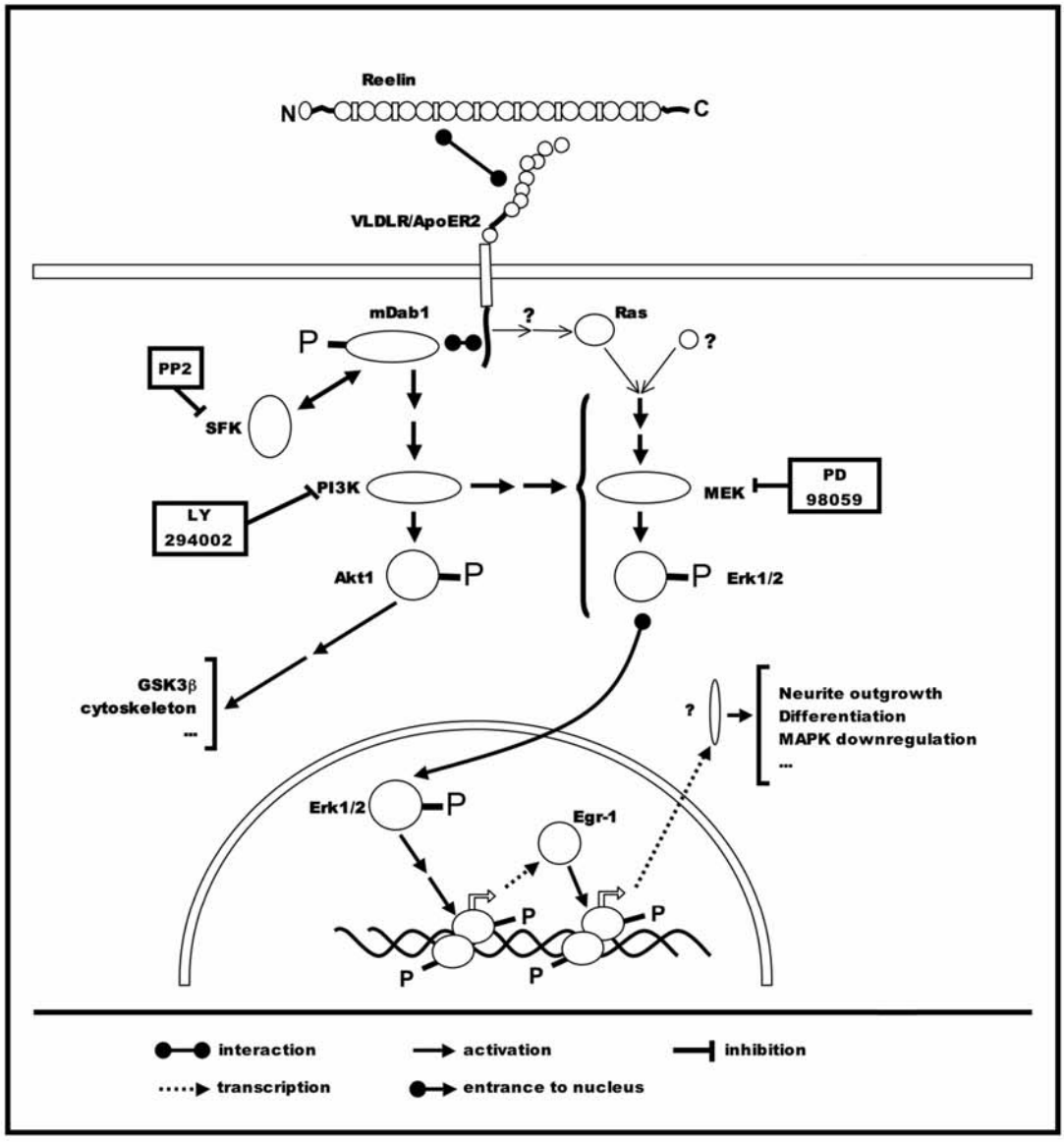
Reelin
N
C
VLDLR/ApoER2
mDab1
P
?
Ras
?
PP2
SFK
PI3K
LY
294002
MEK
PD
98059
Akt1
P
P
Erk1/2
GSK3β
cytoskeleton
...
?
Neurite outgrowth
Differentiation
MAPK downregulation
...
Erk1/2
P
Egr-1
P
P
P
P
interaction
activation
inhibition
transcription
entrance to nucleus

Figure 7

SUPPLEMENTAL FIGURE 1

Proteins of the Reelin signaling pathway are present in neurons migrating from the SVZ

Immunocytochemical analyses of the expression of mDab1, Erk and Ras in cells migrating from SVZ.
(A,B) mDab1 protein is present in neurons migrating in chains out of SVZ explants *in vitro*, as detected with the B3 antibody (A), same field counterstained with β-III-tubulin antibody (B).
(C) Pan-Erk antibody reveals a high immunolabeling in neurons migrating from SVZ, indicating that Erk proteins are present in these neurons (C).
(D) Ras is also expressed in neurons migrating from SVZ explants, although with low labeling levels.
Scale bar, 20 μm (A,B; C,D).

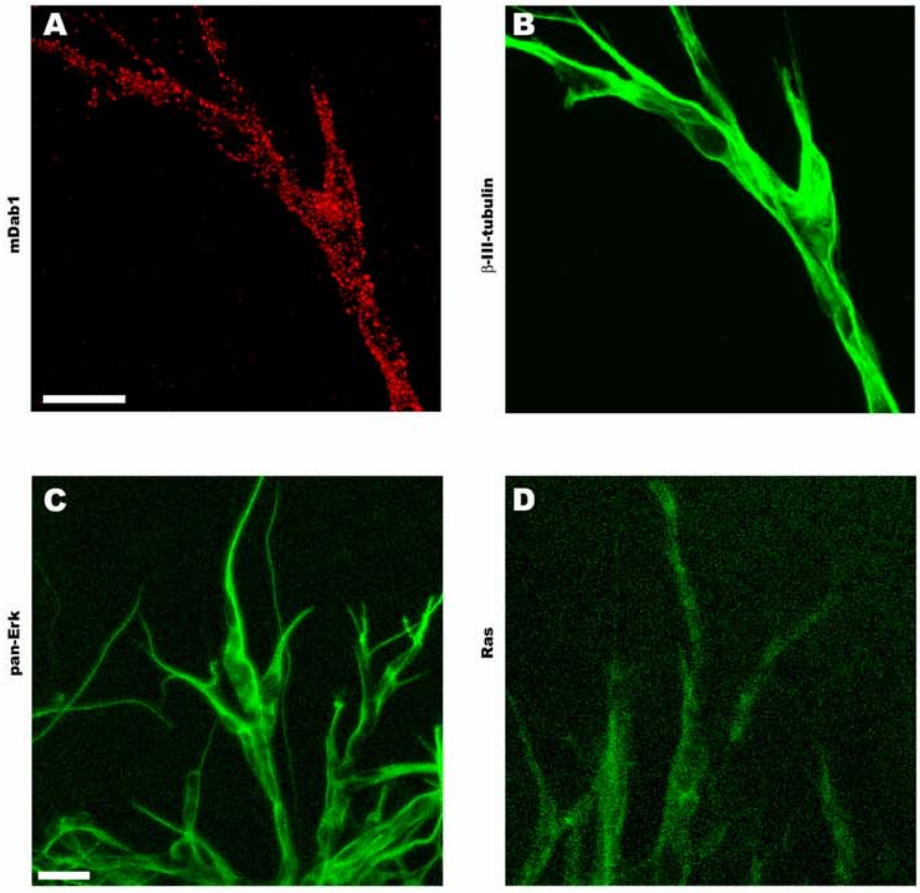

Supplemental Figure 1

SUPPLEMENTAL FIGURE 2

Reelin induces the translocation of P-Erk protein levels in SVZ neuronal cultures and dose dependency of PD 98059 effects on cells migratin from SVZ treated with Reelin

(A) Immunostaining of SVZ neuronal cultures with phospho-Erk1/2 antibodies (left panels) after incubation with control or Reelin-containing media for 15 minutes (Control or Reelin, respectively). SVZ neuronal cultures show and increased phospho-Erk1/2 immunolabeling in the nuclei after Reelin treatment. Middle panels show counterstaining of actin filaments with Texas-Red-phalloidin and right panels show merged images.
(B) 2 DIV explants treated with PD 98059 (PD) at a concentration of 0μM, 25μM or 50μM. Without MEK inhibitor, detached neurons are abundant after Reelin treatment (left panel). Virtually no cell detachment is observed after incubation with 25μM PD 98059. Moreover, chain morphology is similar to untreated cells (middle panel). Similar results are obtained when culturing SVZ explants with 50μM PD 98059 under Reelin stimulation, although chains are more compacted (right panel).
Scale bar, 20 μm (A,B).

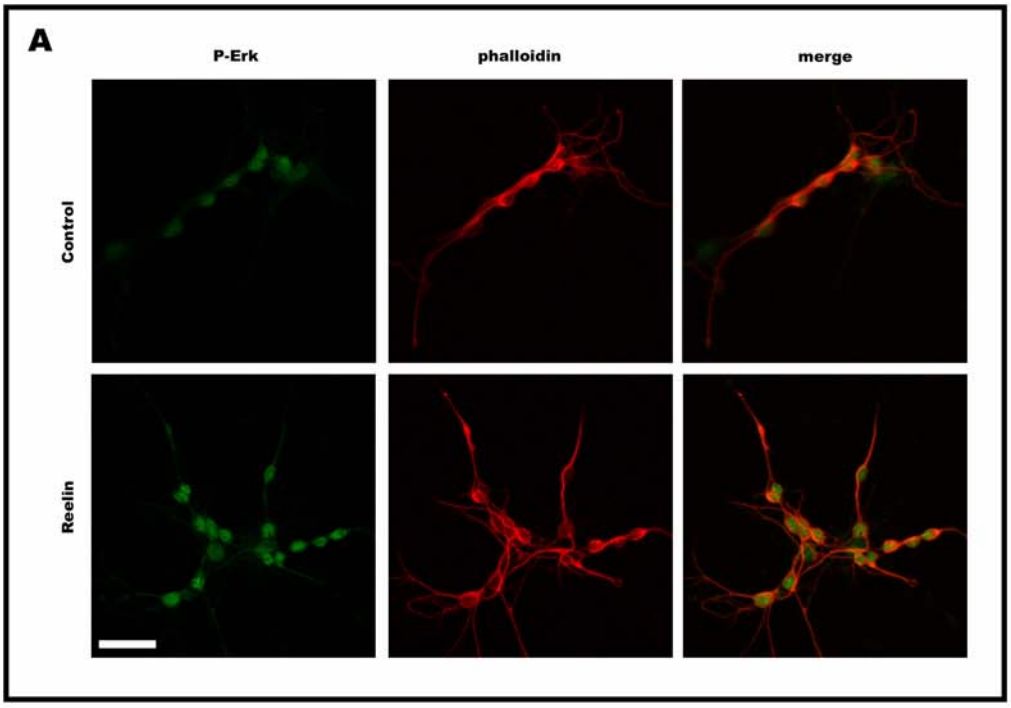

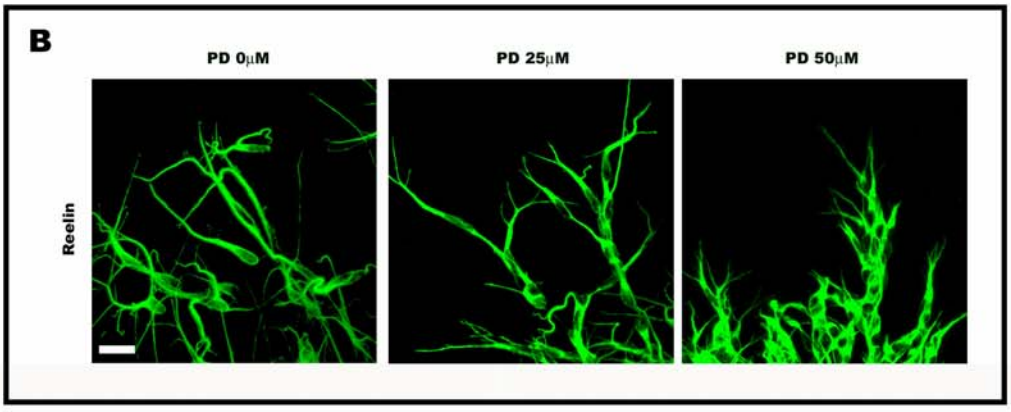

Supplemental Figure 2

SUPPLEMENTAL FIGURE 3

BDNF does not induce detachment of neurons migrating from the SVZ

(A,B) Untreated explants (A) and BDNF-treated explants (B) show neuronal chains of normal thickness at 2 DIV, in both conditions.
(C,D) In the presence of LY 294002, no detachment is observed either in controls (C) or after treatment with BDNF (D). Neuronal chains appear more compact after incubation with LY 294002.
Scale bar, 20μm (A-D).

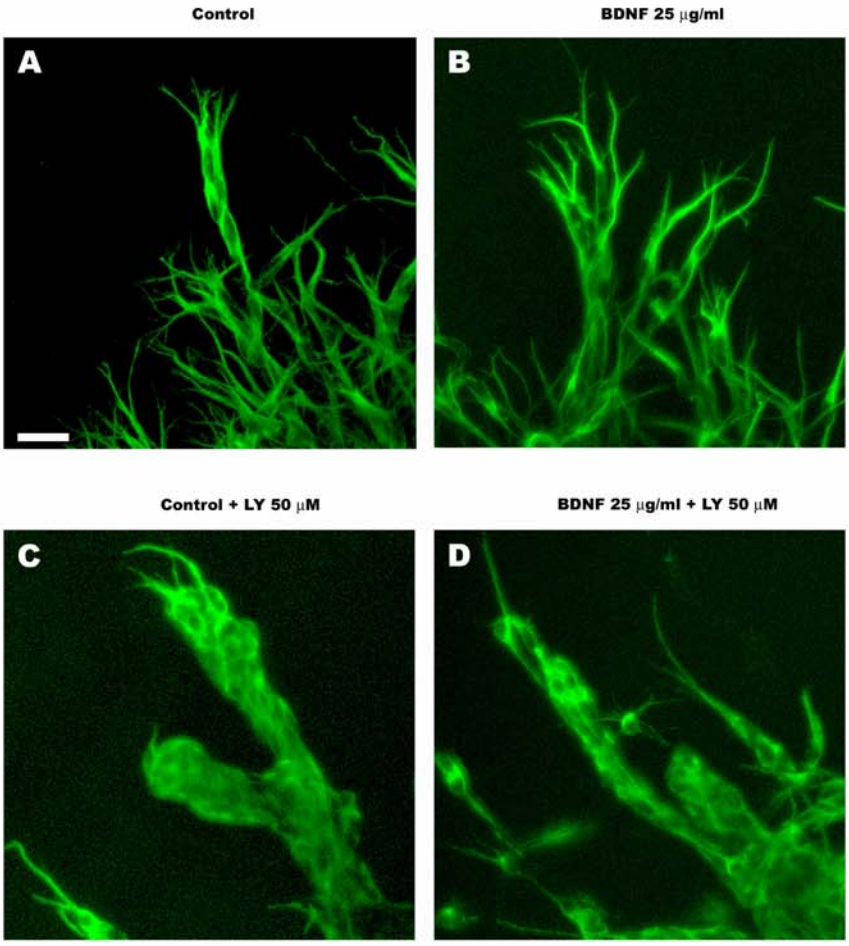

Supplemental Figure 3

Resultats (Capítol 3)

Generació de ratolins transgènics que expressen la Reelina de forma condicional

Els resultats presentats en aquest capítol estan en procés de preparació.

Lluís Pujadas [1*], Luís de Lecea [2], and Eduardo Soriano [1]

[1]**Laboratori de Neurobiologia del Desenvolupament i la Regeneració Neuronal**, Parc Científic de Barcelona-IRB i Departament de Biologia Cel·lular, Universitat de Barcelona, E-08028 Barcelona.
[2]**Department of Molecular Biology**, The Scripps Research Institute, La Jolla, California 92037 USA.

RESUM

Amb l'objectiu de desxifrar el paper de la Reelina a l'edat adulta, s'ha generat un model de ratolí transgènic d'expressió condicional de *reelin*. L'expressió del transgen està controlada pel *tetracicline operator*. La construcció s'injectà en oocits, i els animals nascuts foren creuats amb una soca de transgènics que expressen el *tetraciclin transactivator* (*tTA*) sota el control del *CaMKIIα promoter*.

En els animals dobles transgènics, la Reelina es produeix en neurones que expressen *CaMKIIα*, i conseqüentment es detecta en neurones piramidals de l'hipocamp, en neurones granulars del gir dentat i en l'estriat. L'expressió de la Reelina s'observa a partir d'edat P20, i pot ser abolida per l'administració de la deoxycicline.

Aquests animals són de gran interès per a l'estudi de processos de migració de l'edat adulta en les regions neurogèniques (SVZ i SGZ), i alhora, per a l'estudi de processos de plasticitat: sinaptogènesi, LTP i memòria. A més, l'expressió condicional de *reelin* podrà ser dirigida a d'altres regions per creuament del ratolins transgènics de *reelin* amb altres soques de ratolins que expressin *tTA* sota el control de promotors diversos.

Resultats (Capítol 3)

Generation of transgenic mice conditionally expressing Reelin

ABSTRACT

To elucidate the role of Reelin in adulthood, we generated a mouse model with conditional expression of *reelin*. We directed the expression of *reelin* by the tetracycline operator, thus generating a construct that was later injected into mouse oocytes. These animals were crossed with a transgenic strain that express the tetracycline transactivator (*tTA*) under the control of the *CaMKIIα* promoter.

In double transgenic animals, Reelin was ectopically produced by *CaMKIIα*-expressing neurons and subsequently detected in pyramidal neurons from the hippocampus, in granular neurons from the dentate gyrus and in the striatum. Reelin expression was observed from P20 onwards, and can be suppressed by oral administration of deoxycycline.

This double transgenic mouse model is of great interest for studies on adult migration processes from the neurogenic regions (SVZ and SGZ), and also for the study of plasticity: synaptogenesis, LTP and memory formation. Moreover, the conditional expression of Reelin can be directed to other regions/ages by crossing the *reelin* transgenic animals with strains of mice expressing *tTA* under the control of other promoters.

INTRODUCTION

The function of Reelin during the formation of laminated brain structures has been extensively studied since this protein was described as defective in *reeler* mice (D'Arcangelo et al., 1995). *reeler* animals show an abnormal distribution of neurons in several brain regions, such as hippocampus, cerebral cortex, cerebellum and olfactory bulb, which leads to their characteristic phenotype (Rice and Curran, 2001; Tissir and Goffinet, 2003). Cajal-Retzius cells and the Reelin that they secrete have been studied mainly during embryogenesis because of their participation in cortical and hippocampal layering (Soriano and Del Rio, 2005). In addition, Reelin functions have been examined in early postnatal development, especially in the cerebellum (Miyata et al., 1997), but also in the olfactory bulb (Hack et al., 2002). The identification of the signaling pathways induced by Reelin is of great interest since the mDab1 adaptor protein and also the apolipoprotein E receptor 2 (ApoER2) and the very-low lipoprotein lipoprotein receptor (VLDLR) are known to be crucial for Reelin function (D'Arcangelo et al., 1999; Hiesberger et al., 1999; Rice et al., 1998). Other intracellular proteins are activated by Reelin, including the Src family protein kinases (SFKs) (Fyn and Src), phophatidylinositol 3 kinase (PI3K), Akt1, glycogen synthase kinase 3 beta (GSK3β) and the microtubule associated protein 1B (MAP1B) (Arnaud et al., 2003; Beffert et al., 2002; Bock and Herz, 2003; Bock et al., 2003; Gonzalez-Billault et al., 2005). Moreover, we recently described the involvement of the ERK pathway in the Reelin-induced intracellular signaling network. Reelin induces the activation of the extracellular regulated kinases 1 and 2 (Erk1/2). We also reported the contribution of the ERK pathway to the detachment of neurons migrating from the SVZ and to the up-regulation of the early gene *egr-1* (also known as *zif268*) (Unpublished data).

Moreover, Reelin is crucial for synaptogenesis; indeed, *reeler* animals show a large decrease in the number of hippocampal synaptic contacts of the perforant pathway (Borrell et al., 1999). Finally, this protein also participates in memory-related processes such as long-term potentiation (LTP) (Beffert et al., 2005; Weeber et al., 2002).

Nevertheless, the precise function of Reelin in the cases cited above is not fully understood, and some discrepancies remain in the bibliography. To clarify these divergences, several animal models are now being used to further study Reelin functions in the brain. Mutant animals with a *reeler* phenotype (defective for *reelin*, *mdab1*, or *apoer2/vldlr*) or with *reeler*-like abnormalities (defective for *cdk5*, *p35/p39*, *tbr1*, or *map1b*) have been used to analyze the effect of Reelin signaling deficiency in brain development (Sheldon et al., 1997; Trommsdorff et al., 1999). The ectopic over-expression of Reelin has also been examined in early embryogenesis by generating a transgenic model showing *reelin* expression under the control of the *nestin* promoter (Magdaleno et al., 2002).

To study the developmental processes in adulthood in which Reelin may be involved, here we designed a transgenic mouse model conditionally expressing this protein. This new transgenic model has been developed to clarify the participation of Reelin in the neuronal migration and plasticity during adulthood. However, the model can also be adapted for the study of other processes.

RESULTS

Generation of Reelin-expressing conditional transgenic mice

To clarify the role of Reelin in the postnatal forebrain, we generated a transgenic mouse model of Reelin over-expression. We based the transgenic mouse design on a tet-regulated system of gene expression, setting the *myc*-tagged transgene of *reelin* (*rlM*) under the control of the tetracycline operator (*tetO*) (Gossen and Bujard, 1992; Lewandoski, 2001).

We directed the transgene expression in a spatially and temporally regulated manner by using the tetracycline-controlled transactivator (*tTA*) under control of the calcium-calmodulin-dependent kinase IIα promoter (*pCaMKIIα*) (Mayford et al., 1996). In *pCaMKIIα-tTA* transgenic animals (*Tg1*), *tTA* expression is restricted to forebrain projection neurons throughout the neocortex, hippocampus, amygdala, and striatum, mimicking endogenous *CaMKIIα* expression (Burgin et al., 1990; Mayford et al., 1996). In double transgenic animals carrying both the *tetO-rlM* and *pCamKIIα-tTA* transgenes, Reelin is expected to mimic the distribution of CaMKIIα expression.

To generate a transgenic mouse line expressing *reelin* under *tetO* control, we excised full-length *reelin* cDNA from the pCrlM plasmid, a *myc*-tagged version of pCrl plasmid (D'Arcangelo et al., 1997). *myc*-tagged *reelin* cDNA (rlM) was subcloned into a PCRII-TOPO vector (Invitrogen) to create PCRII-rlM. It was then excised and cloned into a PMM400 vector (Mayford et al., 1996). The PMM-rlM-generated plasmid carried the fragment to be microinjected into single cell embryos. This fragment contained the *tetO* operator, a 5' intron, the rlM, a 3' intron, and a simian virus 40 polyadenylation sequence (SV40-polyA) (Figure 1A). Upstream of the fragment, the PMM-rlM plasmid also contained a cytomegalovirus (*CMV*) promoter (Figure 1A).

Before microinjection, the correct expression of *reelin* from the PMM-rlM plasmid was tested using the *CMV* promoter by transitory transfection of 293T cells. Supernatants from 293T cells transfected with PMM-rlM were analyzed by Western blot (WB) using anti-Reelin antibodies (G10), thus obtaining the same bands as transfection with the pCrlM vector (Figure 1B, upper panel). Supernatants from PMM-rlM, pCrlM, or their Mock control vectors (PMM400 and pCDNA3.1 respectively) were used to stimulate cultured forebrain neurons. PMM-rlM and pCrlM treatments of supernatants produced the phosphorylation of the adaptor protein mDab1, the first step in signaling events caused by Reelin, indicating that the Reelin produced by the PMM-rlM vector was functional (Figure 1B, middle and bottom panel).

The *tetO-rlM* construct was microinjected into oocytes. PCR analyses were performed to determine transgenic founder mice. The number of transgene insertions was evaluated by semi-quantitative PCR and the three *tetO-rlM* transgenic strains (*Tg2*) with a greater number of insertions were selected for characterization: *Tg2-alpha* (*alphaR*), *Tg2-beta* (*betaR*), *Tg2-gamma* (*gammaR*); another transgenic strain, *Tg2-rho* (*rhoR*), with a single insertion of the transgene was also selected for this purpose (Figure 1D).

Tg2 strains were crossed with *Tg1* animals to obtain the double transgenic progeny (*Tg1/Tg2*), expected to overexpress *reelin* but only in those cells that express *tTA* (Figure 1C). Reelin expression can be fully suppressed by oral administration of deoxycycline (Dox).

Expression of Reelin in transgenic mice

Reelin expression in *Tg1/Tg2* mice was analysed by immunohistochemistry using the monoclonal anti-Reelin antibody G10. *Tg1/Tg2* animals, and their control littermates (*wt*, *Tg1* or *Tg2*), were perfused with paraformaldehyde (PF) and processed for histological analysis.

G10 immunostaining was observed in the subset of neurons that normally express Reelin (i.e. mitral and periglomerular neurons of the olfactory bulb; a subset of cortical interneurons, mainly in cortical layer V; a subset of hippocampal interneurons; and the lasting Cajal-Retzius cells in the adult hippocampus) (Alcantara et al., 1998). This endogenous expression of Reelin was observed in all animals without differences in the levels of protein expression (unpublished data).

Moreover, *Tg1/Tg2* animals also expressed Reelin ectopically in the population of neurons known to express CaMKIIα. Therefore, ectopical expression of Reelin was detected in *Tg1/Tg2* animals, but not in controls, in the principal neurons of the CA1 region of the hippocampus (Figure 2A,B), in the granular neurons of the dentate gyrus (Figure 2C,D) and in the striatum (Figure 2E,F). In the hippocampal formation (CA1 and DG) the expression of transgenic Reelin was detected only in adults (P60) while ectopic expression in the striatum was seen from P20 onwards (unpublished data).

DISCUSSION

Here we report the generation of a new transgenic mouse model suitable for studying the participation of Reelin in mature forebrain processes of neuronal migration and plasticity. The further characterization of these mice will clarify the contribution of this protein to functions in which its specific role is still unknown.

A mouse model to analyze the participation of Reelin in adult neuronal migration

The ectopic production of Reelin in *Tg1/Tg2* animals occurred near the main neuronal germinal sites. The neurogenic regions in the mature brain are the subventricular zone (SVZ), positioned in the lateral wall of the anterior horn of the lateral ventricle; and the subgranular zone (SGZ), the neurogenic region of the hippocampal dentate gyrus (Doetsch and Hen, 2005). Once generated, neuroblasts migrate to the target region were they mature and integrate into the existing circuitry (Ming and Song, 2005).

New-born neurons from the SVZ migrate tangentially forward through the rostral migratory stream (RMS), forming chain-like structures by homophilic interactions. When they reach the olfactory bulb, they are exposed to the Reelin produced by mitral cells. Reelin induces neurons to switch from tangential/chain to radial/individual migration in a process that requires the participation of the ERK signaling pathway (Hack et al., 2002). The entire SVZ is located next to the striatum, where Reelin is expressed in *Tg1/Tg2* animals. Studies on the SVZ and the RMS of *Tg1/Tg2* animals will be of great interest to further corroborate the participation of Reelin in the detachment of cells from homophilic chains. The alterations that *Tg1/Tg2* are expected to show during migration could be caused by ectopic striatum Reelin.

The SGZ is located within the hilus and the granular layer in the dentate gyrus. New-born neurons generated in the SGZ migrate short distances to integrate as granular neurons in inner third of the granular layer. Although no studies have related Reelin with the migration of SGZ new-born neurons, the layering of the dentate gyrus is completely broken in *reeler* animals because Reelin is crucial for the migration of granular layers during embryogenesis. *Tg1/Tg2* animals express Reelin in the granular layer and therefore this model is highly suited to study the influence of this protein in a migratory process in which it is not suspected to be involved in the adulthood. Moreover, it will be of interest to compare the response of progenitors of granular neurons to Reelin at distinct developmental stages.

Contribution of Reelin to plasticity: synaptogenesis, LTP, learning, and memory

On the basis of the deficiency observed in the number of the hippocampal synaptic contacts in *reeler* mice (Borrell et al., 1999), it has been hypothesized that Reelin contributes to synaptogenesis. Moreover, the participation of Reelin in adult synaptic plasticity is of great interest since this protein has been described as an inductor of long-term potentiation (LTP) in the CA1 area (Weeber et al., 2002); indeed,

the modulation of NMDA receptor activity, synaptic neurotransmission and memory by Reelin involves differential splicing of the Reelin-receptor ApoER2 (Beffert et al., 2005). The transgenic animals *Tg1/Tg2* express Reelin in the pyramidal neurons of the CA1 area and thus, we assume they will show differences in plasticity, learning and memory processes with respect to control animals.

reeler heterozygous mice (*rl/+*) are considered a model for schizophrenia (Costa et al., 2002; Tueting et al., 1999), although with some controversy (Podhorna and Didriksen, 2004). Thus, the animals with the genotype *rl/+;Tg1/Tg2* are candidates to show a rescued schizophrenic phenotype.

Reelin-signaling in the adult brain

A critical issue to examine in the *Tg1/Tg2* mouse is the state of activation of the signaling network activated by Reelin in the brain regions in which this protein is ectopically produced. The analysis of intracellular signaling downstream of Reelin has been studied mainly in primary neuronal cultures; nonetheless, the signaling pathways that Reelin may activate in the adult brain are suspected to be the same. Therefore, it is of primary interest to analyze the content of mDab1 in *Tg1/Tg2* animals and also the phosphorylation state of this protein in this model. Moreover, the basal phosphorylation/activation state of PI3K, Akt1, Erk1/2, GSK3β and MAP1B may also be altered by ectopic expression of Reelin. Another point to address in *Tg1/Tg2* animals is the Egr-1 transcription factor content and that of its target genes.

Reelin has been related to Tau phosphorylation and consequently to Alzheimer's disease. In *Tg1/Tg2* animals, Reelin is secreted in the hippocampus, a region highly affected by this disease. Therefore, this animal model is specially suited to address this topic.

Development of new Reelin-transgenic animal models for the study of Reelin-regulated processes

tetO-rlM animals were also designed in order to determine the involvement of Reelin in other processes by crossing this strain with other tTA-expressing transgenic models. Using specific promoters, tTA expression can be directed to almost any cell type; and the new transgenic mouse can be used to analyze the consequences of Reelin in these models.

Finally, the *Tg1/Tg2* model is of particular interest in order to rescue phenotypic characteristics of *reeler* animals. For example, by obtaining *Tg1/Tg2* animals on a *reeler* background (*reeler-Tg1/Tg2*), the abnormalities in synaptogenesis described in *reeler* hippocampus could be hypothetically reduced. In contrast, abnormalities such as the embryonic mispositioning of neurons will not be rescued.

MATERIALS AND METHODS

Generation of the injection fragment:

Total digestion of pCrlM (kindly provided by Dr. T. Curran, Memphis) was performed with *NotI* to linearize the 16 kb vector. Then, partial digestion with *EcoRI* was performed for 10 min at 37ºC, obtaining as a result a mixture of partially digested species. The 10.6 kb fragment, containing the Myc-tagged cDNA of Reelin (rlM), was subcloned into the *EcoRI-NotI* sites of the pCRII-TOPO cloning vector (Invitrogen); originating the pCRII-rlM vector. A 10.6 kb fragment was then excised by *SpeI* total digestion, overhanging ends refilled using Cloned Pfu DNA polymerase (Stratagene), and subcloned into the *EcoRV* site of the PMM400 vector (generously provided by Dr. M. Mayford, San Diego). The newly generated PMM-rlM vector was digested with *NotI* to obtain an injection fragment of 12.6 kb, which contained the tetO operator linked to rlM. Microinjections of single-cell CBAxC57BL/6J embryos were performed in Department of Animal Reproduction (INIA, Madrid).

Animals:

Mice were bred in the animal research centre at the Barcelona Science Park (SEA-PCB). They were provided food and water *ad libitum* and maintained in a temperature-controlled environment in a 12/12h light-dark cycle. Founder mice were identified by PCR with primers generated on exon 26 and exon 27: *RLgen-F*: 5'-TTGTACCAGGTTCCGCTGGT-3', *RLgen-R*: 5'-GCACATATCCAGGTTTCAGG-3', amplifying a 320bp fragment. The same primers also amplify the endogenous *reelin* gene fragment of 720bp, containing the 400bp intron 26. Confirmed founder mice (Tg2) were then crossed with wild-type C57BL/6J mice to generate strains. Following generations were crossed with pCaMKIIa-tTA (Tg1) animals, provided by M. Mayford (Mayford et al., 1996), to produce double transgenic mice over-expressing Reelin (Tg1/Tg2).

Antibodies and reagents:

Mouse monoclonal anti-Reelin antibody (clone G10) was provided by A.M. Goffinet and affinity purified antibody anti-mDab1 (B3) was a generous gift from J.A. Cooper. Anti-Myc antibody was purchased from Santa Cruz Biotechnology. The goat-anti-mouse-HRP secondary antibody used for WB was from DAKO and the goat-anti-rabbit-HRP was from Sigma. For immunohistochemistry, Biotinylated-anti-mouse secondary antibody and Streptavidin-biotinylated horseradish peroxidase complex were from Amersham.

Protein G-Sepharose 4B Fast Flow was purchased from Sigma. Diaminobenzidine (DAB) reagent and H_2O_2 were also from Sigma.

Reelin production and neuronal primary cultures stimulation:

Transfection of 293T cells with full-length mouse Reelin expression constructs pCrlM and PMM400-rlM, or control vectors pcDNA3.1 and PMM400 was done using Lipofectamine (Invitrogen) (D'Arcangelo et al., 1997). Culture medium was replaced with Opti-MEM I reduced serum medium (GibcoBRL) the following day. Cells were maintained for 4 days and the conditioned medium was collected, filtered through 0.2μm filter membranes (Orange Scientific), concentrated 60-fold using Amicon Ultra-15 100,000 MWCO (Millipore) centrifugal filters, and maintained at 4ºC. Reelin

production was confirmed by WB using anti-Reelin (G10) antibody. Control supernatants were treated in the same way.

Telencephalon neurons were obtained from E16 mouse embryos (OF1 mice, Charles River Laboratories). Telecephalons were dissected in PBS containing 0.6% glucose, trypsinized and mechanically dissociated. Cells were cultured in 6-well plates (Nunc) coated with Poly-D-Lysine at a density of 3-5 million per well and maintained in serum-free Neurobasal medium (GibcoBRL) with 2mM L-glutamine, 30mM D-+-glucose, 5mM sodium bicarbonate, Penicillin/Streptomycin (100U/ml, 100µg/ml), 25µM sodium glutamate and B27 supplement diluted 1/50 (GibcoBRL). Prior to stimulation, neuronal cultures were starved using Neurobasal-based medium. Reelin or control conditioned media were then used for the treatments at a 1/20 dilution from the stock.

Western blots and immunoprecipitation:

Lysates were collected in Lysis Buffer (Hepes 50mM (pH 7.5), 150mM sodium chloride, 1.5mM magnesium chloride, 1mM EGTA, 10% glycerol and 1% Triton X-100) containing Complete Mini protease inhibitor cocktail (Roche, cat. 1836153) and phosphatase inhibitors (10mM tetra-sodium pyrophosphate, 200µM sodium orthovanadate and 10mM sodium fluoride); insoluble debris was removed by centrifugation (30 min, 16000*g*) and supernatants were stored at -80ºC.

For immunoprecipitation, lysates were incubated with the primary antibody overnight (o/n) at 4ºC (4µg/sample). Protein G-Sepharose beads were added for 90 min at 4ºC, recovered by centrifugation, and washed 3 times with Lysis Buffer.

Samples were diluted 2:3 with 3X Loading Buffer (225mM Tris (pH 6.5), 1.5mM β-mercaptoethanol, 1.5% SDS, 15% glycerol and 0.0375% bromophenol blue), boiled for 10 min at 95ºC, resolved by SDS-polyacrylamide gels and transferred onto nitrocellulose membranes.

Nitrocellulose membranes were blocked for 1 h at room temperature (RT) in TBST (Tris 10mM pH 7.4, sodium chloride 140mM (TBS) with 0.1% Tween 20) containing 5% non-fat milk. Primary antibodies were incubated for 90 min in TBST-0.02% azide (anti-Reelin (clone G10) 1:10000, anti-Myc 1:5000, anti-phospho-tyrosine (clone 4G10) 1:5000, anti-mDab1 (B3) 1:3000). After incubation with secondary HRP-labeled antibodies for 1 h at RT (diluted 1:5000 in TBST-5% non-fat milk), membranes were developed with the ECL+ system (Amersham).

Immunohistochemistry:

For immunohistochemistry, animals were perfused for 20 min with 0.1M phosphate buffer (PB) containing 4% of paraformaldehyde (PF). Brains were postfixed overnight with PB-4% PF, cryoprotected with PB-30% ethylenglycol, sectioned coronally at 30µm and maintained at -20ºC in PB-30% glycerol-30% sucrose. Sections were then blocked with PB saline (PBS) containing 10% of normal goat serum (NGS), and incubated overnight at 4ºC with anti-Reelin antibody (clone G10) at a 1:1000 dilution in PBS-5% NGS. Incubation with biotilated biotinylated secondary antibodies at 1:200 and streptavidin-HRP complexes at 1:400 was performed in PBS-5% NGS (2h at RT). Bound antibodies were visualized by reaction using DAB and H_2O_2 as peroxidase substrates. Finally, sections were mounted dehydrated in Eukitt.

Semi-quantitative PCR:

To quantify the number of insertions of the transgene, PCRs were performed by co-amplification of *reelin* and the control gene *Rps15* (which codes for the ribosomal protein S15). The primers used to amplify the 380bp fragment of the endogenous gene *Rps15* were: *rib/S15-F*: 5'-TTCCGCAAGTTCACCTACC-3' and *rib/S15-R*: 5'-CGGGCCGGCCATGCTTTACG-3'. The primers used to amplify the endogenous gene *reelin* (720bp) and the *reelin*-transgene (320bp) were: *RLgen-F* and *RLgen-R* (sequences above). Pictures were taken from agarose gels using a Gene Genius Bio Imaging System and band intensities were quantified using GeneTools software, both from Syngene.

ABBREVIATIONS

CMV	cytomegalovirus
Dox	deoxicicline
Erk	extracellular regulated kinase
GSK3β	glycogen synthase kinase 3 beta
MAP1B	microtubule-associated protein 1B
PI3K	phosphatidylinositol 3 kinase
SGZ	subgranular zone
SFK	Src family protein kinase
SV40	simian virus 40
SVZ	subventricular zone
tetO	tetracycline operator
tTA	tetracycline-controlled transactivator
WB	Western blot

ACKNOWLEDGEMENTS

We thank Drs. M. Mayford, J. A. Cooper, T. Curran, and A. M. Goffinet for generously providing materials used in this study; C. Díaz-Ruiz, J.M. Ureña and A. La Torre for scientific assistance; and B. Pintado, S. Soriano for technical assistance, and T. Yates for editorial help. L. Pujadas holds postgraduate fellowships from the Spanish Ministry of Education and Science and from the IRB. This work was supported by grant SAF2004-07929 awarded to E. Soriano.

REFERENCES

Alcantara, S., M. Ruiz, G. D'Arcangelo, F. Ezan, L. de Lecea, T. Curran, C. Sotelo, and E. Soriano. 1998. Regional and cellular patterns of reelin mRNA expression in the forebrain of the developing and adult mouse. *J Neurosci*. 18:7779-99.

Arnaud, L., B.A. Ballif, E. Forster, and J.A. Cooper. 2003. Fyn tyrosine kinase is a critical regulator of disabled-1 during brain development. *Curr Biol*. 13:9-17.

Beffert, U., G. Morfini, H.H. Bock, H. Reyna, S.T. Brady, and J. Herz. 2002. Reelin-mediated signaling locally regulates protein kinase B/Akt and glycogen synthase kinase 3beta. *J Biol Chem*. 277:49958-64.

Beffert, U., E.J. Weeber, A. Durudas, S. Qiu, I. Masiulis, J.D. Sweatt, W.P. Li, G. Adelmann, M. Frotscher, R.E. Hammer, and J. Herz. 2005. Modulation of synaptic plasticity and memory by Reelin involves differential splicing of the lipoprotein receptor Apoer2. *Neuron*. 47:567-79.

Bock, H.H., and J. Herz. 2003. Reelin activates SRC family tyrosine kinases in neurons. *Curr Biol*. 13:18-26.

Bock, H.H., Y. Jossin, P. Liu, E. Forster, P. May, A.M. Goffinet, and J. Herz. 2003. Phosphatidylinositol 3-kinase interacts with the adaptor protein Dab1 in response to Reelin signaling and is required for normal cortical lamination. *J Biol Chem*. 278:38772-9.

Borrell, V., J.A. Del Rio, S. Alcantara, M. Derer, A. Martinez, G. D'Arcangelo, K. Nakajima, K. Mikoshiba, P. Derer, T. Curran, and E. Soriano. 1999. Reelin regulates the development and synaptogenesis of the layer-specific entorhino-hippocampal connections. *J Neurosci*. 19:1345-58.

Burgin, K.E., M.N. Waxham, S. Rickling, S.A. Westgate, W.C. Mobley, and P.T. Kelly. 1990. In situ hybridization histochemistry of Ca2+/calmodulin-dependent protein kinase in developing rat brain. *J Neurosci*. 10:1788-98.

Costa, E., Y. Chen, J. Davis, E. Dong, J.S. Noh, L. Tremolizzo, M. Veldic, D.R. Grayson, and A. Guidotti. 2002. REELIN and Schizophrenia:: A Disease at the Interface of the Genome and the Epigenome. *Mol Interv*. 2:47-57.

D'Arcangelo, G., R. Homayouni, L. Keshvara, D.S. Rice, M. Sheldon, and T. Curran. 1999. Reelin is a ligand for lipoprotein receptors. *Neuron*. 24:471-9.

D'Arcangelo, G., G.G. Miao, S.C. Chen, H.D. Soares, J.I. Morgan, and T. Curran. 1995. A protein related to extracellular matrix proteins deleted in the mouse mutant reeler. *Nature*. 374:719-23.

D'Arcangelo, G., K. Nakajima, T. Miyata, M. Ogawa, K. Mikoshiba, and T. Curran. 1997. Reelin is a secreted glycoprotein recognized by the CR-50 monoclonal antibody. *J Neurosci*. 17:23-31.

Doetsch, F., and R. Hen. 2005. Young and excitable: the function of new neurons in the adult mammalian brain. *Curr Opin Neurobiol*. 15:121-8.

Gonzalez-Billault, C., J.A. Del Rio, J.M. Urena, E.M. Jimenez-Mateos, M.J. Barallobre, M. Pascual, L. Pujadas, S. Simo, A.L. Torre, R. Gavin, F. Wandosell, E. Soriano, and J. Avila. 2005. A role of MAP1B in Reelin-dependent neuronal migration. *Cereb Cortex*. 15:1134-45.

Gossen, M., and H. Bujard. 1992. Tight control of gene expression in mammalian cells by tetracycline-responsive promoters. *Proc Natl Acad Sci U S A*. 89:5547-51.

Hack, I., M. Bancila, K. Loulier, P. Carroll, and H. Cremer. 2002. Reelin is a detachment signal in tangential chain-migration during postnatal neurogenesis. *Nat Neurosci*. 5:939-45.

Hiesberger, T., M. Trommsdorff, B.W. Howell, A. Goffinet, M.C. Mumby, J.A. Cooper, and J. Herz. 1999. Direct binding of Reelin to VLDL receptor and ApoE receptor 2 induces tyrosine phosphorylation of disabled-1 and modulates tau phosphorylation. *Neuron*. 24:481-9.

Lewandoski, M. 2001. Conditional control of gene expression in the mouse. *Nat Rev Genet*. 2:743-55.

Magdaleno, S., L. Keshvara, and T. Curran. 2002. Rescue of ataxia and preplate splitting by ectopic expression of Reelin in reeler mice. *Neuron*. 33:573-86.

Mayford, M., M.E. Bach, Y.Y. Huang, L. Wang, R.D. Hawkins, and E.R. Kandel. 1996. Control of memory formation through regulated expression of a CaMKII transgene. *Science*. 274:1678-83.

Ming, G.L., and H. Song. 2005. Adult Neurogenesis in the Mammalian Central Nervous System. *Annu Rev Neurosci*. 28:223-50.

Miyata, T., K. Nakajima, K. Mikoshiba, and M. Ogawa. 1997. Regulation of Purkinje cell alignment by reelin as revealed with CR-50 antibody. *J Neurosci*. 17:3599-609.

Podhorna, J., and M. Didriksen. 2004. The heterozygous reeler mouse: behavioural phenotype. *Behav Brain Res*. 153:43-54.

Rice, D.S., and T. Curran. 2001. Role of the reelin signaling pathway in central nervous system development. *Annu Rev Neurosci*. 24:1005-39.

Rice, D.S., M. Sheldon, G. D'Arcangelo, K. Nakajima, D. Goldowitz, and T. Curran. 1998. Disabled-1 acts downstream of Reelin in a signaling pathway that controls laminar organization in the mammalian brain. *Development*. 125:3719-29.

Sheldon, M., D.S. Rice, G. D'Arcangelo, H. Yoneshima, K. Nakajima, K. Mikoshiba, B.W. Howell, J.A. Cooper, D. Goldowitz, and T. Curran. 1997. Scrambler and yotari disrupt the disabled gene and produce a reeler-like phenotype in mice. *Nature*. 389:730-3.

Soriano, E., and J.A. Del Rio. 2005. The cells of cajal-retzius: still a mystery one century after. *Neuron*. 46:389-94.

Tissir, F., and A.M. Goffinet. 2003. Reelin and brain development. *Nat Rev Neurosci*. 4:496-505.

Trommsdorff, M., M. Gotthardt, T. Hiesberger, J. Shelton, W. Stockinger, J. Nimpf, R.E. Hammer, J.A. Richardson, and J. Herz. 1999. Reeler/Disabled-like disruption of neuronal migration in knockout mice lacking the VLDL receptor and ApoE receptor 2. *Cell*. 97:689-701.

Tueting, P., E. Costa, Y. Dwivedi, A. Guidotti, F. Impagnatiello, R. Manev, and C. Pesold. 1999. The phenotypic characteristics of heterozygous reeler mouse. *Neuroreport*. 10:1329-34.

Weeber, E.J., U. Beffert, C. Jones, J.M. Christian, E. Forster, J.D. Sweatt, and J. Herz. 2002. Reelin and ApoE receptors cooperate to enhance hippocampal synaptic plasticity and learning. *J Biol Chem*. 277:39944-52.

FIGURE 1

Generation of transgenic mice containing myc-tagged reelin cDNA

(A) The construction of the insertion fragment to generate the transgenic mouse *tetO-rlM* (Tg2) starts from the *myc*-tagged version (pCrlM) of the pCrl vector, which contains the cDNA of the *reelin* gene (1st and 2nd panels). The excision of the *reelin* cDNA from pCrlM was inserted into the PCRII vector (PCRII-rlM) (3rd panel), re-excised, and inserted into the PMM vector to generate PMM-rlM (4th panel). The insertion fragment from the PMM-rlM vector was excised by digestion with NotI (bottom panel).
(B) Supernatants from 293T cells transfected with the pCrlM and PMM-rlM vectors (and their control Mock vectors: pCDNA3.1 and PMM400) were analyzed by WB (top panel). Both pCrlM and PMM-rlM supernatants contained Reelin, as detected with the G10 anti-Reelin antibody (lines 2 and 4). Telencephalon neurons treated for 15 min with Reelin-containing supernatants showed increased levels of phosphorylated mDab1 (middle panel, lines 2 and 4) compared with control Mock treatments (lines 1 and 3). This observation indicatesthat the Reelin produced from the PMM-rlM vector is functional, as is Reelin derived from pCrlM. Bottom panel shows the loading controls for the middle panel.
(C) Double transgenic mice *Tg1/Tg2* were obtained by crossing *tetO-rlM* (*Tg2*) mice with *pCaMKIαI-tTA* (*Tg1*). *Tg1* mice expressed the *tTA* transactivator in neurons that express the *CaMKIIα* promoter. *Tg2* mice did not express *rlM* because the *tetO* promoter is inactive. *Tg1/Tg2* mice express. *rlM* by transactivation of its promoter *tetO* by *tTA* in neurons that express *CaMKIIα*.
(D) The number of insertions in 8 transgenic strains was estimated by semi-quantitative PCR. Strains *alphaR* (6 insertions), *betaR* (6 insertions), *gammaR* (5 insertions) and *rhoR* (1 insertion) were selected for maintenance and further characterization.

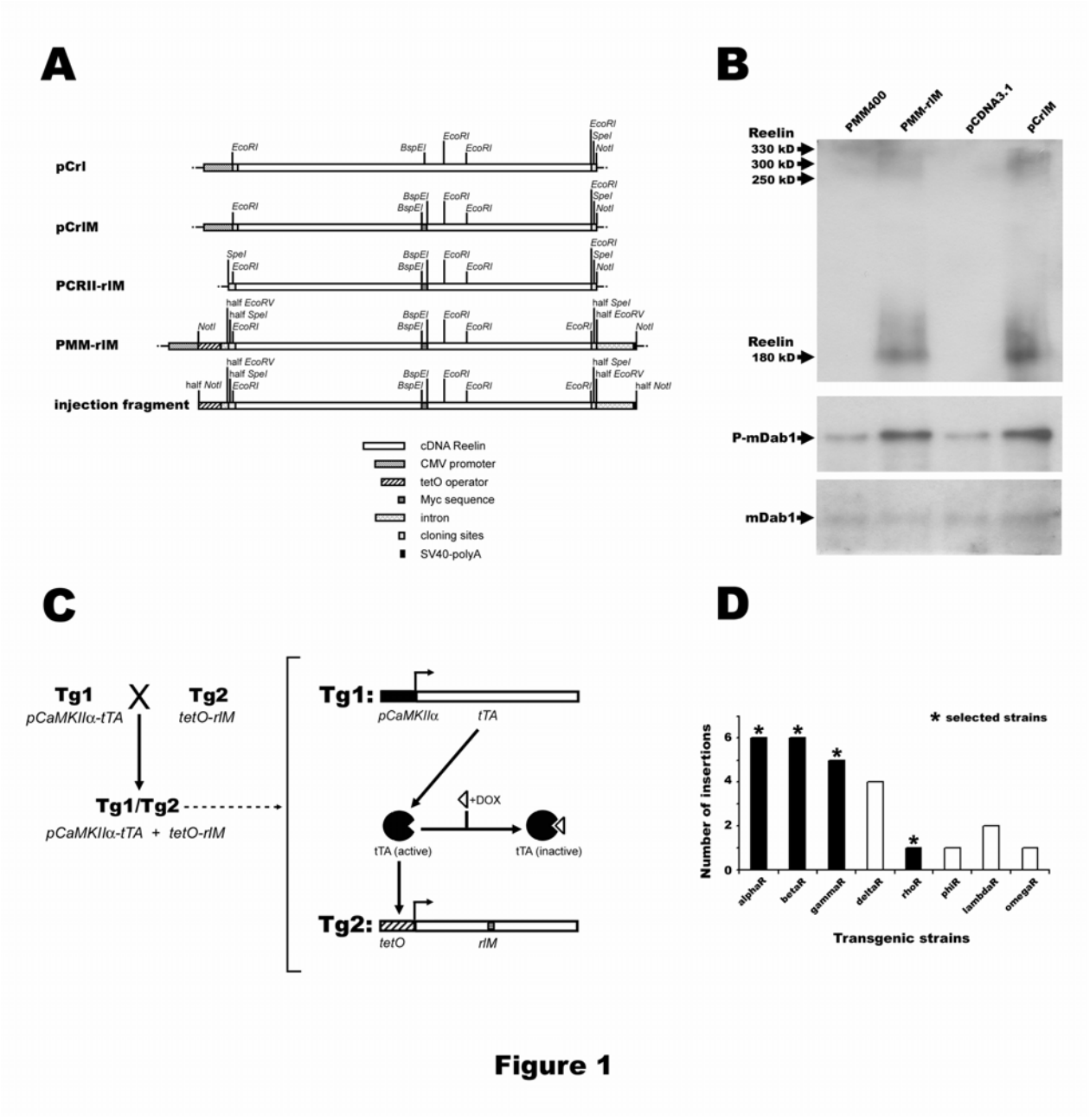
A
pCrl
pCrlM
PCRII-rlM
PMM-rlM
injection fragment
EcoRI
BspEI
SpeI
NotI
half EcoRV
half SpeI
half NotI
cDNA Reelin
CMV promoter
tetO operator
Myc sequence
intron
cloning sites
SV40-polyA
B
PMM400
PMM-rlM
pCDNA3.1
pCrlM
Reelin
330 kD
300 kD
250 kD
Reelin
180 kD
P-mDab1
mDab1
C
Tg1
pCaMKIIα-tTA
Tg2
tetO-rlM
Tg1/Tg2
pCaMKIIα-tTA + tetO-rlM
Tg1:
pCaMKIIα
tTA
+DOX
tTA (active)
tTA (inactive)
Tg2:
tetO
rlM
D
* selected strains
Number of insertions
0
2
4
6
alphaR
betaR
gammaR
deltaR
rhoR
phiR
lambdaR
omegaR
Transgenic strains

Figure 1

FIGURE 2

Expression of Reelin in transgenic mice

(A-F) *Tg1/Tg2* mice originated by crossing the *CamKIIα* (*Tg1*) and the *alphaR* (*Tg2*) strains, and their control littermates (*wt*, *Tg1* and *Tg2*) were processed for immunohistochemistry at age P60, and the expression of endogenous and transgenic Reelin was analyzed with the G10 antibody.
(A,B) The CA1 hippocampal region showed endogenous expression of Reelin in the lasting Cajal-Retzius cells of the hippocampal fissure and in a subset of interneurons located in several layers, both in control and *Tg1/Tg2* mice (A,B). Moreover, Reelin was also expressed in the pyramidal neurons of the CA1 region of the hippocampus in double transgenic mice (B, black arrowheads).
(C,D) In the DG, Reelin was endogenously expressed by a subset of interneurons in both control and *Tg1/Tg2* mice (C,D). *Tg1/Tg2* animals also showed low expression levels of Reelin in granular neurons (D, black arrowheads).
(E,F) Reelin was not expressed at high levels in any neuron in the striatum of control mice (E), but was abundant in *Tg1/Tg2* animals (F, black arrowheads).
Scale bar, 100μm (A,B); 100μm (C,D); 200μm (E,F).
Abbreviations: ML, molecular layer; HF, hippocampal fissure; SLM, stratum lacunosum moleculare; SR, stratum radiatum; SP, stratum piramidale; SO, stratum oriens; WM, white matter; DG, dentate gyrus; H, hilus; SGZ, subgranular zone; GL, granular layer; ML, molecular layer; CC, corpus callosum; S, septum; LV, lateral ventricle; SVZ, subventricular zone; STR, striatum; CX, cortex.

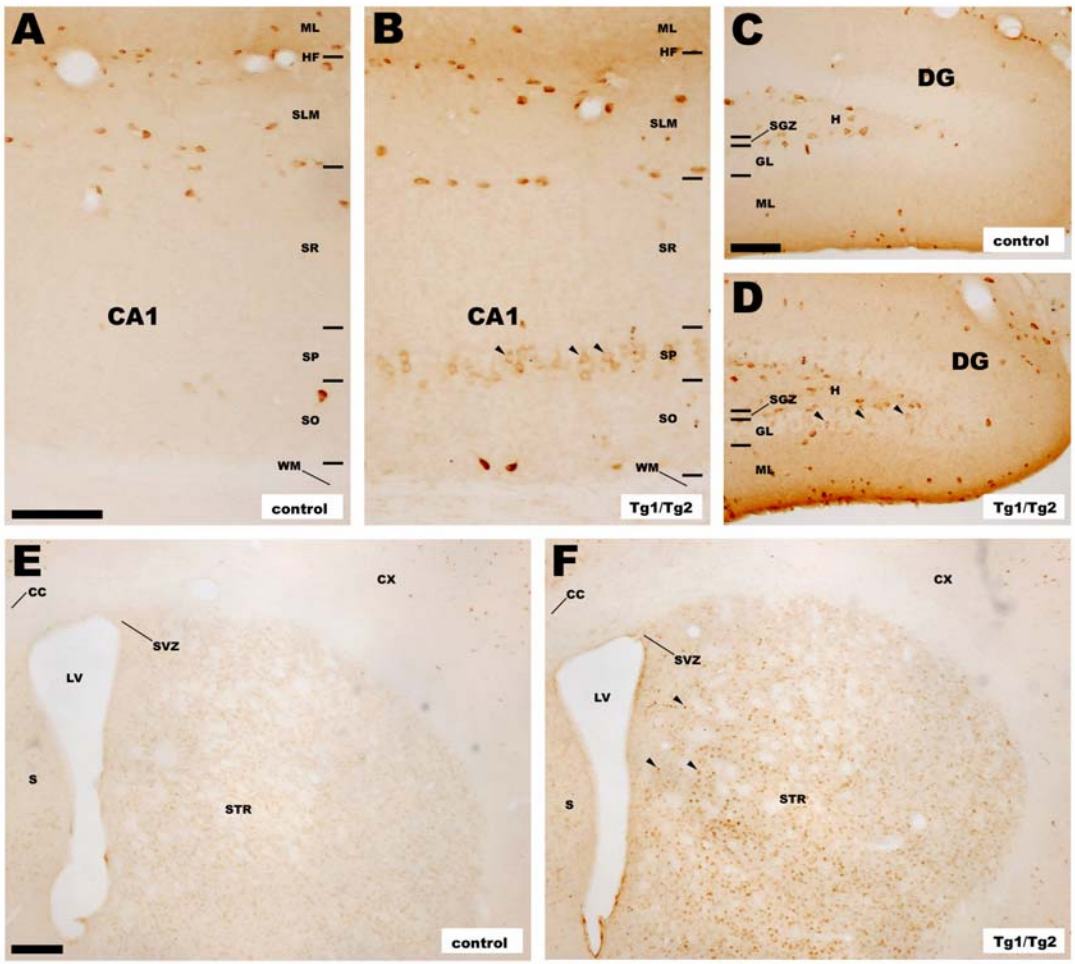
A
ML
HF
SLM
SR
CA1
SP
SO
WM
control
B
ML
HF
SLM
SR
CA1
SP
SO
WM
Tg1/Tg2
C
DG
SGZ
H
GL
ML
control
D
DG
SGZ
H
GL
ML
Tg1/Tg2
E
CC
CX
SVZ
LV
S
STR
control
F
CC
CX
SVZ
LV
S
STR
Tg1/Tg2

Figure 2